

THE EFFECT OF SHORT CHAIN FATTY ACIDS ON
PICORNAVIRUS REPLICATION

THESIS

Submitted in Fulfilment of the
Requirements for the degree of
MASTER OF SCIENCE
of Rhodes University

By

NAZEEM ISMAIL-CASSIM

January 1993

CONTENTS

	<u>PAGE</u>
CONTENTS	ii
ABSTRACT	vi
ACKNOWLEDGEMENTS	viii
PUBLICATIONS	ix
TABLES	x
FIGURES	xi
<u>CHAPTER 1</u>	
INTRODUCTION	
1.1 CLASSIFICATION	1
1.2 THE RNA CHROMOSOME AND ITS GENE PRODUCTS	2
1.2.1 Structure of picornaviral RNAs	2
1.2.2 The protein-coding region	3
1.3 THE VIRION	9
1.3.1 Physical properties	9
1.3.2 The protomer	10
1.3.3 Dodecahedral nature of the protein shell	12
1.3.4 Buoyant density of picornaviruses	14
1.4 OVERVIEW OF THE MULTIPLICATION CYCLE	16
1.5 ADSORPTION, UNCOATING, AND PENETRATION	19

1.6 EFFECTS ON THE HOST CELL	22
1.7 SYNTHESIS OF VIRAL RNA AND PROTEIN	27
1.7.1 RNA synthesis	28
1.7.2 Role of VPg in regulating the infection cycle	30
1.7.3 Synthesis and cleavage of the polyprotein	31
1.8 MORPHOGENESIS	34
1.9 PICORNAVIRAL STRUCTURE	40
1.9.1 Functions of the protomer	41
1.9.2 Location of the four segments	42
1.9.3 Structure of Poliovirus	43
1.9.4 Atomic resolution structure of HRV14	46
1.9.5 Atomic structure of Mengo virus	50
1.9.6 Receptor recognition	54
1.9.7 Immunogenic sites on picornaviruses	55
1.9.8 Antiviral drug binding	58
1.9.9 Unique features of FMDV	63
1.10 MYRISTYLATION OF PICORNAVIRUS CAPSID PROTEIN VP4	66

CHAPTER 2

MATERIALS AND METHODS

2.1 REAGENTS	70
2.2 APPARATUS	70
2.3 VIRUSES AND CELLS	71

2.4 TOXICITY OF FATTY ACIDS	71
2.5 MYRISTIC ACID COMPETITION IN BHK-21 CELLS	72
2.6 TITRATION OF VIRUS HARVESTS CONTAINING FATTY ACIDS	73
2.7 VIRUS PURIFICATION	74
2.8 RADIOLABELLING OF BHK-21 CELLS	75
2.9 FATTY ACID TREATMENT OF BHK-21 CELLS	75
2.10 RADIOLABELLING OF VIRUS	79
2.11 RADIOLABELLING OF VIRUS-DIRECTED PROTEINS	79
2.12 FATTY ACID TREATMENT OF VIRUSES	80

CHAPTER 3

RESULTS

3.1 MYRISTIC ACID COMPETITION EXPERIMENTS	81
3.1.1 Incorporation of lauric acid into VP4 of BEV	81
3.1.2 Toxicity of fatty acids for BHK-21 cells	83
3.1.3 Competition with myristylation of BHK-21 cell proteins	86
3.1.4 Titration of virus harvests grown in the presence and absence of fatty acid	86
3.1.5 Effect of lauric acid on virus yield	89
3.2 LAURIC ACID EXPERIMENTS	94
3.2.1 Effect of fatty acids on normal cell protein synthesis	94
3.2.2 Effect of fatty acids on virus-directed protein synthesis	96
3.2.3 Attachment of virus to susceptible cells	108

3.2.4 Binding of lauric acid to virus particles	110
3.2.5 Stabilization of virus particles with lauric acid	110
3.2.6 Inhibition of cell-mediated uncoating	114

CHAPTER 4

DISCUSSION AND CONCLUSIONS

4.1 MYRISTIC ACID COMPETITION EXPERIMENTS	117
---	-----

4.2 LAURIC ACID EXPERIMENTS	118
-----------------------------	-----

APPENDICES	122
------------	-----

REFERENCES	128
------------	-----

ABSTRACT

Picornavirus proteins VP1 to VP3 are exposed on the surface of the virus particle whereas VP4 is internal and modified at its amino terminus by the addition of myristic acid (Chow et al., 1987; Paul et al., 1987). Myristic acid occupies a position in the core of mature poliovirus particles; it has been suggested that it may be important for particle integrity or in the localization of the capsid protein precursor on the hydrophobic membranes during virion assembly (Chow et al., 1987).

To determine the function of the amino-terminal myristylation of VP4 in picornaviruses, and to establish whether competition for the acylation site is a possible approach to antiviral chemotherapy, the effect of fatty acids on virus replication has been examined. Some fatty acids are able to enter picornavirus-infected cells and compete for the myristylation site on VP4. Unexpectedly, it was found that short chain fatty acids also inhibit an early event in the replication of bovine enterovirus (BEV) at concentrations which have no detectable effect on cellular macromolecular synthesis and cloning. These findings indicate that fatty acids inhibit cell-mediated uncoating.

Short chain fatty acids inhibit the replication of bovine enterovirus but are almost ineffective against poliovirus type 1, coxsackievirus B5, encephalomyocarditis virus and human rhinovirus 1B. Lauric acid binds to bovine enterovirus, thereby stabilizing the virus particle to heat degradation. Fatty acid-bound virions attach to susceptible cells but fail to undergo cell-mediated uncoating. The inhibitory effect is reversible with chloroform and may result from a hydrophobic interaction between the fatty acid and a specific site on the virus particle.

ACKNOWLEDGEMENTS

I would like to thank:

Professor J. F. E. Newman, for his supervision and assistance throughout this project

Professor R. Kirby, for taking over supervision after the departure of Professor Newman, and for his patience and understanding through a difficult time

Professor D. A. Hendry, for his supervision, and assistance with the photographs

Miss Claudia Chezzi for contributing publishable versions of figures 3.15, 3.16 and 3.19

Miss M. Poggrund and Mrs G. Hagemann, for all their assistance throughout my studies

My wife and my parents, for their support and encouragement during my studies.

I also acknowledge a bursary from the Poliomyelitis Research Foundation.

This research was in part funded by the Council for Scientific and Industrial Research.

PUBLICATIONS

Part of this work was published as a paper:

ISMAIL-CASSIM, N., CHEZZI, C. & NEWMAN, J. F. E. (1990).
Inhibition of the uncoating of bovine enterovirus by short
chain fatty acids. Journal of General Virology 71,
2283-2289.

TABLES

	<u>PAGE</u>
TABLE 1.1 Physical properties of the poliovirion	9
TABLE 1.2 Mass of some picornaviral coat proteins	12
TABLE 1.3 Physical properties of picornaviruses	15
TABLE 1.4 Key to nomenclature of picornaviral proteins	33
TABLE 1.5 Amino-terminal sequences of myristylated proteins	68
TABLE 3.1 Maximum concentration of fatty acids that are not toxic to BHK-21 cells	85

FIGURES

PAGE

Figure 1.1: Model of proteolytic processing of the initial translation product of poliovirus by two virus-encoded proteinases.	4
Figure 1.2: Structure of the picornaviral genome for some picornaviruses.	6
Figure 1.3: Proposed autocatalytic cleavage of VP0.	8
Figure 1.4: Structural organization of the picornaviral capsid.	11
Figure 1.5: Experimental basis for the dodecahedral model of picornaviral capsid structure.	13
Figure 1.6: Overview of the picornaviral infection cycle.	17
Figure 1.7: One-step growth experiment for human rhinovirus 14 in a HeLa cell suspension culture.	20
Figure 1.8: Model for attachment of the virions, dismantling of the protective protein shell, and delivery of the RNA to a site where translation can begin.	23

Figure 1.9: Synthesis of protein in poliovirus-infected HeLa cells infected at high multiplicity.	25
Figure 1.10: Replicative form (RF) of poliovirus RNA illustrating end structure of the complementary (+) and (-) strands.	29
Figure 1.11: Spectrum of proteins synthesized in poliovirus-infected HeLa cells at 3.5 hours after infection.	32
Figure 1.12: Picornaviral morphogenesis.	35
Figure 1.13: Schematic representation of the poliovirus capsid proteins.	44
Figure 1.14: Diagrammatic drawings showing the polypeptide fold of SBMV and of each of the three capsid proteins of HRV14.	47
Figure 1.15: The fivefold β -cylinder formed by the amino-terminal ends of VP3 at the protein/RNA interface.	49
Figure 1.16: Ribbon drawings of the three larger viral proteins VP1, VP2, and VP3 for Mengo virus and HRV14.	52

Figure 1.17: Pentameric 14S assembly unit as seen from the outside, showing the course of VP4 represented by a ribbon in (A) HRV14 and (B) Mengo virus.	53
Figure 1.18: The presence of depressions on the picornavirus surface suggests a strategy for the evasion of immune surveillance.	56
Figure 1.19: Formulae of the two antiviral compounds, WIN 51711 and WIN 52084.	59
Figure 1.20: (A) Ribbon drawing of VP1 with WIN compound binding site. (B) Diagrammatic representation of antiviral compound binding site.	61
Figure 1.21: Picornavirus structure illustrating the disposition of the structural proteins VP1-4 with respect to the icosahedral symmetry axis.	65
Figure 2.1: Typical virus peak obtained by sucrose density gradient fractionation of bovine enterovirus.	76
Figure 2.2: PAGE separation of BEV proteins.	77
Figure 2.3: Determination of molecular weights of the structural proteins of BEV by PAGE.	78

Figure 3.1: Identification of the protein-linked fatty acid on VP4.	82
Figure 3.2: SDS-PAGE separation of radiolabelled BEV proteins.	84
Figure 3.3: Inhibition of the incorporation of [³ H] myristic acid into cell proteins by various fatty acids, as measured by scintillation counting.	87
Figure 3.4: Titres of BEV grown in the presence and absence of lauric acid and capric acid.	88
Figure 3.5: Sedimentation through a 15-45% sucrose gradient of BEV grown in normal MEM and BEV grown in MEM containing 30 uM lauric acid.	90
Figure 3.6: Sucrose density gradient fractionation of BEV radiolabelled with [S]methionine and [H]uridine showing that BEV empty particles do not contain RNA.	92
Figure 3.7: PAGE separation of BEV grown in the presence and absence of 30 uM-lauric acid.	93
Figure 3.8: PAGE of radiolabelled proteins from BHK-21 cells grown in the presence and absence of lauric acid and capric acid.	95

Figure 3.9: PAGE of radiolabelled proteins from BHK-21 cells grown in the presence of fatty acids and related compounds.	97
Figure 3.10: PAGE of radiolabelled proteins from BHK-21 cells infected with BEV in the presence and absence of lauric acid and capric acid.	98
Figure 3.11: PAGE of radiolabelled proteins from BHK-21 cells infected with EMCV in the presence and absence of lauric acid and capric acid.	100
Figure 3.12: PAGE of radiolabelled proteins from HeLa cells infected with HRV-1B in the presence and absence of 30 μ M-lauric acid.	101
Figure 3.13: PAGE of radiolabelled proteins from BHK-21 cells infected with BEV in the presence of 100 μ M-lauric acid.	102
Figure 3.14: PAGE of radiolabelled proteins from BHK-21 cells infected with BEV in the presence and absence of myristic- and palmitic acids.	104
Figure 3.15: PAGE of radiolabelled proteins from cells infected with picornaviruses in the presence and absence of lauric acid.	105

Figure 3.16: PAGE of radiolabelled proteins from BHK-21 cells infected with BEV in the presence of fatty acids and related compounds.	107
Figure 3.17: Kinetics of attachment [³⁵ S]methionine-labelled BEV to BHK-21 cells at 37°C.	109
Figure 3.18: Sucrose gradient of [³ H]lauric acid bound to purified BEV.	111
Figure 3.19: PAGE of radiolabelled proteins from BHK-21 cells infected with BEV.	112
Figure 3.20: Sucrose gradients showing the protective activity of fatty acids against degradation by heating at 52°C.	113
Figure 3.21: Sucrose gradients showing the inhibition of cell-mediated uncoating by lauric acid.	115

CHAPTER 1

INTRODUCTION

The Picornaviridae are among the smallest riboviruses known. They comprise one of the largest and most important families of human and agricultural pathogens, including poliovirus, human hepatitis A virus, the human rhinoviruses (the single most important cause of the common cold), and foot-and-mouth disease virus (the most important single pathogen of livestock). Because of their economic and medical importance the picornaviruses have been prominently involved in the development of modern virology.

1.1 CLASSIFICATION

The family is divided into four genera: Enterovirus, Cardiovirus, Rhinovirus, and Aphthovirus. The enteroviruses are so-called because most inhabit the alimentary tract. They include the polioviruses, coxsackieviruses and Echoviruses (Auvinen, 1990), together with enterovirus types 68-72, including human hepatitis A virus (Coulepsis et al., 1982; Melnick, 1983a), and a number of nonhuman enteric viruses (Melnick, 1976; Melnick, 1983b). The cardioviruses, the best studied being encephalomyocarditis virus (EMCV), all belong to one serotype and are generally regarded as murine viruses. Rhinoviruses (so-called because of their adaptation to the nasopharyngeal region) are the

most important etiologic agents of the common cold in adults and children (Gwaltney, 1982). There are officially 89 serotypes (Kapikian, 1971), but additional candidate viruses have continued to accumulate and the number now probably exceeds 113 (Matthews, 1982). Most of the picornaviruses isolated from the human respiratory system are acid labile, and this lability has become a defining characteristic of rhinoviruses (Melnick, 1974; Melnick, 1983b). The seven serotypes of foot-and-mouth disease virus (FMDV) constitute the aphthoviruses. Some viruses, such as "equine rhinoviruses" 1 and 2 (Newman et al., 1977) and a collection of insect picornaviruses (Longworth, 1978; Moore & Tinsley, 1982) have not yet been assigned genera.

1.2 THE RNA CHROMOSOME AND ITS GENE PRODUCTS

1.2.1 Structure of Picornaviral RNAs

The picornaviral genome consists of a single strand of messenger-active RNA which has a molecular weight of $2-2.8 \times 10^6$, and constitutes about 30% of the particle mass. The RNA is polyadenylated at the 3' terminus and covalently attached to a small protein called VPg at the 5' terminus. The first picornaviral RNA to be completely sequenced was that of type 1 poliovirus (Kitamura et al., 1981; Racaniello, 1981). A number of other picornaviral RNAs were then sequenced and the results revealed significant variations in length ranging from 7-8.5 kilobases (kb). The longer RNAs, such as those of EMCV (7.8 kb) and FMDV (8.5

kb), carry a tract of polycytidylic acid between VPg and the beginning of the protein-coding region. This is not found in the entero- and human rhinoviruses (Brown et al., 1974). The biologic function of these poly (C) tracts is unclear. However, removal of poly (A) with the enzyme ribonuclease H markedly reduces the specific infectivity of poliovirus RNA, suggesting that poly (A) serves an essential function (Spector & Baltimore, 1974). RNA molecules with short poly (A) tracts appear to have a lower specific infectivity (Hruby & Roberts, 1976). On the other hand, VPg is not required for infectivity of the RNA (Nomoto et al., 1976). The presence of VPg is peculiar to picornaviruses because many other viral RNAs and eucaryotic mRNAs have a 7 methyl-G-cap at the 5' terminus. The exact function of VPg is not known but it has been suggested that VPg might be an important element in packaging of RNA into virions. There is also increasing evidence that it plays an important role in initiation of picornaviral RNA synthesis (Hershey & Taylor, 1987).

1.2.2 The Protein-Coding Region

The overall features of the pattern of protein synthesis used by picornaviruses are now fairly clear since this has been studied for over a decade. The RNA is translated as a single polyprotein which is subsequently cleaved into its functional proteins by two virally coded proteases (Fig. 1.1) (Palmenberg, 1982; Jacobson et al., 1970; Toyoda et al., 1986).

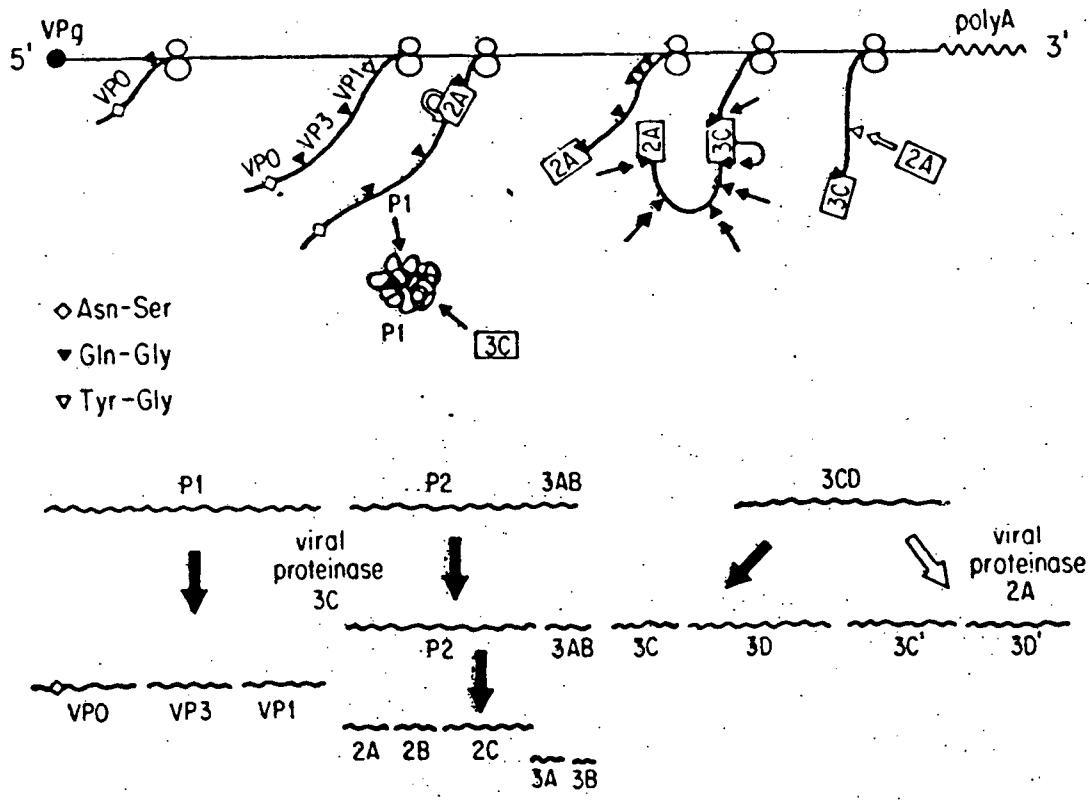


Figure 1.1: Model of proteolytic processing of the initial translation product of poliovirus by two virus-encoded proteinases. Soon after its synthesis, polypeptide 2A cleaves intramolecularly the Y-G site (∇) at its amino terminus. A similar event might occur at the amino terminus of 3C, the other proteinase specific for Q-G cleavages (\blacktriangledown). It is likely that 3C acts initially also at its carboxy-terminal Q-G site by an intramolecular mechanism, then cleaves the other Q-G sites in trans, freeing 2A from the P2 precursor. 2A then can cleave 3CD in trans to produce 3C' and 3D'. In infected cells, polypeptide P2-3AB is seen only in the presence of Zn^{2+} ions. The mechanism of the N-S cleavage (\diamond), which occurs only during (or after) encapsidation of viral RNA is obscure. (Toyoda *et al.*, 1986)

Proteolytic processing of virus-encoded translation products is common in animal virus replication, but only the picornaviruses produce all of their gene products by proteolytic cleavage of a single polyprotein precursor. In the case of poliovirus, three types of cleavages occur during proteolysis: one at an asparagine-serine (N-S) amino acid pair, two at tyrosine-glycine pairs (Y-G), and eight at glutamine-glycine (Q-G) pairs. In poliovirus replication, the virus-encoded polypeptide 3C cuts the polyprotein at Q-G sites. However, recent studies have shown that the specificity of the 3C protease in poliovirus is not restricted to Q-G sites (Kean et al., 1990). The processing sites for the enzyme 3C in various picornaviruses are shown in Fig. 1.2. Most protease 3C-directed cleavages, deduced initially by comparison with poliovirus cleavages, occur between glutamic acid or glutamine and glycine (or serine) dipeptide pairs (Arnold et al., 1987).

It is unknown how the structural precursors and RNA finally form the virion. However, during the last step of viral maturation, VP0 is cleaved into VP2 and VP4, thus completing the final stages of both processing and assembly. The cleavage of VP0 apparently occurs only after the RNA has been packaged (Jacobson et al., 1970). One or two copies of VP0 remain uncleaved in each capsid, the functional significance of this being unclear (Stanway, 1990). The structures of HRV14 (Rossman et al., 1985), poliovirus (Hogle et al., 1985), and Mengo virus (Luo et

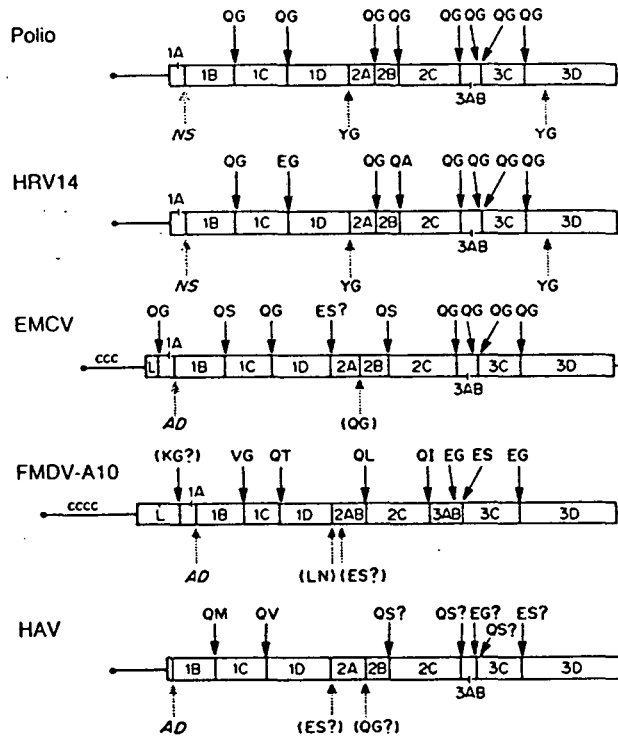


Figure 1.2: Structure of the picornaviral genome for some picornaviruses. Peptide nomenclature is according to standard convention (Rueckert & Wimmer, 1984). The P1 region is composed of 4 peptides [1A(VP4), 1B(VP2), 1C(VP3), 1D(VP1)], the P2 region is composed of 3 peptides (2A, 2B, and 2C), and the P3 region is composed of 4 peptides (3A, 3B, 3C, and 3D). Proteolytic cleavages of the polyproteins occur between amino acid pairs indicated. Cleavages produced by protease 3C are shown above each genome. Protease 2A (hatched arrowhead) and VP0(1AB) (stippled arrowhead) cleavage sites are shown below the genome. Sites for which the proteolytic agent has not been specifically identified are enclosed in paranthesis. Question marks denote sites where the sequence has not been established precisely. (Arnold *et al.*, 1987)

al., 1987), all show the close proximity of a serine residue to the carboxy-end of VP4. This structural proximity as well as the conservation of Ser¹⁰ suggest that the serine acts as a nucleophile for an autocatalytic cleavage of VP0 into VP2 and VP4 (Rossman et al., 1985). By analogy with other proteases, it would be necessary to have a proton-abstracting base to activate the nucleophile for catalysis (Fig. 1.3). However, none of the available virus structures have any suitable base in the vicinity of the cleavage site. It has been suggested, therefore, that an RNA provides the essential base (the amino groups in adenine, guanine and cytosine) and thereby initiates the catalytic step during assembly (Arnold et al., 1987; Rossman et al., 1985). This proposed mechanism is unusual in that the catalysis is produced by a combination of protein and nucleic acid functionalities. Apparently intact VP0 is necessary for correct assembly of the protomers, whereas processing of VP0 is necessary for the final assembly of the virion. Particles which are eluted from cell membranes after "tight binding" or which have been heat treated are missing VP4 and sometimes also VP2. It is possible that the cleavage of VP0 is a prerequisite for uncoating in that it renders VP4 mobile (Arnold et al., 1987).

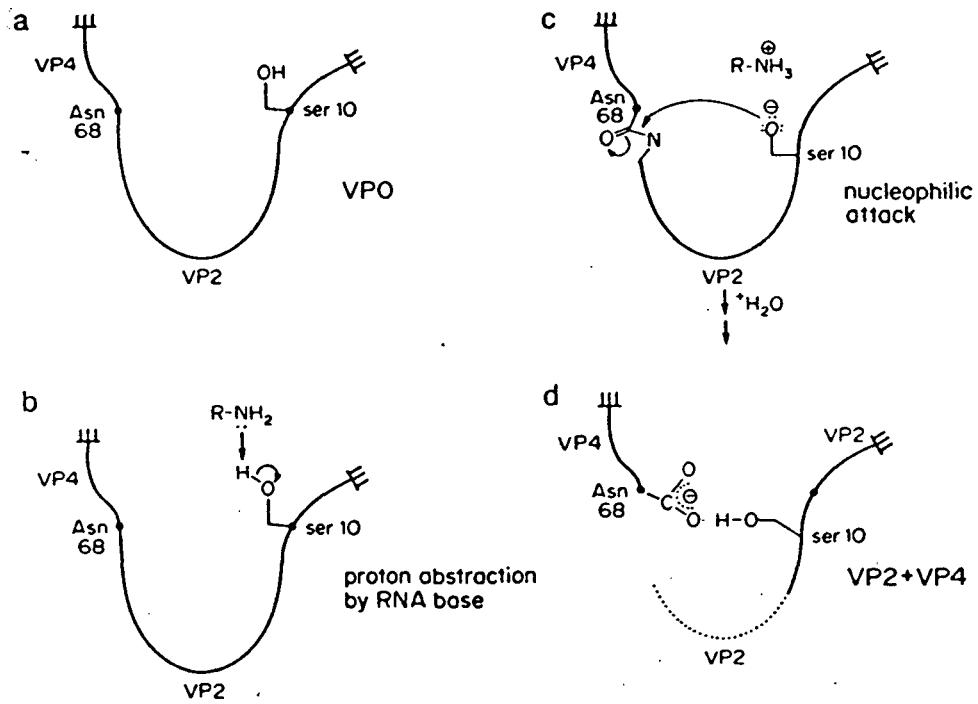


Figure 1.3: Proposed autocatalytic cleavage of VP0. (a) Partial structure of VP0 before cleavage. (b) Abstraction of a proton from HRV14 Ser-10 (Ser-11 in Mengo virus). (c) Nucleophilic attack on the neighbouring peptide bond. (d) Partial structure of cleaved VP2 and VP4 as observed in HRV14. (Arnold et al., 1987)

1.3 THE VIRION

1.3.1 Physical Properties

Poliovirus is one of the most thoroughly characterized viruses and some of its physical properties are listed in Table 1.1. The virion is roughly spherical with no lipid envelope. Its infectivity is, therefore, generally unaffected by shaking virus-containing fluids with organic solvents such as ether or chloroform. Particle diameters reported from electron micrographs range from 24 to 30 nm. The virion contains an RNA core which resides in the central cavity of a thin protein shell.

TABLE 1.1: PHYSICAL PROPERTIES OF THE POLIOVIRION

Shape	Slightly spheroidal
Diameter (hydrated)	About 30.5 nm
Symmetry (X-ray)	5:3:2 (icosahedral)
Capsomers (EM)	Indistinct (32, 42, 60)
$S_{20,w}$	$156 \times 10^{-13} \text{ sec}^{-1}$
$D_{20,w}$	$1.40 \times 10^{-7} \text{ cm}^2\text{sec}^{-1}$
\bar{v}	0.685 ml g^{-1}
Virion mass	8.58 million
%RNA (as K salt)	31.6
% Protein	68.4
Virions/mg	7.07×10^{13}
Virions/OD ₂₆₀ -unit	9.4×10^{12}

(Rueckert, 1986)

1.3.2 The Protomer

All picornaviruses, including poliovirus (Maizel, 1964), cardioviruses (Rueckert et al., 1969), human rhinoviruses (Medappa et al., 1971), and aphthoviruses (Talbot & Brown, 1972), contain four polypeptide chains: VP1, VP2, VP3, and VP4 (Fig. 1.4, right). These chains are elements of identical four-segmented protein subunits called "mature" protomers. The protomer is defined as the smallest identical subunit of an oligomeric protein. Picornaviruses typically display traces of a fifth protein, VP0, which, as mentioned before, is cleaved to form VP4 and VP2 during the viral maturation step (Arnold et al., 1987). This implies that VP0 chains reside in "immature" protomers (VP0,3,1), i.e., subunits that have not undergone maturation cleavage (Rueckert et al., 1969). The number of VP0 chains is rarely, if ever, less than two (Rueckert, 1976). However, the biologic significance of these residual chains is currently unclear. The genome sequences of viruses representing different genera reveal significant differences in the size of homologous viral polypeptides (Table 1.2). VP4, the smallest protein, is easily lost during purification of some picornaviruses and is thus sometimes overlooked.

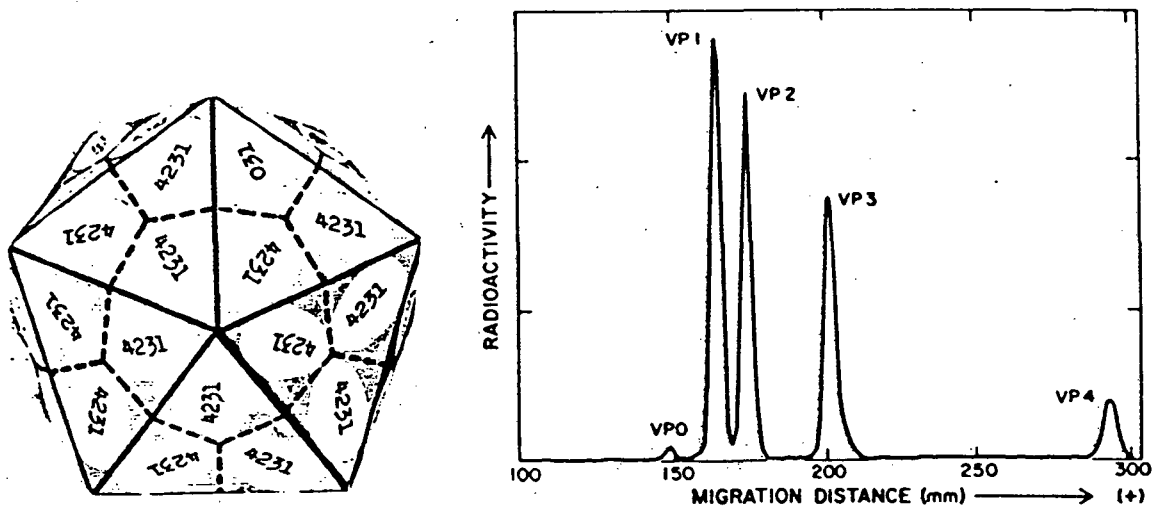


Figure 1.4: Structural organization of the picornaviral capsid. Left: The shell contains 60 subunits called protomers. Of these subunits $60 - n$ are identical "mature" protomers (VP1,2,3,4) and n are "immature" protomers (VP0,1,3). VP0 represents an uncleaved precursor of chains VP2 and VP4. Picornavirions rarely, if ever, contain fewer than two immature subunits. Right: Electrophoretic profile on an SDS-polyacrylamide gel of protein from EMC virions radiolabelled with a mixture of [14 C]amino acids. (Rueckert, 1986)

TABLE 1.2: MASS OF SOME PICORNAVIRAL COAT PROTEINS

Protein	Polio ^a	EMC ^b	FMDV ^c	HRV14 ^d
VP1	33,521	31,703	23,267	32,381
VP2	29,985	29,026	24,669	28,503
VP3	26,410	25,141	24,323	26,195
VP4	7,385	7,247	8,480	7,178
VP1,2,3,4	97,301	93,117	80,648	94,257

(a) Kitamura *et al.*, 1981

(b) Palmenberg *et al.*, 1984

(c) Carroll *et al.*, 1984

(d) Callahan *et al.*, 1985

1.3.3 Dodecahedral Nature of the Protein Shell

Insight into the basic organization of the proteins (Fig. 1.4, left), and into the dodecahedral nature of the picornaviral shell, was first provided by analysis of the acid dissociation products of ME virus (a cardiovirus). In the presence of 0.1 M chloride or bromide ion at pH 6 the virion can be thermally dissociated and yields infectious RNA, VP4, and two kinds of pentamers: a soluble 13.4S pentamer and an insoluble precipitate which has been attributed to a still hypothetical structure, the I-pentamer (Fig. 1.5). In the presence of 2 M urea, which disrupts hydrogen bonds and hydrophobic interactions, the 13.4S pentamers are degraded into 4.7S subunits. From

molecular weight determinations and measurements of chain stoichiometry it was shown that the 4.7S subunit is a monomer composed of one chain each of (VP1,2,3), while the 13.4S subunit is a pentamer of the 4.7S monomer. Thus, the protein shell of EMC virus behaves as an assembly of 12 pentamers held together by one kind of acid-sensitive bonding domain. The pentamers, in turn, are held together by a second type of urea-sensitive domain. As will be seen later, the assembly of the picornaviral shell can be understood as the operation of these domains in reverse order (Dunker & Rueckert, 1971).

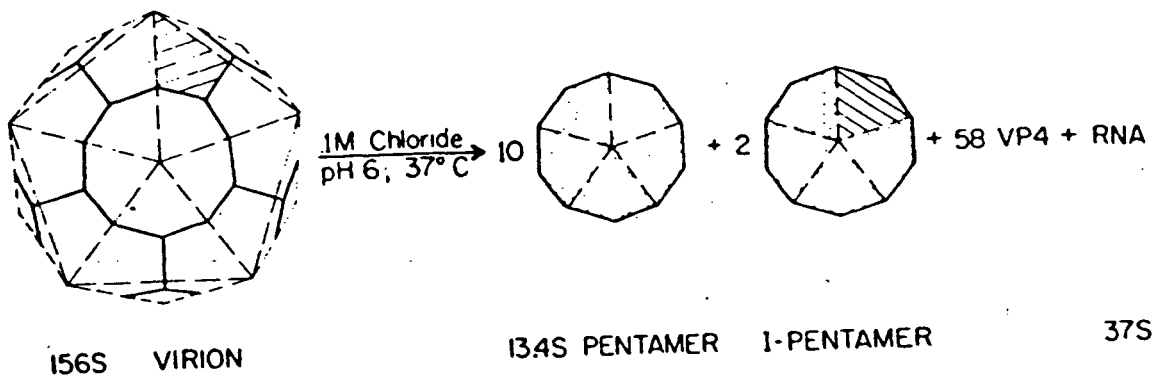


Figure 1.5: Experimental basis for the dodecahedral model of picornaviral capsid structure. (Dunker & Rueckert, 1971)

1.3.4 Buoyant Density of Picornaviruses

The sedimentation coefficients and the buoyant densities of picornaviruses appear to differ among certain groups (Table 1.3). The enteroviruses and cardioviruses band at a density of 1.34 g/ml, whereas the equine rhinoviruses and some of the aphthoviruses band at 1.45 g/ml. The latter density is characteristic of viruses with RNA contents in the order of 30 to 35%. Poliovirus is abnormally light because its cesium-impermeable shell prevents binding of these heavy atoms to the viral RNA (Mapoles et al., 1978). It is necessary to point out that the apparent buoyant density of a virus is influenced by the hydrodynamic properties of the particles in solution which, in turn, are dependent on the degree to which the capsids are permeable to the dissolved solute (e.g. Cs⁺) and the amount of solvation. It has been demonstrated that cesium can be incorporated into poliovirions by growing infected cells in medium enriched in cesium chloride. When artificially substituted with a full complement of 7 500 cesium atoms, poliovirus has an expected buoyant density of 1.45 g/ml (Mapoles et al., 1978). Poliovirus "dense" particles of this density have been observed (Rowlands et al., 1975; Wetz et al., 1983; Yamaguchi-Koll et al., 1975), but are practically noninfectious. The high buoyant density of the aphthoviruses and equine rhinoviruses (Table 1.3) indicates that the RNA is more accessible to cesium ions. The intermediate buoyant density of the human rhinoviruses,

TABLE 1.3: PHYSICAL PROPERTIES OF PICORNAVIRUSES

Group	pH stability	Buoyant density (CsCl)		Sedimentation coefficient
		Virions	Shells	
Enterovirus	Stable 3-9	1.34	1.30	156S
Cardiovirus	Stable 3-9	1.34	1.30	156S
Human rhinovirus	Labile < 6	1.39-1.42	1.29	149S
Aphthovirus	Labile < 7	1.43-1.45	1.30	142-146S
"Equine rhinovirus"	Labile < 6	1.45	1.29	156S

near 1.40 g/ml, is due to incomplete substitution with cesium ion, about 5 000 atoms per virion. The remaining unexchanged sites are occupied by the polyamines spermine and spermidine, which are too large to diffuse out of the semipermeable protein envelope and cannot therefore be exchanged out of the RNA core (Rueckert, 1986).

1.4 OVERVIEW OF THE MULTIPLICATION CYCLE

The initial event in infection is attachment of the virion to specific "receptor units" located in the plasma membrane (Fig. 1.6, top left). These receptors mediate delivery of the viral genome to the cytoplasm. This process is still poorly understood, but involves loss of VP4 and release of viral RNA from the protein shell (Fig. 1.6, step 1). The incoming RNA strand forms polysomes (Fig. 1.6, step 2), using host cell machinery, as it directs the synthesis of a "polyprotein". The latter is proteolytically cleaved during synthesis to form proteins P1, P2, and P3. P1 is the coat protein precursor and P3 cleaves itself autocatalytically (Palmenberg & Rueckert, 1982) into three smaller proteins: a protease required for cleaving the viral proteins; a protein that gives rise to VPg and is probably necessary for initiating RNA synthesis; and an RNA polymerase required for copying the (+)RNA strand to form the complementary minus-strand RNA with poly(U) at its 5' end (Fig. 1.6, step 3).

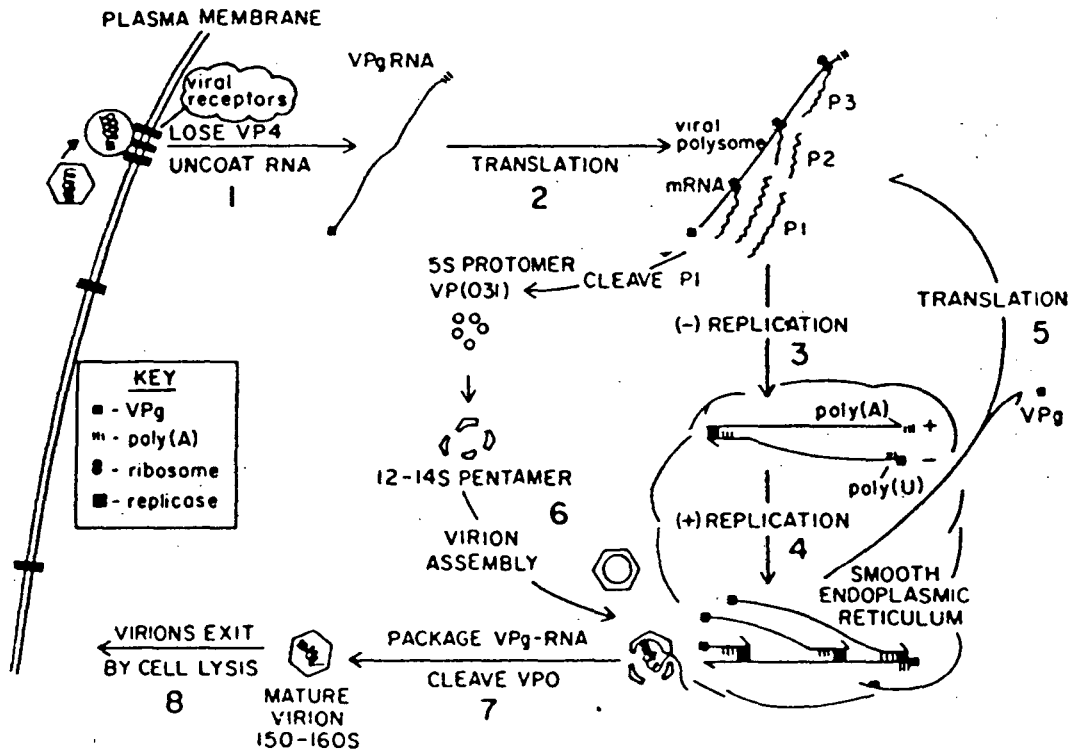


Figure 1.6: Overview of the picornaviral infection cycle. (Rueckert, 1986)

Further synthesis of (+)RNA leads to formation of the multistranded replicative intermediate (RI) with the 3' poly(A) being transcribed from the poly(U) tract in the RI. This RI is associated with smooth endoplasmic reticulum (Fig. 1.6, step 4) and generates a pool of (+)RNA for translation (Fig. 1.6, step 5) and some for synthesis of additional (-)RNA. As the concentration of protein increases, an increasing fraction of the (+)RNA in the replication complex is packaged into virions (Fig. 1.6, step 7). As a preliminary step in shell assembly (Fig. 1.6, step 6), coat precursor protein P1 is cleaved by the virus-coded protease to form a 5S subunit (immature protomer) composed of three tightly aggregated proteins (VP0,1,3). The 5S subunits assemble into pentamers, 12 of which are required to form the 60-subunit protein shell enveloping the RNA genome. Formation of infective 150-160S virions (Fig. 1.6, step 7) is accompanied by a "maturation cleavage" in which most of the VP0 chains are cleaved to form the "mature" four-chain subunits (VP4,2,3,1) characteristic of picornaviruses. Completed virus particles are ultimately released by infection-mediated disintegration of the host cell (Fig. 1.6, step 8). The time required for a complete multiplication cycle, from infection to completion of virus assembly, ranges from 5 to 10 hours. The precise timing depends on variables such as temperature, pH, the virus, the host cell, the nutritional vigour of the cell, and the number of particles that infect the cell (Baltimore et al., 1966). The precise characteristics have to be determined experimentally for

each virus-cell system. This can be done by constructing a single-step growth experiment in which an entire population of cells is infected more or less simultaneously by inoculating cultured cells with enough virus to infect every cell (Fig. 1.7). During the initial stages of the cycle there is a lag period, also called the "latent" or "eclipse" period, in which infectivity is due to residual inoculum virus that fails to be uncoated. This "eclipse" of infectivity reflects particles engaged in the process of infection, i.e., releasing their RNA, synthesizing protein and RNA, but not yet assembling new virions. The lag period typically lasts 2 to 4 hours; it can often be reduced by increasing the multiplicity of infection (Baltimore et al., 1966). The lag period is followed by a "rise" period which consists of an "exponential" phase, when the concentration of infectivity doubles at a constant rate, followed by a declining rate of increase that finally reaches a maximum or "plateau". Timing of virus release depends upon the virus-cell system. The "plateau" is often followed by a "decay" period of declining infectivity, particularly with rhinoviruses and aphthoviruses, in which the RNA genome may fragment spontaneously inside the otherwise intact virion (Denoya et al., 1978; Gauntt & Griffith, 1974).

1.5 ADSORPTION, UNCOATING, AND PENETRATION

Different picornaviruses have different host ranges and this is presumably caused by differential availability of specific receptors on the cell surface which are necessary

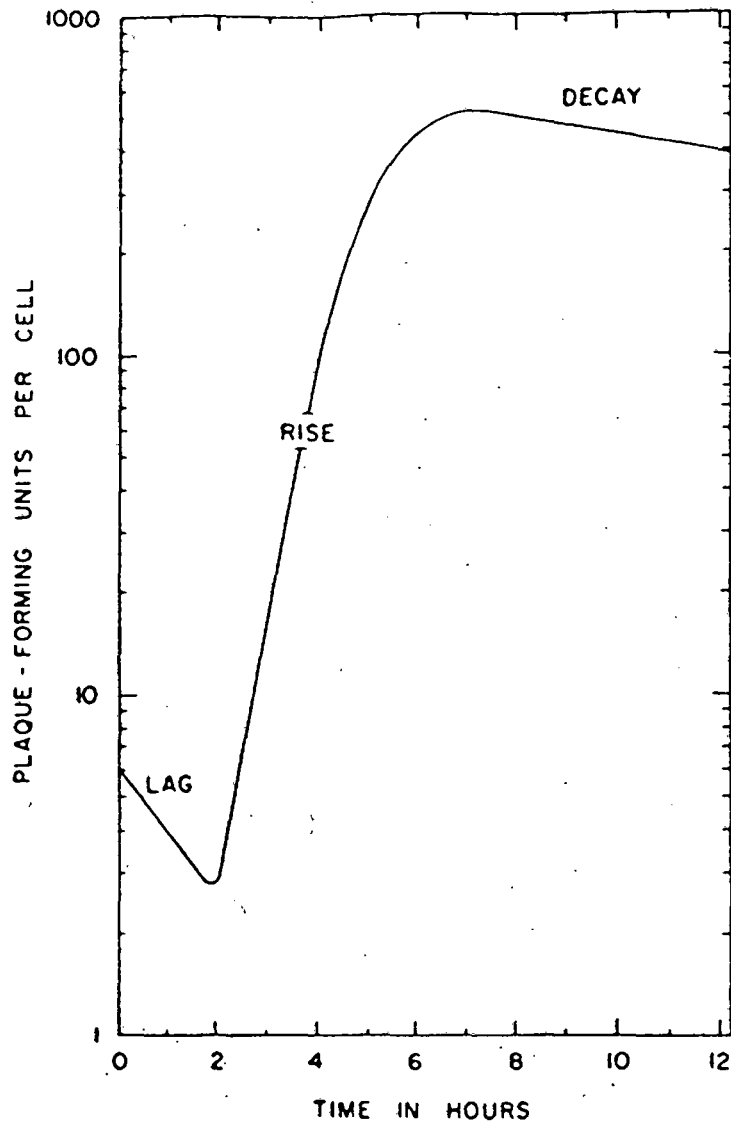


Figure 1.7: One-step growth experiment for human rhinovirus 14 in a HeLa cell suspension culture. (Rueckert, 1986)

for virus attachment. It has also been suggested that ionizable groups on the surface of the virus or cell play an important role in the attachment process. The attachment of group B coxsackieviruses and of echovirus 6, for example, changes markedly with pH, each with a distinct pH profile (Crowell & Landau, 1983); attachment of the polioviruses, on the other hand, is almost independent of pH over the range 4.5 to 8.5. Additional evidence for the attachment process being governed by electrostatic events comes from a study of the effects of ionic composition on virus attachment. Binding of poliovirus, for example, is accelerated by monovalent ions. A number of picornaviruses require the divalent ions Ca^{2+} or Mg^{2+} . These include rhinoviruses (Brown, 1983; Lonberg-Holm & Whitely, 1976), some coxsackieviruses (Cords et al., 1975), and FMDV (Brown et al., 1962). The chelating agent EDTA (ethylene diamine tetra-acetic acid) inhibits attachment of viruses requiring divalent ions (Lonberg-Holm & Korant, 1972). Thus, electrostatic attraction appears to be important in fostering optimum attachment of virus to cell. The exact role of the ions, however, is not clear. Several workers have demonstrated that VP4 plays some role in the adsorption process. Crowell & Philipson (1971) and Lonberg-Holm & Korant (1972) have shown that coxsackievirus and rhinovirus eluted from cells, to which they had briefly been adsorbed, lack polypeptide VP4. The eluted viruses are not capable of reattachment. Some conformational change within the capsid may take place upon adsorption, causing VP4 to be lost. Lonberg-Holm and co-workers have proposed

that the tight binding is caused by gradual envelopment of virus with receptor units whose lateral mobility in the plasma membrane is enhanced by elevated temperature (Fig. 1.8).

1.6 EFFECTS ON THE HOST CELL

Infection by picornaviruses causes dramatic changes in macromolecular metabolism. During the eclipse period, the virus exerts its most significant effect on the metabolism of the host cell. The rate of RNA synthesis declines shortly after infection. This is accompanied by synthesis of a vigorously expanding pool of viral RNA in the cytoplasm. Picornaviruses inhibit cellular protein synthesis soon after infection. In the case of poliovirus-infected HeLa cells, the most intensively studied system, shutoff occurs within the half-hour or so required for attachment, penetration, and uncoating of the RNA genome (Fig. 1.9). Protein synthesis is studied by incorporation of radioactive amino acids into acid-insoluble material, and the declining phase reaches a minimum at about 2 hours. The following wave of incorporation, which peaks at about 3 hours, reflects vigorous synthesis of viral proteins. Finally, there is a decline of viral protein synthesis associated with gross leakage of intracellular components and cell death. Most picornaviruses induce characteristic morphologic changes in the infected cells. Synthesis of cellular ribosomal and messenger RNA begins to decline soon after infection with many picornaviruses, including

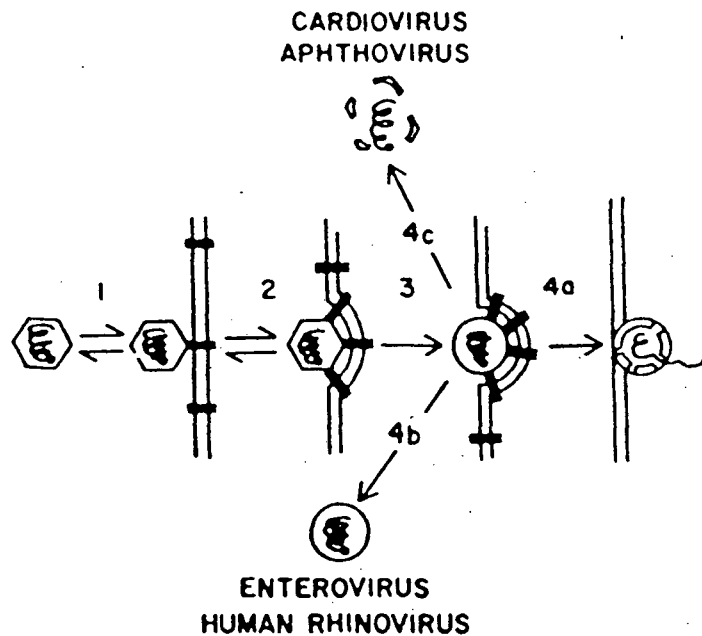


Figure 1.8: Model for attachment of the virions, dismantling of the protective protein shell, and delivery of the RNA to a site where translation can begin. 1: Loose reversible attachment of antireceptor on the virion surface to one of the membrane-associated "receptor" units. 2: Attachment becomes tighter as mobile receptor units are recruited from the membrane surface; the membrane is drawn around the virion to begin the invagination process. 3: Conformational alteration of the protein shell, as indicated by susceptibility of the particle to digestion with proteases, and loss of VP4 to form "A particles". Step 4a: "Entry" of particle into the cytoplasm; this process is accompanied by many abortive events including "elution" or "sloughing" into the medium of A particles in the cases of polio-, coxsackie-, echo-, and human rhinoviruses (Step 4b); or release of free RNA and 12-14S protein subunits in the case of cardio- and aphthoviruses, whose shells are less stable (Step 4c). (After Boulanger & Lonberg-Holm, 1981)

poliovirus, mengovirus, EMC virus, human rhinoviruses, and FMDV. The kinetics of decline appear to vary with the host cell. The inhibition of nuclear RNA synthesis is paralleled by a decline in the ability of isolated nuclei or crude DNA-protein complexes from infected cells to make RNA. Measurements on alpha-amanitin-sensitive transcription indicate that polymerase II is most strongly affected; polymerase I and III are also slightly inhibited. However, when freed from their nucleoprotein complexes, all three polymerases are active. Previous studies suggested that the target is an unidentified factor required by polymerase II (Crawford et al., 1981). Inhibitors of protein synthesis block this inhibition, suggesting that shutoff of cellular RNA synthesis is mediated by a viral protein, but the responsible protein has not yet been identified. The poliovirus-induced decline in host protein synthesis (Penman & Summers, 1965) is accompanied by dissociation of ribosomes from host messenger RNA. This dissociation of polysomes is not caused by degradation of host mRNA molecules, because when extracted from infected cells they remain fully able to direct protein synthesis in a cell-free translation system (Kaufmann et al., 1976). One of the most interesting questions about host protein shutoff has been the mechanism by which virus inhibits host protein synthesis without at the same time blocking synthesis of viral proteins. The key to this question appears to be in the discovery that poliovirus RNA, unlike cellular mRNA, is not capped at its 5' end. It terminates in pUp instead of the 7 methyl G "cap", found on almost all

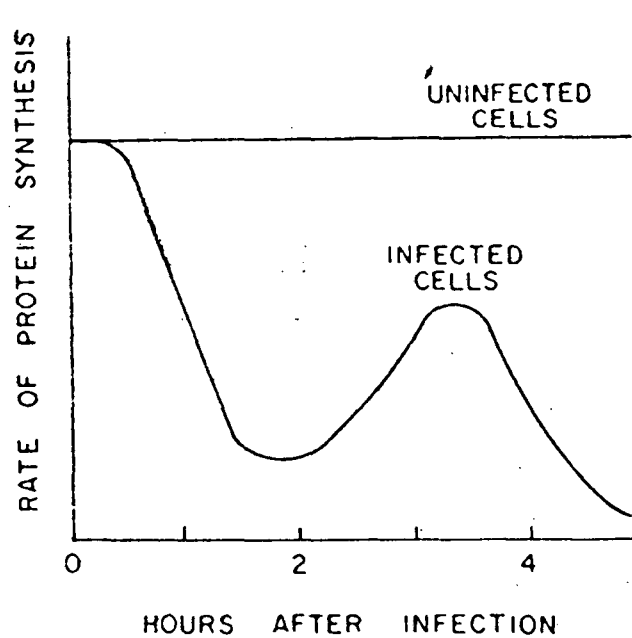


Figure 1.9: Synthesis of protein in poliovirus-infected HeLa cells infected at high multiplicity. The rate of decline and the magnitude and timing of the new wave of protein synthesis vary significantly with virus, multiplicity of infection, and identity of the host cell. Use of the drug actinomycin D, which blocks synthesis of cellular RNA but not of picornaviral RNA, hastens shutoff of host cell protein synthesis. (Rueckert, 1986)

other mRNAs (Fernandez-Munoz & Darnell, 1976; Hewlett et al., 1976; Nomoto et al., 1976). This discovery intensified the search for mechanisms that might inactivate cap-binding factors essential for initiating translation of host mRNAs but indispensable for translation of poliovirus RNA. Previous studies indicated that the inhibition is caused by a virus-induced inactivation of a cellular structure, the "cap-binding complex" (CBC), required for attachment of "capped" mRNAs to ribosomes (Etchison et al., 1984). The CBC contains three proteins: p220, p49, and p24/28. Protein p220 is cleaved early after infection; moreover, this cleavage is inhibited by the same compounds (N-ethylmaleimide, iodacetamide, and zinc ions) that inhibit processing of polioviral proteins, suggesting that p220 is cleaved by the virus-coded protease. A similar mechanism appears to operate in HeLa cells infected with human rhinovirus 14 but not when infected with cardioviruses. However, inhibition of protein synthesis in murine L cells with EMC or mengovirus appears to result from a different mechanism, i.e., competition between viral and host cell mRNAs (Jen & Thach, 1982). In this case it appears that as viral mRNA accumulates it outcompetes cellular mRNA for one or more of the factors involved in initiating protein synthesis. The kinetics of inhibition also vary with cell type. This suggests that inhibition of host protein synthesis is an accidental feature of the picornaviral life cycle, one that lends the virus a competitive advantage in certain biological situations but is not essential for productive infection. The mechanism of

cellular protein shutoff has variously been attributed to accumulation of double-stranded RNA,, toxic effects of viral coat protein, increase in cytoplasmic sodium and decrease in cytoplasmic potassium concentration associated with changes in the plasma membrane, inactivation of factors required for initiation of protein synthesis, and ability of viral RNA to outcompete host mRNA for critical components of the protein synthetic machinery (Ehrenfeld, 1982). The mechanism of host protein shutoff has been one of the most controversial in the picornavirus literature.

1.7 SYNTHESIS OF VIRAL RNA AND PROTEIN

The initial events in the picornaviral multiplication cycle are not readily observable, since, the fraction of virus particles that succeed in establishing a productive infection is small (usually less than 1% of the input virus), and the minute amount of viral material synthesized is masked by vigorous macromolecular metabolism of the host cells. It is assumed that the first task of the virus is to translate its genome and thereby supply the proteins necessary for replication of its RNA since infected cells do not contain all the components necessary for viral replication. Most of the experimental evidence supports the hypothesis that the viral proteins are synthesized by translating a single large coding region on the genome. The protein products are then produced by cleavage of the nascent polyprotein (see Fig. 1.1).

1.7.1 RNA synthesis

In addition to serving as a template for the translation of protein, an infecting RNA molecule functions as a template for RNA replication. Intracellular synthesis of the polyprotein takes about 10 to 15 minutes (Butterworth & Rueckert, 1972; Taber et al., 1971). This probably represents the minimum time between uncoating and the moment when synthesis of viral RNA can begin. Synthesis is carried out by protein 3D^{pol}. This protein is found tightly associated with its RNA template (Flanegan & Baltimore, 1977; Lundquist et al., 1974) and with cellular membranes (Caliguiri & Tamm, 1970) in the cytoplasm of infected cells. Studies on cell-free synthesis of (-) strands from the (+) template indicate that at least three proteins are required: virus protein 3C^{pol}, a VPg donor, and a host factor (HF) protein of molecular weight 67 000. The VPg donor is thought to donate a "primer", such as VPg-pUpU, from which the nascent (-) strand is elongated by protein 3D^{pol} (Crawford & Baltimore, 1983; Das Gupta et al., 1980; Flanegan & Baltimore, 1979; Nomoto et al., 1977; Van Dyke & Flanegan, 1980). Not much is known of the requirements for the synthesis of (+) strands from (-) templates, nor is it known if the enzyme required for synthesis of (+) strands is identical to that which makes (-) strands. Replication takes place via a structure known as the replication intermediate (RI) which consists of a full-length template strand with about 6 to 8 nascent daughter strands. The RI is probably predominantly

single-stranded (Richards et al., 1984), with short stretches of base-pairing in the vicinity of the polymerase molecule (Fig. 1.6, step 4). Double-stranded RNA molecules called replicative form (RF) are also found in infected cells (Fig. 1.10); the role of the RF in replication is not clear. Replicating forms of picornaviral RNA and newly made virions are associated with smooth membranes (Butterworth et al., 1976; Caliguiri & Tamm, 1970; Lazarus & Barzilai, 1974) that proliferate as viral RNA multiplies (Bienz et al., 1980). The proliferation and vacuolization are blocked by guanidine, which inhibits multiplication of viral RNA (Tamm & Eggers, 1963).

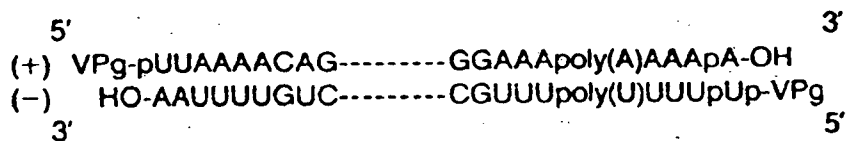


Figure 1.10: Replicative form (RF) of poliovirus RNA illustrating end structure of the complementary (+) and (-) strands. -pApA residues at or near the 3' terminus of each strand provide a potential recognition site for a UpUp-VPg primer. (Rueckert, 1986)

Once initiated, polioviral RNA synthesis proceeds exponentially. The rate of synthesis doubles every 15 minutes during this early stage until about 10% of the final yield is produced. At this point the rate of synthesis becomes constant, accumulating linearly for an additional hour until the number of RNA molecules reaches about 4×10^5 per cell. About 5-10% of the total RNA in infected cells consists of minus strands (Baltimore & Girard, 1966), however, the mechanism controlling this differential synthesis of plus and minus strands is not clear. A significant amount of the RNA synthesized during the exponential phase is destined to become mRNA (Baltimore et al., 1966), while about 50% of that made during the linear phase is packaged into virions. The switch from exponential to linear synthetic rate may reflect siphoning of the RNA pool into virions (Rueckert, 1986).

1.7.2 Role of VPg in Regulating the Infection Cycle

According to Rueckert (1986), it is possible that VPg also plays a role in the switchover from exponential to linear RNA synthesis. Although VPg-containing poliovirus RNA can act as mRNA in vitro (Golini et al., 1980) and are sometimes found in polysomes late in replication (Sangar, 1979), most (+) strands found in polysomes end in 5'-pUU-3' and have had the VPg removed, presumably by a host enzyme found in uninfected cells. Since this mRNA, lacking VPg, is as infective as genomic RNA, it is clear that VPg is not essential for infectivity (Flanegan et al., 1977). Despite

the in vitro findings, it seems likely that removal of VPg plays an important regulatory role within the intact cell by favouring flow of viral mRNA to ribosomes, which then associate with membrane to form patches of rough endoplasmic reticulum, a site of viral protein synthesis (Roumiantzeff et al., 1971).

1.7.3 Synthesis and Cleavage of the Polyprotein

As shown in Fig. 1.9, the virus-induced decline in cellular protein synthesis is followed by a wave due to vigorous synthesis of viral proteins. This was demonstrated by adding radioactive amino acids to infected cells and analyzing the radioactive products by electrophoresis on SDS-polyacrylamide gels. In this way Summers et al., (1965) discovered a complex spectrum of proteins like that shown in Fig. 1.11 and thereby set the stage for unraveling the synthesis and cleavage of the virus-encoded proteins. Earlier recognition that all of the proteins were derived from a single large polyprotein made the task of mapping these proteins on the picornaviral genome much simpler. This made it possible to order the genes by analyzing the specific activity of viral proteins synthesized in the presence of the drug pactamycin (Butterworth & Rueckert, 1972; Summers & Maizel, 1971; Taber et al., 1971). The drug inhibits initiation of new protein chains while allowing nascent proteins on the viral polysome to be completed. Thus, when a radioactive amino acid is added to infected cells with pactamycin-blocked polysomes, proteins encoded

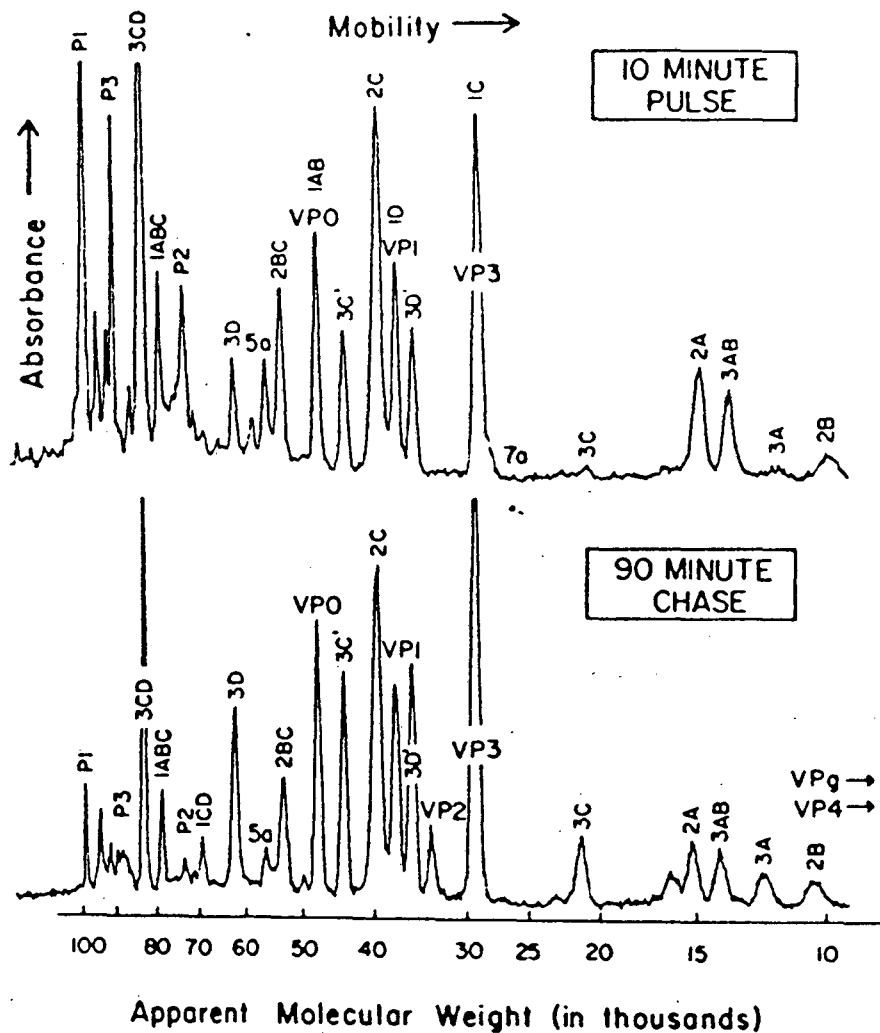


Figure 1.11: Spectrum of proteins synthesized in poliovirus-infected HeLa cells at 3.5 hours after infection. Cells were dissolved with SDS and proteins in the lysate were separated by PAGE. Top: After exposing the cells to radioactive [35 S]methionine for a 10-minute incorporation. Bottom: As above, except cells were further incubated for 90 minutes in medium lacking radiolabel to allow additional time for cleavage. (Pallansch *et al.*, 1984; Rueckert *et al.*, 1979)

TABLE 1.4: KEY TO NOMENCLATURE OF PICORNAVIRAL PROTEINS

L434 name	Polio		FMDV		HRV-2	EMC
L			p16	p16/20		p12/14
L-1-2A						pre-A
1-2A						A
1 or P1	1a	P1-1a	p91	p88	1A	B
2 or P2	3b	P2-3b			58	
2BC	5b	p2-5b			X(43)	
2A	8	p2-8	p14	p20c		G
2B	10	p2-10				I
2C	X	P2-X	p41	p34	38	F
2AB	7a	P2-71				
3 or P3	1b	P3-1b	p102	p100	1B	C
3AB	9	P3-9	p19	p14		H
3C	7c	P3-7c	p118	p20b	7c	p22
3D	4	P3-4b	p16	p56a		E
3D	2	P3-2	p18	p72	2	D
1A	VP4	VP4	VP4	VP4	VP4	alpha
1B	VP2	VP2	VP2	VP2	VP2	beta
1C	VP3	VP3	VP3	VP3	VP3	gamma
1D	VP1	VP1	VP1	VP1	VP1	delta
1AB	VP0	VP0	VP0	VP0	VP0	epsilon

at the 5' end of the polysomal mRNA incorporate less radiolabel than those at the 3' end as synthesis is completed. The order of the completed proteins is then deduced from the gradient of specific activity, which increases in the direction of translation, 5'-3'. Precursor-product relationships were established by relating the patterns of proteins fragmented with trypsin or cyanogen bromide and by analyzing the flow of radioactivity through proteins (Butterworth & Rueckert, 1972). Radiochemical sequencing of polioviral proteins, which became feasible once the genome sequence was known, confirmed the map constructed from earlier studies. In addition, they identified the precise location of the cleavage sites and showed that the termini of the products are not further trimmed (Kitamura et al., 1981; Pallansch et al., 1984). A key to the old nomenclature of some of the most intensively studied picornaviruses is provided in Table 1.4.

1.8 MORPHOGENESIS

Picornaviral morphogenesis can be described (Fig. 1.12) as a three- or four-stage process in which monomers are converted to a pentamer (step 1). Pentamers are then assembled into a provirion consisting of the RNA genome within a 12-plated capsid (step 2). It is not clear whether the RNA is inserted during (step 2a) or after completion of the capsid (step 2d). In the final step mature virus is formed (step 3); this step involves cleavage of most, if

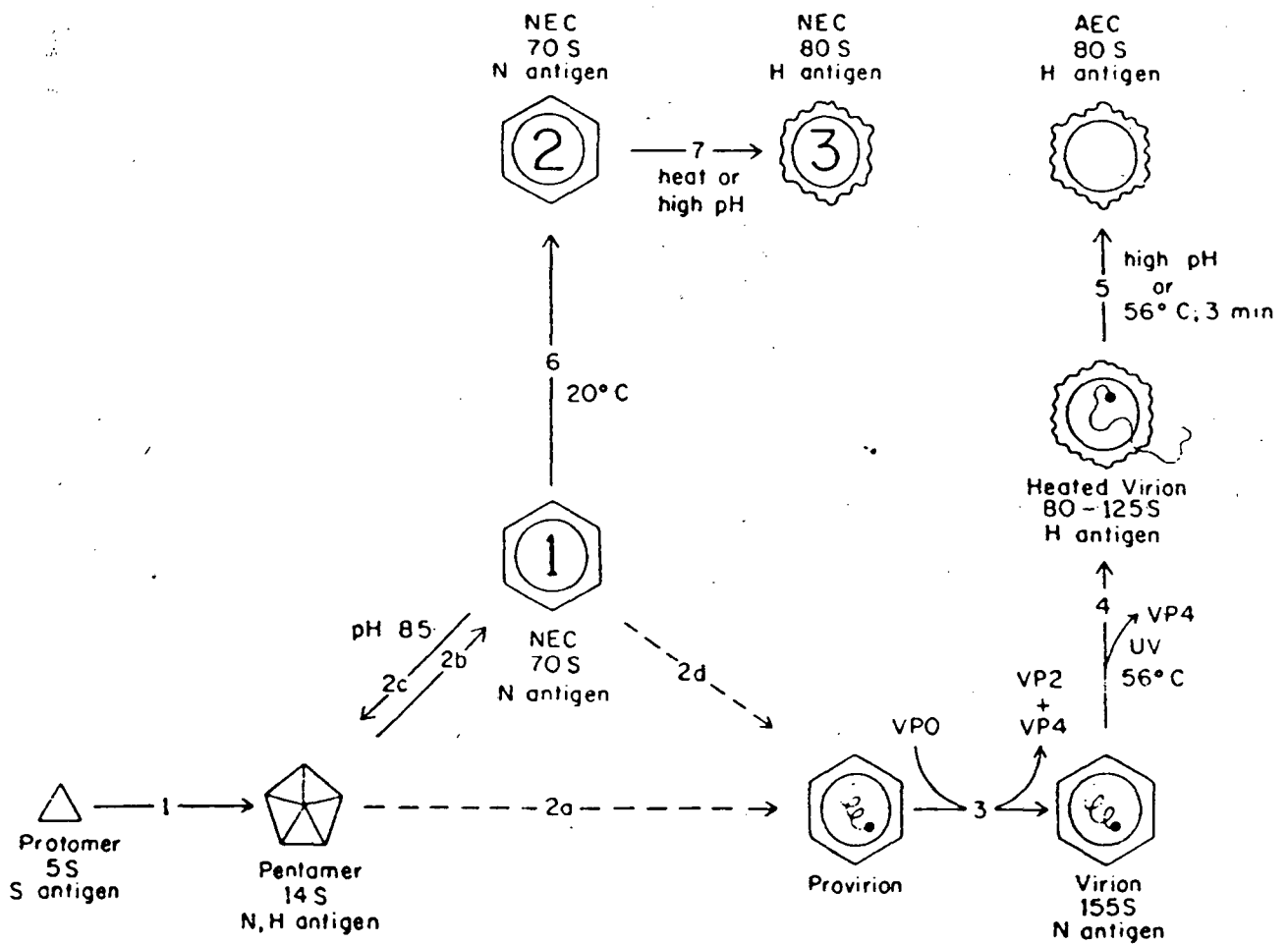


Figure 1.12: Picornaviral morphogenesis. (Rueckert, 1986)

not all, of the VP0 chains in the 60-subunit capsid. There has been experimental evidence for the existence of configurational changes during assembly from crude serologic studies, however the structural basis for these changes is only now beginning to be probed with monoclonal antibodies (Rombaut et al., 1984). Picornaviruses are attractive models for studying the mechanism of viral assembly because the 60-subunit shell is relatively simple, involving assembly of only 12 units of coat protein (Rueckert et al., 1969), yet, experimental progress in this field has proven tortuous and slow (Putnak & Phillips, 1981).

Using rate-zonal centrifugation, Mayer et al. (1957) separated partially purified preparations of poliovirus into four bands designated A, B, C, and D. A and B were impurities. The fastest sedimenting band, D, contained infective virions, while band C contained virion-sized particles subsequently identified as RNA-free shells, now called natural empty capsids (NEC). Since these empty capsids sediment half as fast as virions, and have a lighter buoyant density, they are often referred to as natural top component (NTC).

When infective poliovirions (called N antigen) are heated in neutral saline for 2 to 3 minutes at 56°C, RNA is released and the protein shell is simultaneously converted to a new antigenicity, called H antigen, for "heated" (Fig. 1.12, step 4). There is little or no immune cross-reaction

between the H and N components, thus, antiserum raised against H antigen does not neutralize the infectivity of native virions, nor does it even bind to them. Heated particles are also no longer able to attach to cells. In other words, when native virions are heated they lose all of their characteristic surface features. Empty shells produced by heating virions also lack VP4 (Maizel et al., 1967) and are called artificial empty capsids (AEC) or artificial top component (ATC). The conversion from N to H antigenicity can also be brought about by other means, such as UV radiation, high pH, mercurials, phenol, and dessication. Loss of RNA is not required for this conversion, therefore, the virion can also be converted to H antigenicity without loss of its encapsulated RNA by shorter heating at 56°C or by treatment with UV light (Katagiri et al., 1967). Finally, this conversion from N to H antigenicity is irreversible and occurs by a process called concerted transition; i.e., particles are either N antigenic or H antigenic.

Another antigen, S antigen, is produced by immunization with a 2S protein produced by degrading poliovirus with 6 M guanidine hydrochloride. This antibody reacts with a 5S antigen in extracts from infected cells (Scharff et al., 1964) and also with nascent viral protein associated with polysomes (Scharff & Levintow, 1963).

In addition to 5S subunits and NEC, a 14S particle (Phillips, 1969) is present in extracts from

poliovirus-infected cells. A study of the polypeptide composition of these particles showed that the NEC, the 14S, and probably also the 5S component contained roughly similar amounts of VP0, 1, and 3 but lacked VP2 and VP4, which are found in the mature virion. It was also showed that extracts from infected cells had the ability to promote assembly of the 14S particles into NEC; this was shown to be virus specific due to the lack of activity in extracts from uninfected cells.

Phillips (1981) and co-workers showed that there are two kinds of assembly: self-assembly and extract-mediated assembly. Self-assembly requires high concentrations of 14S particles and produces H antigenic shells. Extract-mediated assembly occurs at lower 14S concentrations and produces N antigenic shells. The assembly-catalyzing activity, which is sensitive to trypsin but not to ribonuclease, was traced to rough membranes carrying 14S, NEC, and an unidentified 110S structure that could be released by solubilizing the membrane with deoxycholate (Perlin & Phillips, 1973). Extracts of cells infected with defective interfering (DI) particles, a form of poliovirus whose only known defect is a deletion in its coat protein, lacked assembly-promoting activity (Phillips et al., 1980). This suggests that the morphopoietic factor associated with rough endoplasmic reticulum is a form of membrane-bound coat protein.

Other experiments suggest that morphogenesis takes place in association with the viral replication complexes that are

found on smooth membranes. The crucial evidence is that virus particles associated with fractionated complexes from cells labelled for a short time with radioactive uridine reportedly exhibit a specific activity some 3- to 8-fold higher than virions in other fractions (Caliguiri & Mosser, 1971). This higher specific activity suggests that these virions are the ones most recently made and are therefore formed on the replicating complex. Empty shells can be recovered in a stable condition by treating these membrane-associated replication complexes with ribonuclease (Yin, 1977).

Studies on the effect of the drug guanidine provided additional evidence for a link between RNA synthesis and virion formation. Guanidine specifically blocks assembly of virions at concentrations (1-3 mM) that have no known effects on the macromolecular synthesis of the host cell (Tamm & Eggers, 1963). Recent evidence suggests that the drug acts at the initiation step of RNA synthesis. When it is added midway through the infection cycle, movement of newly made RNA from the replication complex into virions ceases abruptly, and this is accompanied by accumulation of empty shells, a halt in cleavage of VP0, and a block in the flow of radioactive protein into virions. When the drug is removed, RNA synthesis resumes, label in empty shells flows rapidly and completely into virions, and VP0 is cleaved in parallel (Jacobson et al., 1970). From this it was established that the difference in polypeptide composition of the capsid and the capsid precursors is due to cleavage

of VP0 to VP2 + VP4 during the final stage of morphogenesis when virions acquire infectivity. This theory of a final maturation cleavage of VP0 was supported by identification of an RNA-containing particle called a provirion, originally reported to sediment at 120S (Fernandez-Tomas & Baltimore, 1973) but later reported to cosediment with mature 155S virions (Guttman & Baltimore, 1977). The particle is richer in VP0 than virions are and, unlike virions, is dissociable with SDS, 3 M CsCl, or 20 mM EDTA, a chelator of divalent cations such as Ca^{2+} and Mg^{2+} .

One of the most controversial aspects of picornavirus assembly is the mechanism by which the RNA becomes packaged into virions. Jacobson and Baltimore proposed the procapsid hypothesis, in which the final step in morphogenesis is association of the RNA with the preformed shell. They suggested two possible mechanisms by which this might happen: (a) RNA is somehow inserted into the empty shell (insertion model), or (b) the RNA wraps around the procapsid, fitting into appropriate channels and thereby triggering changes in the structure of the shell that internalize the RNA and precipitate maturation cleavage (transfiguration model).

1.9 PICORNAVIRAL STRUCTURE

The structures of the protein shell of a number of icosahedral RNA plant and animal viruses are now known at atomic resolution. These structures have provided

information of viral assembly, disassembly, the antigenic surface on viruses available to neutralizing antibodies, the host cell receptor attachment site, fusion of viral proteins with the host cell, processing of polyproteins during maturation and the manner in which antiviral agents can interfere with the function of a viral capsid.

Picornaviruses are small, spherical RNA viruses which can frequently form single crystals. There has been a rapid expansion of information on the three dimensional, atomic resolution structures of such viruses. Plant viruses were the first to be investigated by crystallography, as they were readily available in large quantities. However, with the experience gained in the analysis of plant viruses, it has been possible to study animal viruses where only small quantities were available (Rossmann & Rueckert, 1987).

1.9.1 Functions of the Protomer

Coat protein serves four important functions. (a) It protects the RNA genome from nucleases in the environment. (b) It recognizes specific cell-coded receptor sites in the plasma membrane and may therefore be an important determinant of host range and tissue tropism (disease pathology). (c) The protomer carries directions for selecting and packaging the viral genome and possibly also a protease involved in maturation of the virion (see Morphogenesis). (d) Finally, the capsid is an effective machine for penetrating the plasma membrane and delivering

the RNA genome into the cytoplasm of susceptible host cells.

1.9.2 Location of the Four Segments

With general acceptance of the 60-protomer model of capsid structure, attention has now focused upon the structural organization and functions of the four chains within the picornaviral subunit. The first three picornaviruses to be described in atomic detail were human rhinovirus 14 (HRV14) (Rossmann et al., 1985), poliovirus (Hogle et al., 1985), and Mengo virus (Luo et al., 1987). Not only were these three viruses (Rossmann et al., 1987) strikingly similar, but the tertiary structure of each of the three larger viral proteins, VP1, VP2 and VP3, were similar to each other and similar to those found for the plant viruses. The three-dimensional structure of foot-and-mouth disease virus (FMDV) (Acharya et al., 1989) has also been determined. The virus shows similarities with the other picornaviruses but also several unique features. In all four of these viruses the three larger structural viral proteins (VP1, VP2 and VP3) form the exterior of the viral capsid, while VP4 is at the interface between the capsid and the RNA. Among the great surprises and exciting discoveries in the structures of the small icosahedral RNA plant and animal viruses, are the folding patterns of their proteins and the similarity of organization of these proteins in the shell. These viruses are composed of 60 T.n protein subunits, where n is the number of different

proteins in the capsid and T is the 'triangulation' number. In the picornaviruses, VP1, VP2 and VP3 are each folded into an eight-stranded antiparallel β -barrel and are organized in the capsid with a pseudo T = 3 surface lattice.

1.9.3 Structure of Poliovirus

The quality of the electron density map obtained by Hogle et al., (1985) was such that it was possible to locate and identify almost all of the residues in all four capsid protein subunits. However, no electron density was present for residues 1 to 20 at the NH₂-terminus of VP1, residues 1 to 7 at the NH₂-terminus of VP2, residues 1 to 12 at the NH₂-terminus of VP4 (all of which are in the interior of the particle) and residues 234 to 238 at the COOH-terminus of VP3 (on the outside surface of the virion). There was also no significant density that could correspond to the viral RNA or to VPg. This lack of density for the NH₂-terminal residues and the RNA implies that the interior of the virion is spatially disordered with respect to the icosahedrally symmetric protein shell.

The structures of VP1, VP2 and VP3 (Fig. 1.13) are remarkably similar to one another. Each of these proteins consists of a "core" with variable elaborations. The cores are topologically identical and each core is composed of an 8-stranded antiparallel β -barrel with two flanking helices. Four strands (B, I, D, and G in Fig. 1.13a) make up a large

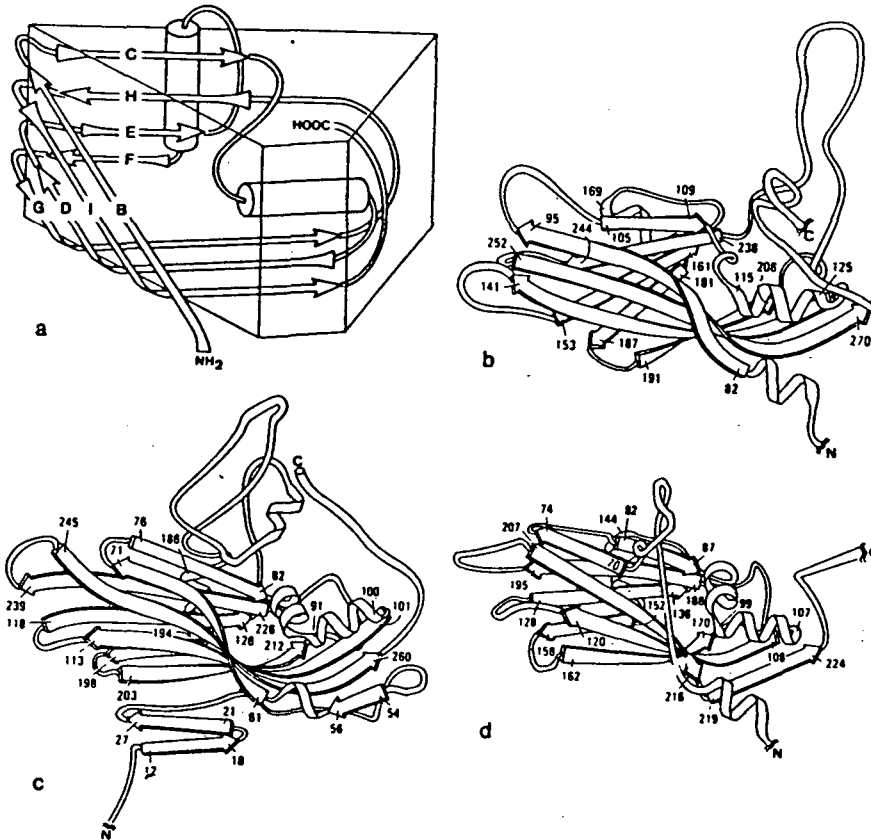


Figure 1.13: Schematic representation of the poliovirus capsid proteins. (a) Diagram showing the topology of the conserved "core". Beta strand designations are consistent with those used to describe the capsid proteins of the plant viruses. Ribbon diagrams show (b) VP1, (c) VP2, and (d) VP3. (Hogle et al., 1985)

twisted β sheet which forms the front and bottom surfaces of the barrels (Fig. 1.13 b to d). The remaining four strands (C, H, E, and F) make up a small, flat β sheet which forms the back surface of the barrel. The strands comprising the front and back surfaces are joined at one end by four short loops, giving the barrel the shape of a triangular wedge. In poliovirus, each of the three coat proteins has different NH_2 - and COOH -terminal extensions, and includes a different set of internal insertions. The largest internal insertion in VP1 is the loop connecting β strands G and H. The largest insertion in VP2 connects β strand E with the radial helix on the back surface of the barrel. The insertion in VP3 connects the NH_2 -terminal strand to β strand B. The NH_2 -terminal strands of all three proteins fold beneath the barrels, while the internal insertions and COOH -terminal additions are located on the top surface of the barrel.

VP4 has a more extended conformation, in contrast to the compact structures of the other three coat proteins. The only significant compact structure in VP4 is a short two-stranded antiparallel sheet near its NH_2 -terminus. VP4 is similar in its position and conformation to the NH_2 -terminal strands of VP1 and VP3, and thus it appears to function as the NH_2 -terminal extension of VP2 rather than as an independent capsid protein.

1.9.4 Atomic Resolution Structure of Human Rhinovirus 14 (HRV14)

It was shown by Rossmann *et al.*, (1985) that rhinovirus and poliovirus capsids were very similar. The structures of these capsid proteins of HRV14 are shown in Fig. 1.14. Large sequence insertions form protrusions on VP1, VP2, and VP3 and create a deep cleft or "canyon" on the HRV14 viral surface. The canyon separates the major part of five VP1 subunits (in the "north") clustered about a pentamer axis from the surrounding VP2 and VP3 subunits (in the "south"), thus forming a moat around the VP1 protrusions on the fivefold axis. The south canyon walls are lined with the carboxy-terminal ends of VP1 and a large sequence insertion in VP1 corresponding to helices β D and β E in the equivalent SBMV capsid protein. The north canyon wall is partially lined with the carboxy terminus of VP3. VP2 is hardly associated at all with the canyon, whereas VP1 is the major contributor to the residues lining the canyon. The canyon is 25 Å deep and 12-30 Å wide.

VP1 has additional elaborations on the surface relative to VP2 and VP3 and because of this, its overall shape is that of a kidney, with the depression forming a large part of the canyon. The small insertion between β B and β C in rhinovirus and poliovirus is not found in FMDV. This loop forms a major immunogen, NIm-IA, in HRV14 and poliovirus. The names NIm-IA and NIm-III are used to identify them as

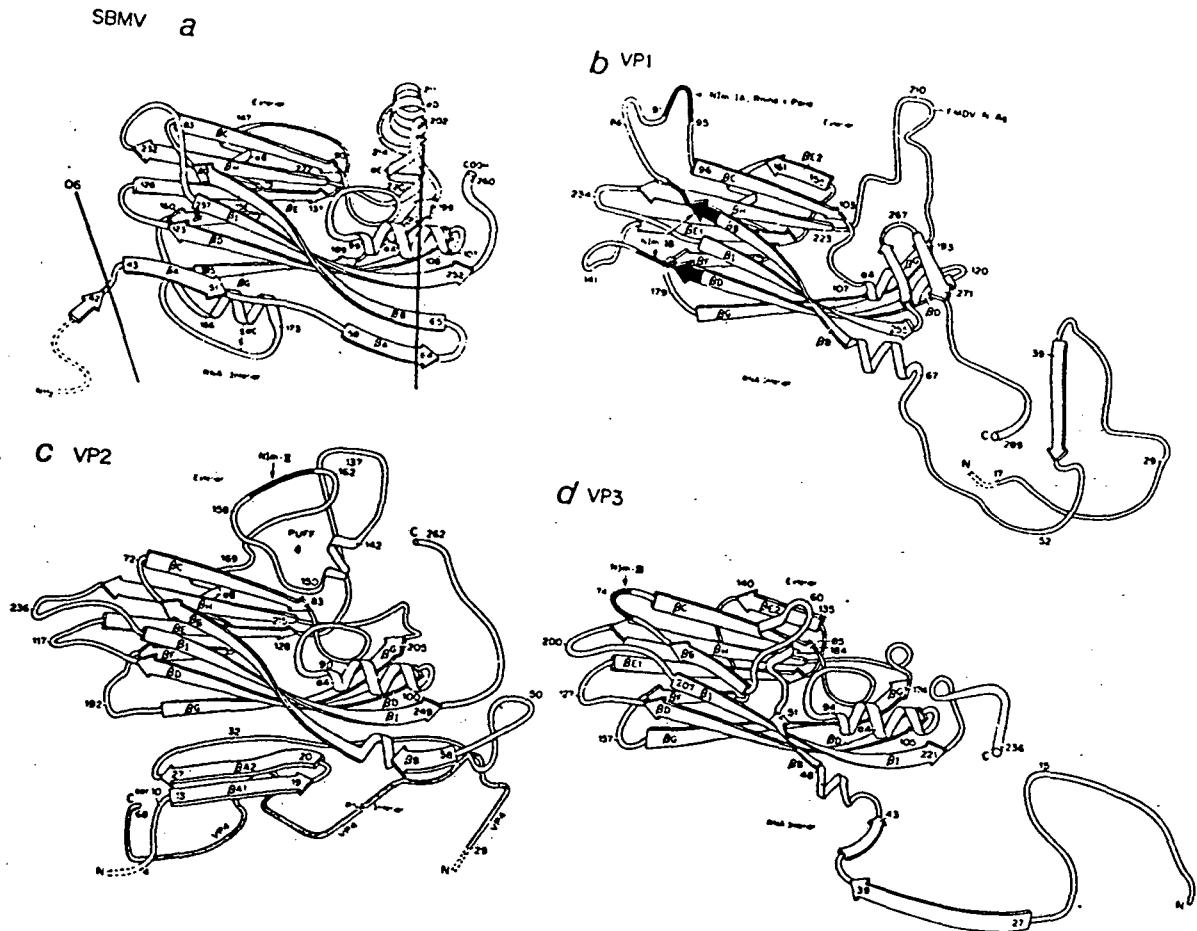


Figure 1.14: Diagrammatic drawings showing the polypeptide fold of SBMV and of each of the three larger capsid proteins of HRV14. The nomenclature of the secondary structural elements is derived from that of SBMV. Amino-acid sequence numbers, appropriate for each protein, are also shown. (a) SBMV, (b) VP1 of HRV14, (c) VP2 and VP4 of HRV14, (d) VP3 of HRV14. (Rossmann *et al.*, 1985)

neutralizing immunogens and to indicate their major coat protein locations on VP1 and VP3 respectively. The residues in VP1 of HRV14 that are analogous to α D and α E helices in SBMV protrude to the surface and form part of the canyon, but do not form helices in HRV14. The external portion of this segment contains the major antigenic site of FMDV.

There is a large 43-residue insertion in the VP2 position, corresponding to β E2 of VP1 and VP3 and forming an external mushroom-shaped "puff". This is positioned next to the VP1 elaborations, associated with the major antigenic site in FMDV. The most external residues of this puff correspond to NIm-II of HRV14. In contrast to VP1 and VP3, the carboxy-terminus of VP2 has no extension beyond the shell domain. All residues of VP3 can be seen in the electron-density map. The 26 amino-terminal residues form a fivefold β -cylinder about the pentamer axis (Fig. 1.15). This fivefold cylinder extends down into the RNA to a radius of 111 Å. The polypeptide emerges from the β -cylinder and circles around the base of the VP1 shell domain, probably making extensive contact with the RNA in the central cavity. It then emerges on the viral surface near residue 61 and enters the shell domain at residue 72. The top corner of the VP3 shell domain, between β B and β C, is the NIm-III site of HRV14, structurally equivalent to NIm-IA in VP1.

The capsid protein VP0 (the precursor to VP2 and VP4) is cleaved into its components only in the final stages of assembly. Since in HRV14 the cleavage occurs at an Asn-Ser

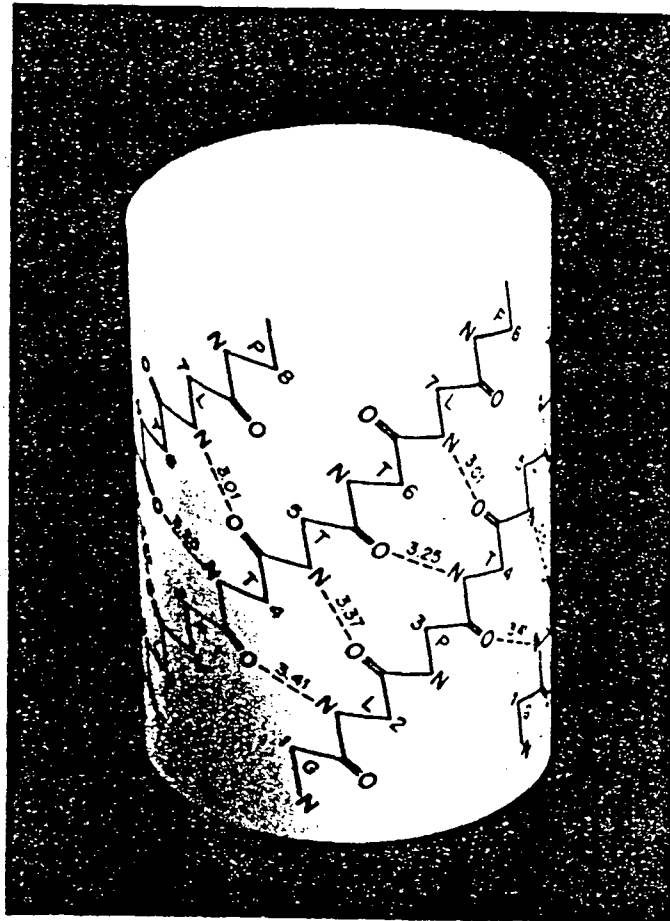


Figure 1.15: The fivefold β -cylinder formed by the amino-terminal ends of VP3 at the protein/RNA interface. (Luo et al., 1987)

site it cannot be performed by the viral protease, specific for Glu-Gly peptides. The proximity of Ser¹⁰ in VP2 to the carboxy-terminus of VP4 suggests that the cleavage of VP0 is autoproteolytic. There is no histidine next to Ser¹⁰ and the carboxy end of VP4. However, nucleotide bases of the RNA could act as proton acceptors in the autocatalysis. Thus, the insertion of RNA into the growing capsids could trigger the cleavage of VP0 into VP2 and VP4. This "enzyme" is, therefore, composed both of protein and RNA components.

1.9.5 Atomic Structure of Mengo Virus

The structure of Mengo virus, a member of the cardioviruses, is substantially different from the structures of rhino- and polioviruses. Although the organization of the capsid proteins is essentially similar to that of rhino- and polioviruses, large insertions and deletions, mostly in VP1, radically alter the surface features. In particular, the "canyon" of HRV14 becomes a deep "pit" in Mengo virus because of polypeptide insertions in VP1 that fill part of the canyon. VP4 is completely internal in Mengo virus, but its association with the other capsid proteins is different from that in rhino- or poliovirus. However, its carboxy-terminus is located at a position similar to that in HRV14 and poliovirus, suggesting the same autocatalytic cleavage of VP0 to VP4 and VP2 takes place during assembly in all these picornaviruses.

The electron density map of Mengo virus had a quality comparable to that of HRV14. The overall structure of Mengo virus resembles HRV14 and poliovirus. The largest differences occur in the surface features of VP1 and the relocation of VP4 (Fig. 1.16). The pentameric clusters of VP1 comprise an even larger proportion of the surface area in Mengo virus than in HRV14 because of a series of insertions in VP1 and deletions in VP2 and VP3. The amino terminal arm of VP1 is 32 residues shorter than VP1 of HRV14. The top corner, equivalent to the NIm-IA site of HRV14 is foreshortened in Mengo virus. Two protrusions, loop I and loop II, are inserted in Mengo virus at the carboxyl end of β C in VP1, and fill the narrow part of the canyon close to the VP2 puff present in HRV14. Loop II is the most external peptide in Mengo virus. Mengo virus and HRV14 show greater similarity between A and the carboxyl terminus of VP1. The third corner (between β D and β E) and the second corner down (between β H and β I) are also shorter in Mengo virus than in HRV14 VP1. As a result there is a shallow depression (as opposed to the HRV14 protrusion) at the fivefold vertices and there is an electron density peak on the fivefold axis. The stereochemistry is consistent with this being a cationic ligand chelated by the carbonyl oxygens of the fivefold-related Pro¹⁷⁸ residues on the fourth corner down. A similar electron density peak is observed in HRV14 associated with Asn¹⁴¹ on the third corner down. The structures of VP2 and VP3 (Fig. 1.16) have a greater similarity to HRV14 VP2 and VP3 than do the structures of VP1 in Mengo virus and HRV14. The first ten

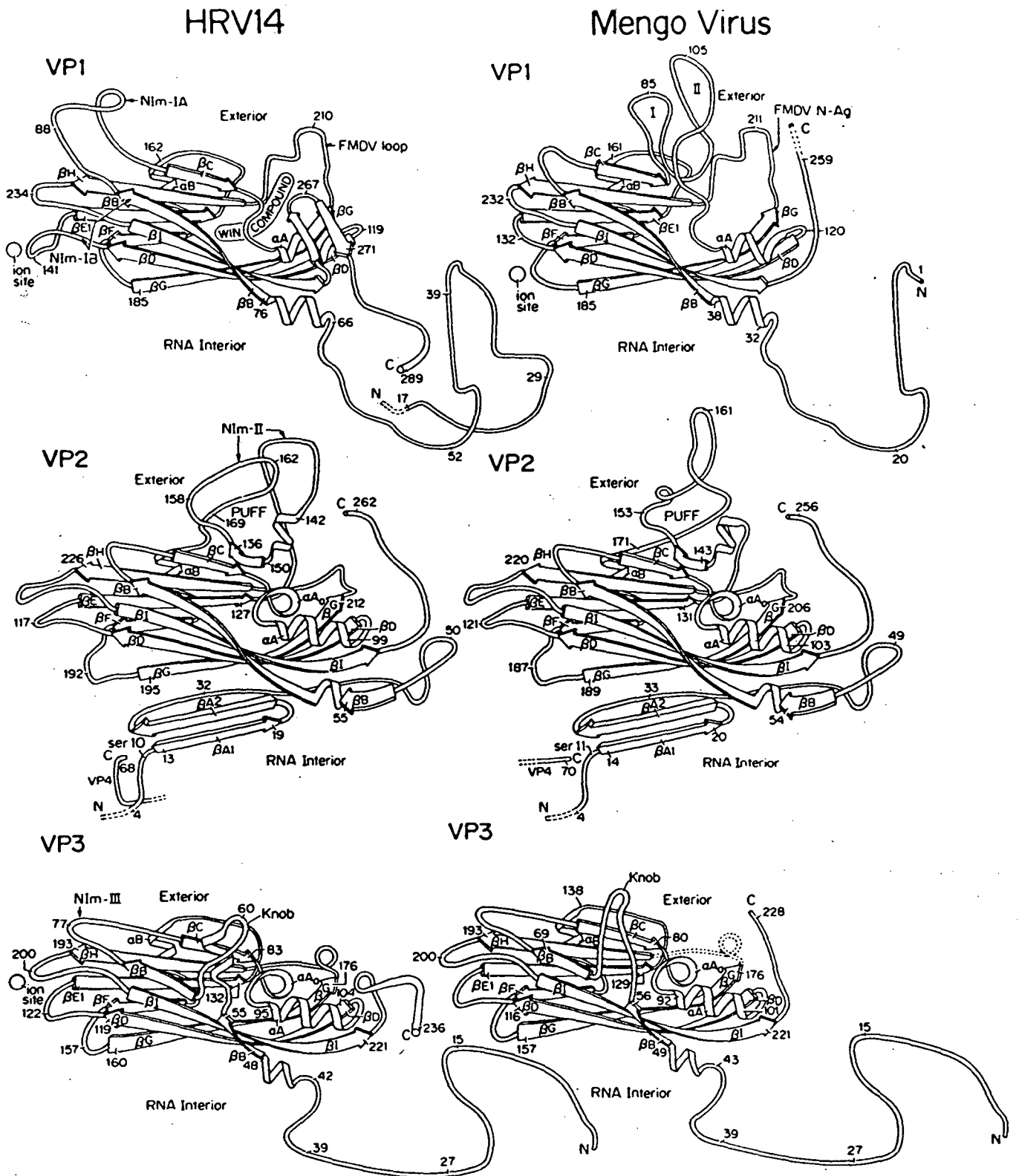


Figure 1.16: Ribbon drawings of the three larger viral proteins VP1, VP2, and VP3 for Mengo virus and HRV14. Each protein has the same wedge-shaped, antiparallel β -barrel but differs because of insertions and deletions mostly at the ends of the β strands. The amino acid numbering and secondary structural nomenclature is also shown. (Luo et al., 1987)

residues of Mengo VP2 are disordered. The Ser¹⁰ residue in VP2 of HRV14 was identified as a possible nucleophile for the autocatalytic cleavage of VP0 into VP2 and VP4, and this residue is homologous with Ser¹¹ of Mengo VP2. However, the side chains of these residues are oriented in different directions in Mengo virus and HRV14.

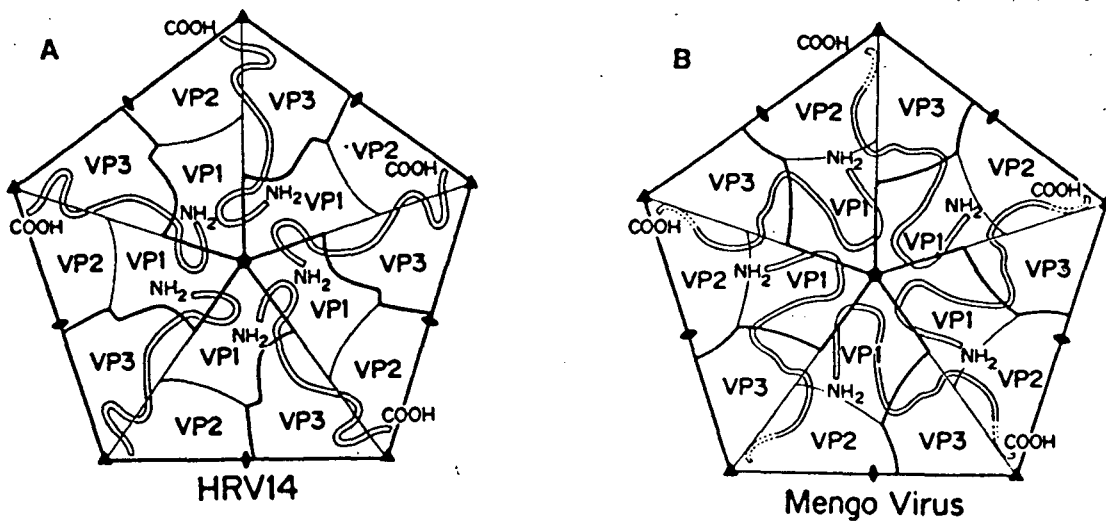


Figure 1.17: Pentameric 14S assembly unit as seen from the outside, showing the course of VP4 represented by a ribbon in (A) HRV14 and (B) Mengo virus. (Luo *et al.*, 1987)

The external VP2 puff is much shorter in Mengo virus and the NIm-II site of HRV14 is deleted in Mengo virus. The major difference in VP3 is that the "knob" (as shown in Fig. 1.16) is mostly deleted in Mengo virus compared to HRV14. In HRV14, VP4 is associated with peptides from only one protomer, running from the fivefold to the threefold axis. However, in Mengo virus VP4 begins near the fivefold axis of one protomer, interacts with the amino terminus of VP3, and ends near the amino terminus of a VP2 in the neighbouring, fivefold anticlockwise related protomer (Fig. 1.17). VP4 is far more exposed to RNA in Mengo virus than in rhino- or poliovirus.

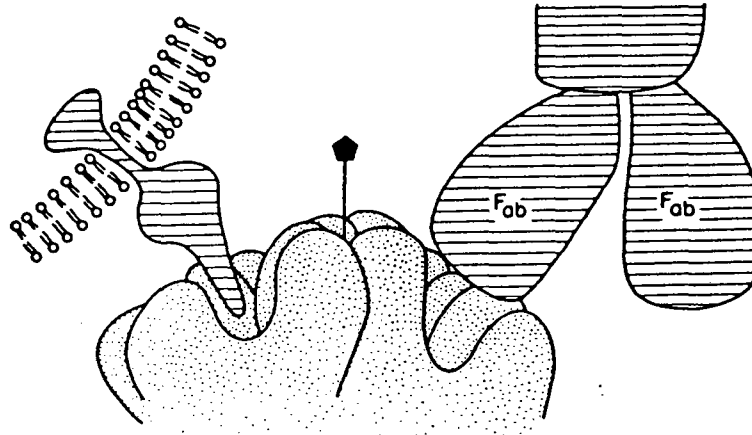
1.9.6 Receptor Recognition

Picornaviruses initiate infection and entry into host cells by attaching to receptors on the host cell membrane. Thus, in order for the viruses to continue to bind to the same receptors, it is important that the receptor attachment site remains sufficiently conserved. However, in viruses that infect animals with an immune system, the viral surface undergoes rapid change to escape neutralizing antibodies and there is a conflict between the requirements for cell attachment and avoidance of antibody binding. Despite the sequence and surface similarities of picornaviruses, they have different host and tissue specificity. This is particularly obvious in a comparison of HRV14 and Mengo virus. The presence of the 25 Å deep canyon, circulating around each of the 12 pentamer

vertices, suggests that this is the site for cell receptor binding. An antibody molecule, whose Fab fragment would have a diameter of the order of 35 Å, would have difficulty in reaching the canyon floor, its entrance being blocked by the canyon rim. Thus the residues in the deeper recesses of the canyon would not be under immune selection and could remain constant, permitting the virus to retain its ability to seek out the same cell receptor. The canyon and pit structures of HRV14 and Mengo virus, respectively, may thus provide a viable receptor binding site inaccessible to host antibodies (Fig. 1.18). The difference between the HRV14 canyon and the Mengo virus pit may reflect differences in recognition and binding of their respective host cell receptors. Amino acid differences between EMCV and Mengo virus and, in particular, Theiler's virus and Mengo virus are on the surface of the virus, but with residues lining the pit remarkably well conserved. It is possible, therefore, that the coronaviruses all use the same, or very similar, cellular receptors. Tissue specificity is perhaps controlled by differential stability of the virion, the flexible polypeptide in the pit or other factors.

1.9.7 Immunogenic Sites on Picornavirions

The immunological response to a virus, i.e. antibody neutralization of viruses, is a major defence against disease in animals. Antibodies can bind to viruses but they do not necessarily neutralize infectivity. Despite the sixtyfold equivalence of each potential binding site on the



THE CANYON HYPOTHESIS

Figure 1.18: The presence of depressions on the picornavirus surface suggests a strategy for the evasion of immune surveillance. The dimensions of the putative receptor binding sites (the canyon in HRV14, the pit in Mengo virus) sterically hinder an antibody's (top right) recognition of residues at the base of the site, while still allowing recognition and binding by a smaller cellular receptor (top left). This would allow for receptor specificity while at the same time permitting evolution of new serotypes by mutating residues about the rim of the canyon or pit. (Rossmann & Rueckert, 1987)

virus, as few as four neutralizing antibodies per virion can be sufficient to inhibit infectivity of poliovirus (Icenogle et al., 1983). Neutralizing antibodies often change the isoelectric point of picornavirions (Mandel, 1976; Emini et al., 1983), indicating that a conformational change may accompany neutralization. Antibodies may neutralize by interfering with cell attachment (antibodies to NIm-II and IA), membrane penetration or virus uncoating (antibodies to NIm-III). Some antibodies that bind to poliovirus may require bivalent attachment that cross-links pentamers in order to neutralize the virus (Emini et al., 1983).

Amino acid residues within the major neutralization immunogens of HRV14 have been identified by Sherry et al., (1986) by screening for escape mutants to neutralizing monoclonal antibodies. Similar results had earlier been obtained in the study of neutralizing immunogenic sites of poliovirus (Hogle et al., 1985). The escape mutants of HRV14 were found to group into four distinct epitopes. Some of the epitopes were composed of residues from different viral proteins. The four neutralizing immunogenic sites (NIm-IA and NIm-IB on VP, NIm-II primarily on VP2 and NIm-III primarily on VP3) occur at the most exposed and external parts of the capsid. They also correspond to hypervariable regions among rhino- and poliovirus sequences. A combination of results for the three polio serotypes showed a similar distribution (Hogle et al., 1985). However, Mengo virus has a different surface and

therefore, may have a different distribution of neutralizing immunogenic sites. Lund et al. (1977) have shown, using polyclonal antibodies, that only isolated VP1 and VP2 induce the production of neutralizing antibodies. The structure shows only one type of extensive protrusion consisting of the top corner (residues 58 to 64), loop I (residues 78 to 83), loop II (residues 93 to 105) in VP1, and the puff (residues 157 to 162) of VP2. These residues are positioned at a radius between 150 Å. and 163 Å., whereas no other parts of the virus extend to a radius greater than 150 Å. Furthermore, these loops are in regions that correspond to the greatest frequency of changes between Mengo virus, EMCV, and Theiler's virus. Hence, this protrusion may represent the immunodominant NIm site on Mengo virus.

1.9.8 Antiviral Drug Binding

Arildone (McSharry et al., 1979; Caliguiri et al., 1980), WIN 51711 and WIN 52084 (Fig. 1.19), as well as some other chemical classes of compounds, inhibit picornavirus infection by preventing viral uncoating without affecting cellular attachment and penetration. These compounds stabilize the virion against alkaline and heat denaturation, loss of VP4 and induce a significant pI change. The effect of these substances on the virion properties in some ways resembles that of neutralizing antibodies or of sulfhydryl reagents. By virtue of their conformation, these compounds can bind specifically to

defined sites on the virion, and have proven a most useful tool to study the structure of the viral particle at the subatomic level.

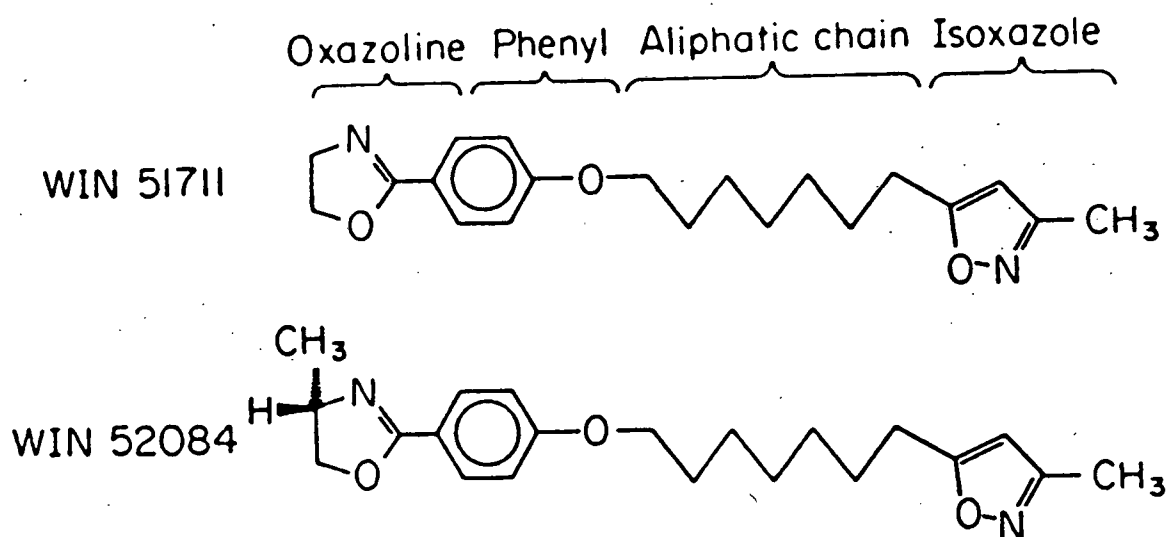


Figure 1.19: Formulae of the two antiviral compounds, WIN 51711 and WIN 52084. They differ only by an additional methyl group on the oxazoline group in WIN 52084. (Rossmann & Rueckert, 1987)

WIN 51711 represents a class of compounds which inhibits picornavirus infection in tissue culture (Otto et al., 1985) and in animal models of human enterovirus disease (McKinlay et al., 1986). Arildone, WIN 51711 and a large number of related compounds have been synthesized at the Sterling-Winthrop Research Institute and tested against several different picornaviruses. The site of binding of WIN 51711 and WIN 52084 on HRV14 has been determined by Smith et al. (1986). As shown in Fig. 1.19, these compounds consist of an isoxazole group (I) connected by a seven-membered aliphatic chain to an oxazoliny1 phenol group (OP). The I group inserts itself into a hydrophobic pocket in the interior of the VP1 β -barrel of HRV14 while the OP group blocks a "pore" in the base of the canyon (Fig. 1.20). The pore opens into large channels leading to the RNA interior. Binding of the compounds is accompanied by large conformational changes in the structure of VP1 in the vicinity of the drug binding site. Various lines of evidence show that these compounds stabilize the virion capsid by inhibiting conformational changes that would otherwise be necessary for viral uncoating (Fox et al., 1986).

The WIN antiviral compounds do not bind to Mengo virus or EMCV and, hence, do not inhibit infection. Loops I and II of VP1 in Mengo virus fill the part of the canyon containing the pore, thus sterically hindering the entry of

the antiviral compounds into the VP1 binding site. Although the pore is blocked in Mengo virus, the cavity within the VP1 β -barrel has sufficient space for the binding of the WIN compounds. The occurrence of such a large cavity lined with hydrophobic residues in VP1 of Mengo virus, rhinovirus, and poliovirus suggests that it might be a functional requirement for the disassembly of these viruses (Luo et al., 1987). Viral disassembly may be inhibited by preventing the collapse of the VP1 hydrophobic pocket or by blocking the flow of ions into the virus interior (Smith et al., 1986).

Numerous substitutions of these compounds have been tested. The most important observation is that the drug becomes inactive on replacing the nitrogen and oxygen atoms in the oxazoline ring by carbon. Similarly, the compounds are inactive in those viruses (viz. EMCV, Mengo, hepatitis A and FMDV) which do not conserve Asn²¹⁹ of HRV14 as Asn or Asp (although the entrance to the pocket is far more constricted in Mengo virus). The hydrogen bond between the drug N or O atoms and Asn²¹⁹ is, therefore, probably essential to the drug function. The structure of poliovirus Mahoney type 1 (Hogle et al., 1985) shows electron density at the precise binding site of the WIN compounds. Thus a "co-factor" appears to bind to the same site as is occupied by the WIN compounds. This co-factor (perhaps a peptide or lipid component) would permit the virion to penetrate the membrane as a complete virion. The WIN compound might

compete with the co-factor but binds more tenaciously, thus inhibiting disassembly.

1.9.9 Unique Features of Foot-and-mouth Disease Virus

The structure of FMDV differs from other picornaviruses in several important respects. The canyon hypothesis proposes that the site of cell attachment is at a depression on the surface which is inaccessible to antibody, and this shields it from immune surveillance. Such depressions have been found on the surface of HRV14 (Rossmann et al., 1985), poliovirus (Hogle et al., 1985), and Mengo virus (Luo et al., 1987). The major antigenic sites for both HRV14 and poliovirus are exposed on the surface, as is the major antigenic site of FMDV, the so-called "FMDV loop" (residues 140-160 of VP1). In contrast to the other picornaviruses, this loop alone (as a synthetic peptide) can induce high levels of neutralizing and protective antibodies. Furthermore, part of the loop has been implicated in cell attachment. These apparently contradictory properties can be understood in terms of the observed disorder of this structure, but cannot be accommodated within the canyon hypothesis.

The close structural relationship of FMDV to HRV14 and Mengo virus is shown in Fig. 1.21. Unlike the other picornaviruses, FMDV does not seem to possess any major canyons or pits. As VP1-3 are substantially smaller in FMDV, the protein shell is generally thinner. The "cores"

of VP1-3 are placed at essentially the same radius and in a similar orientation to those of the other picornaviruses. VP1 shows the most significant rearrangement. For VP2 and VP3 the axis of the β -barrel is approximately in the plane of the capsid whereas in VP1 it is canted up from the plane towards the 5-fold axis. Although this is the case in all picornaviruses it is more pronounced in FMDV where there is a further displacement of 1.5 Å .

VP1 of FMDV comprises 213 residues whereas in HRV14, poliovirus and Mengo virus it comprises 279, 306 and 277 residues respectively. The structure is "trimmed" largely at the loops of the 5-fold axis end of the subunit, and this, together with the canting of the barrel, produces a 5-fold axis naked of VP1 loops, in contrast to other picornaviruses where the VP1 loops approach close enough to form a putative calcium-binding site. Although most of the residues are well-ordered there are some disordered regions which coincide with the major antigenic site (residues 141-160) and part of a minor antigenic site comprising residues 200-213. The 17 C-terminal residues of VP1 form a long "arm" quite unique among the picornaviruses.

In FMDV, VP2 comprises 218 residues whereas in HRV14, poliovirus and Mengo virus it comprises 262, 272 and 256 residues respectively. As with VP1, loops decorating the outside of the FMDV particle are trimmed compared with those of the other picornaviruses (Fig. 1.21). The very close association of the N-terminal residues around the 3-fold

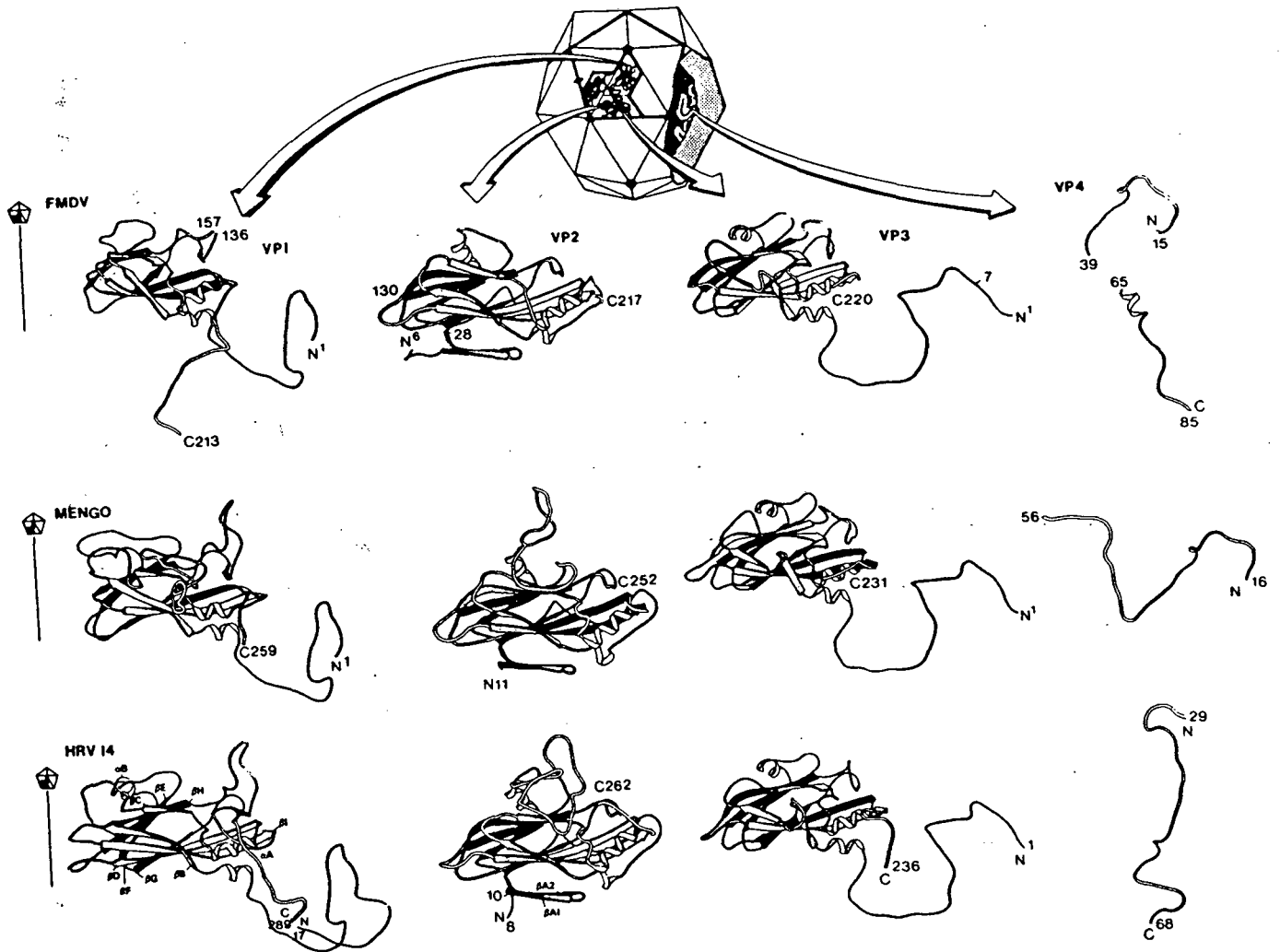


Figure 1.21: Picornavirus structure illustrating the disposition of the structural proteins VP1-4 with respect to the icosahedral symmetry axis. The figure shows the detailed folding of each of the proteins in the three picornaviruses FMDV, Mengo virus and HRV14. The appropriate direction of the icosahedral 5-fold axes is shown for VP1. (Acharya *et al.*, 1989)

axis generates a structure that is not observed in the other picornaviruses. In FMDV, VP3 comprises 220 residues whereas in HRV14, poliovirus and Mengo virus it comprises 238, 236 and 231 residues, respectively. It is the most highly conserved of the coat proteins of the picornaviruses. (Fig. 1.21).

VP4 varies considerably among the members of the picornavirus family. VP4 in FMDV is the longest, comprising 85 residues whereas in HRV14, poliovirus and Mengo virus it has 69, 69 and 70 residues, respectively. The N-terminal portions of VP4 in Mengo virus and FMDV are similar but different from that in HRV14 and lie close to the 5-fold axis. Beyond this region the chain in FMDV forms a well-defined helix of three turns, a novel structure for a picornavirus VP4.

1.10 MYRISTYLATION OF PICORNAVIRUS CAPSID PROTEIN VP4

Chow et al. (1987) and Paul et al. (1987) obtained evidence that poliovirus and other picornaviruses are specifically modified by having myristic acid covalently bound to VP4. In two cases, poliovirus and bovine enterovirus (BEV), myristylation is shown to occur by an amide linkage to the N-terminus of VP4. In all known picornavirus sequences, the N-terminus of VP4 is consistent with a consensus N-terminal sequence previously identified in other myristylated proteins (Table 1.5). These observations defined for the first time the structure of a fatty-acid moiety in the

three-dimensional structure of an acylated protein.

The precise function of the myristyl group in myristylated proteins is still elusive, however, in three cases where a direct test has been made it has proved to be essential.

Mutant unmyristylated p60^{src} loses membrane association and transforming function while maintaining tyrosine kinase activity (Kamps et al., 1985; Pellman et al., 1985). In murine leukemia virus, unmyristylated gag polyprotein does not participate in virus assembly; it no longer associates with plasma membranes, and no discernable viral structures can be found in the infected cell (Rein et al., 1986). In Mason-Pfizer monkey virus, a similarly constructed mutant does form intracellular particles, but they fail to bud (Rhee & Hunter, 1987). While these three cases suggest that myristylated proteins have an affinity for the inner plasma membrane surface, the present results with poliovirus do not fit such a simple mechanism. VP4 of poliovirus is an internal component of a virion that is completely free of membranous elements, and intracellular, mature poliovirions are not membrane-associated. Apparently myristylation need not simply cause attachment of the protein to the nearest available membrane surface.

Paul et al., (1987) entertain two possibilities for the function of the myristic acid residue in VP4 of poliovirus; that it is involved in the process of uncoating of the virus and or in the events leading to the encapsidation of genomic RNA.

TABLE 1.5: AMINO-TERMINAL SEQUENCES OF MYRISTYLATED
PROTEINS (Chow *et al.*, 1989)

Protein		Sequence							
Polio (Type 1)	VP4	Gly	Ala	Gln	Val	Ser	Ser	Gln	Lys
BEV (VG-27)	VP4	Gly	Ala	Gln	Leu	Ser	Arg	Asn	Thr
EMCV	VP4	Gly	Asn	Ser	Thr	Ser	Ser	Asp	Lys
FMDV (01-K)	VP4	Gly	Ala	Gly	Gln	Ser	Ser	Pro	Ala
HRV (1B)	VP4	Gly	Ala	Gln	Val	Ser	Arg	Gln	Asn
RSV	60 ^{src}	Gly	Ser	Ser	Lys	Ser	Lys	Pro	Lys
MuLV	15	Gly	Gln	Thr	Val	Thr	Thr	Pro	Leu
FeLV	15	Gly	Gln	Thr	Ile	Thr	Thr	Pro	Leu
BaeV	12	Gly	Gln	Thr	Leu	Thr	Thr	Pro	Leu
HTLV	19	Gly	Gln	Ile	Phe	Ser	Arg	Ser	Ala
BLV	15	Gly	Asn	Ser	Pro	Ser	Tyr	Asn	Pro
HIV1	17	Gly	Ala	Arg	Ala	Ser	Val	Leu	Ser
cAMP protein kinase		Gly	Asn	Ala	Ala	Ala	Ala	Lys	—
Calcineurin B		Gly	Asn	Glu	Ala	Ser	Tyr	Pro	Leu

PROPOSED CONSENSUS SEQUENCE FOR MYRISTYLATION:

Gly - X - X - X - Ser / Thr

X = other amino acids

Initially the aim of this study was to determine the function of the myristyl group and to establish whether competition for the acylation site is a possible approach to antiviral chemotherapy. The effect of short chain fatty acids on virus replication was therefore examined. Some fatty acids were observed to compete with the myristylation of normal BHK-21 cell proteins and it was thought that this type of competition could be possible in virus-infected cells since it was previously shown that some fatty acids are able to enter picornavirus-infected cells and compete for the myristylation site on VP4 (J. F. E. Newman, unpublished observations). However, somewhat unexpectedly, it was found that lauric acid inhibits an early event in the replication of bovine enterovirus at a concentration which has no detectable effect on normal BHK-21 cell protein synthesis. It was then attempted to determine the actual step in the replication cycle that lauric acid was affecting. The effect of fatty acids on BEV as well as other picornaviruses was examined.

CHAPTER 2

MATERIALS AND METHODS

2.1 REAGENTS

All radiochemicals; [³⁵S]methionine (15 μCi/μl), [¹⁴C]lauric acid (100 μCi/ml), [³H]myristic acid (1 μCi/μl), [³H]uridine (1 μCi/μl), [³H]lauric acid (1 μCi/μl) and [¹⁴C]protein hydrolysate (50 μCi/ml), as well as "Amplify" were obtained from Amersham Radiochemical Centre (England). Scintillation cocktail reagents; (PPO) primary fluor diphenyl oxazole was from Saarchem (SA) and bis-MSB (para-bis-(ortho-methylstyryl)-benzene) was from Packard Instrument Company (Switzerland). All other chemicals were purchased from Merck (Germany).

2.2 APPARATUS

For clarification of virus a Sorvall (Type GSA rotor) centrifuge was used. The Beckman ultracentrifuge was used for pelleting the virus (Type 30 rotor) and for sucrose density gradient centrifugation (SW 41 rotor). A Pye-Unicam ultraviolet (UV) spectrophotometer (model SP8-400) was used for measuring absorbance (optical density) at 260 nm and radioactivity was measured using a Beckman LS 5801 scintillation counter. Electrophoresis was carried out using a dual vertical slab electrophoresis cell (SE 600) from Hoefer Scientific Instruments and gels were dried on a

slab gel dryer (SE 540) also from Hoefer Scientific Instruments. Multiwell plates used for titrating virus were from Nunclon Delta (Denmark). Roentgen Cronex 4 x-ray film was used for autoradiography .

2.3 VIRUSES AND CELLS

Bovine enterovirus (BEV) (VG-5-27; McFerran, 1962) and encephalomyocarditis virus (EMCV) (ATCC VR-129B) were cultivated in BHK-21 (Baby Hamster Kidney) cells; Poliovirus type 1 (NIV-D149/86) and coxsackievirus B5 (ATCC VR-185) were cultivated in Vero cells, and human rhinovirus type 1B (HRV-1B) (obtained from Dr D. V. Sangar, Wellcome Biotechnology, Beckenham, U.K.) was cultivated in Hela cells. All cells were grown as monolayers in 25 or 75 ml plastic flasks in Eagle's minimal essential medium (MEM) (Gibco) containing 10% foetal calf serum (FCS) (State Vaccine Institute, SA), penicillin (pen) and streptomycin (strep), both at a final concentration of 200 ug/ml. HRV-1B was grown at 33°C whereas all other viruses were grown at 37°C.

2.4 TOXICITY OF FATTY ACIDS

The toxicity of fatty acids for BHK-21 cells was initially determined by microscopic observation. BHK-21 cells were grown in 24-well plates by using a 1:12 split of two small flasks (25 ml). Each well containing 2 ml MEM. By incubating at 37°C in a CO₂ incubator confluent

monolayers were obtained after 2-3 days.

Fatty acids at 17.5 mM in ethanol were rapidly injected into 2 ml MEM in glass bottles whilst being vigorously stirred on a vortex mixer. A dilution series of the fatty acid was used to obtain final concentrations of 87.50-, 65.63-, 43.75-, 32.82-, 21.88- and 16.41 μ M in 2 ml MEM. Each of these were placed into a well of the 24-well plate when the cells were at 75% monolayer. The control well contained 2 ml MEM with no fatty acid. The plates were sealed, incubated at 37°C, and examined microscopically after 1-, 2- and 3 days for metabolic inhibition as well as altered morphology.

2.5 MYRISTIC ACID COMPETITION IN BHK-21 CELLS

BHK-21 cells at monolayer in 24-well plates were used. The medium in each well was replaced with 500 μ l serum-free MEM. 5 μ Ci [3 H]myristic acid was then added to each well. A two-fold dilution series of fatty acids at 100 mM was made and 5 μ l of each dilution was added to a BHK-21 cell monolayer. The control well contained 5 μ Ci [3 H]myristic acid but no fatty acid. The plates were incubated for 5 hours with shaking at 37°C. Cells were washed three times with fresh MEM and allowed to drain well. 0.5 ml of 5% trichloroacetic acid (TCA) was added to each well and left for 1 hour at room temperature. The TCA was removed and the cells were washed twice with ethanol. After the cells had dried they were removed with 0.2 ml 0.1 M NaOH containing

1% SDS. 50 μ l aliquots were counted in a liquid scintillation counter.

2.6 TITRATION OF VIRUS HARVESTS CONTAINING FATTY ACIDS

BHK-21 cells in 25 ml flasks were infected with a high multiplicity of BEV. At 1 hour post infection the cells were washed three times with serum-free MEM at 37°C and reincubated with 5 ml fresh serum-free MEM containing fatty acids. The culture was harvested after about 7 hours, when the cells were completely detached from the flask, and titrated for virus infectivity (T.C.I.D.₅₀) using a modified method of Bey and Golombick (1984).

A ten-fold dilution series of each culture was made in a total volume of 2 ml serum-free MEM. 0.1 ml of each dilution, starting with the highest, was inoculated into 8 wells of a 96-well microtitre plate. 0.1 ml of medium was then added to each well, and finally 50 μ l BHK-21 cells (8×10^5 cells/ml) suspended in MEM were added to each well. The plates were incubated at 37°C in a CO₂ incubator for about 48 hours when cells reached monolayer in control wells (i.e. wells lacking virus). Cells were fixed with 5% formalin in 0.01 M phosphate-buffered saline (PBS) pH 7.5 for 2-3 hours. Cells were then stained with 0.1% crystal violet in 50% ethanol for a few hours, rinsed with water and drained. T.C.I.D.₅₀ of each plate was determined according to the Reed and Meunch formula (Whitaker, 1972).

2.7 VIRUS PURIFICATION

Virus was purified using a modified method of Brown & Cartwright (1963).

Monolayers of BHK-21 cells were infected with BEV at a multiplicity of approximately 100 p.f.u./cell at 37°C. After 8-10 hours, when the cells had become detached from the flask, the culture was transferred to -20°C. After freezing and thawing, twice, cell debris was removed by centrifugation at 10 000 r.p.m. for 15 minutes. The supernatant was collected and ultracentrifuged at 25 000 r.p.m. for 120 minutes in a Beckman Type 30 rotor, to pellet the virus. The supernatant was discarded and the virus pellet allowed to drain until dry. The pellet was then resuspended in a total volume of 500 µl of Tris-buffer (0,01 M Tris-HCL pH 7.5 containing 0.1 M NaCl). The virus sample was concentrated by centrifugation on a 15% - 45% sucrose density gradient made up in Tris-buffer (Appendix B). The sample was made 1% with SDS and layered onto the gradient with a pasteur pipette. Ultracentrifugation was carried out at 40 000 r.p.m. for 105 minutes using the Beckman SW41 rotor. The gradient was fractionated (0.5 ml fractions) immediately after spinning and the optical density of each fraction was recorded at 260 nm. The fractions containing the virus were pooled and virus proteins were precipitated by adding one volume of Tris-buffer and two volumes of acetone and storing at -20 °C.

Fig. 2.1 shows a typical virus peak obtained by sucrose density gradient fractionation.

To recover BEV proteins the precipitate was spun down in a Sorvall centrifuge at 10 000 r.p.m. for 10 minutes, drained, and resuspended in dissociation buffer (Appendix C). The sample was heated at 100°C for 2-3 minutes to destroy the tertiary protein structure and analysed on 10% polyacrylamide gels (Appendix C) (Laemmli, 1970). Fig. 2.2 shows a PAGE separation of BEV proteins. These were identified by using standard molecular weight markers (Fig. 2.3).

2.8 RADIOLABELLING OF BHK-21 CELL PROTEINS

Monolayers of BHK-21 cells were washed three times with methionine-free medium (MFM) and then incubated in MFM containing 15 μ Ci [³⁵S]methionine for 1 hour at 37°C with shaking. The monolayers were washed with phosphate-buffered saline and the radiolabelled proteins recovered with dissociation buffer and analysed by polyacrylamide gel electrophoresis (Laemmli, 1970). Radioactive proteins were detected by autoradiography (Appendix C).

2.9 FATTY ACID TREATMENT OF BHK-21 CELLS

Fatty acids at 10 mM in ethanol were added to the medium, when passaging BHK-21 cells, to give final concentrations

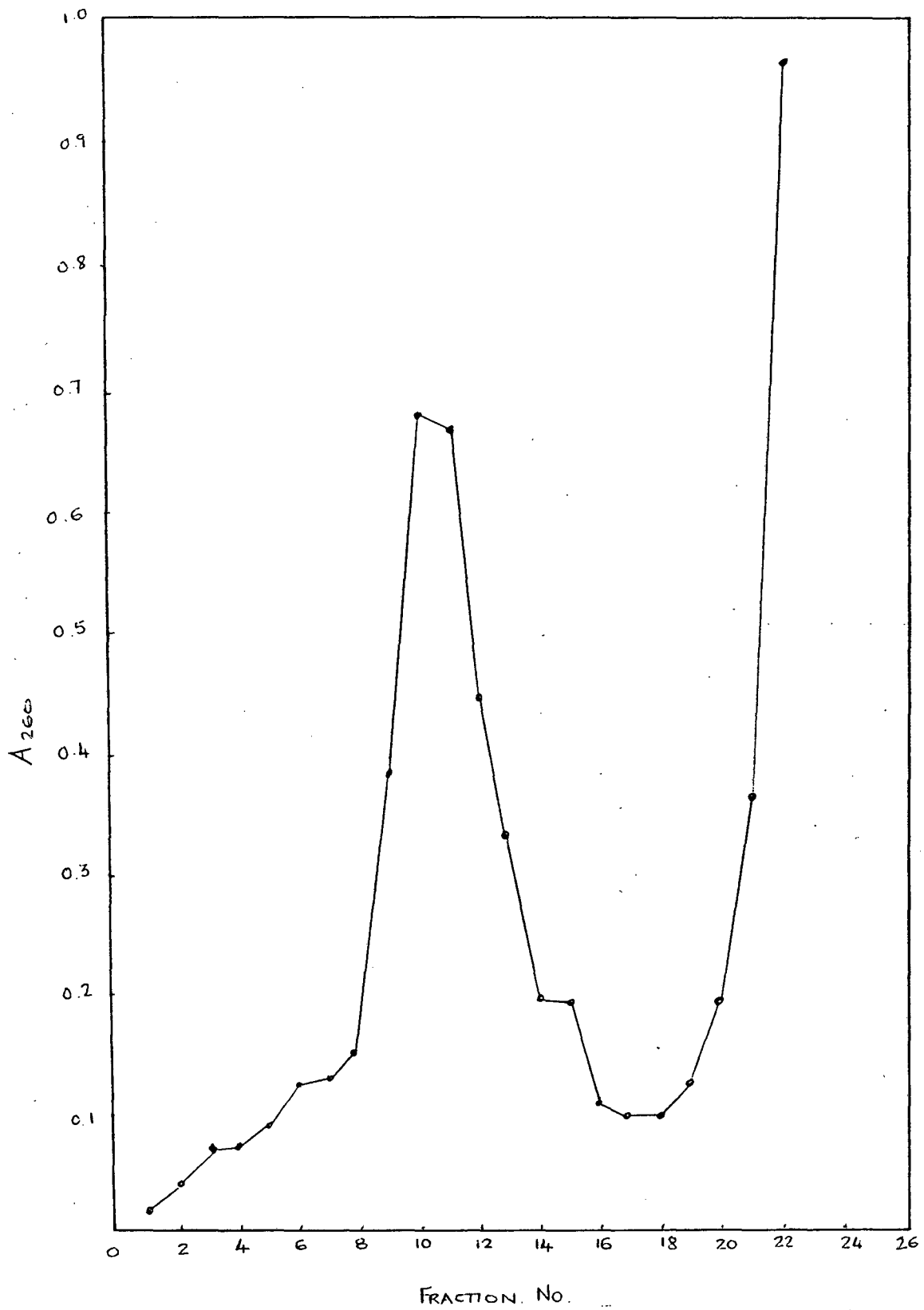


Figure 2.1: Typical virus peak obtained by sucrose density gradient fractionation of bovine enterovirus (BEV).

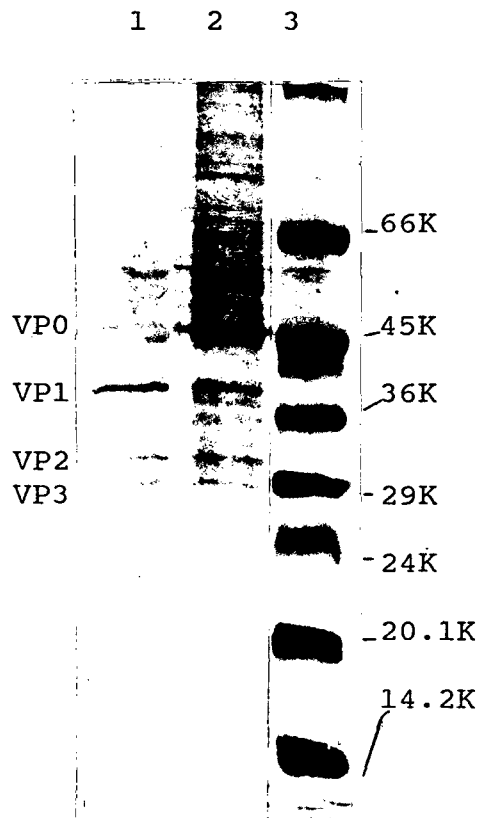


Figure 2.2: PAGE separation of BEV proteins. Pure BEV, lanes 1 and 2; molecular weight markers, lane 3.

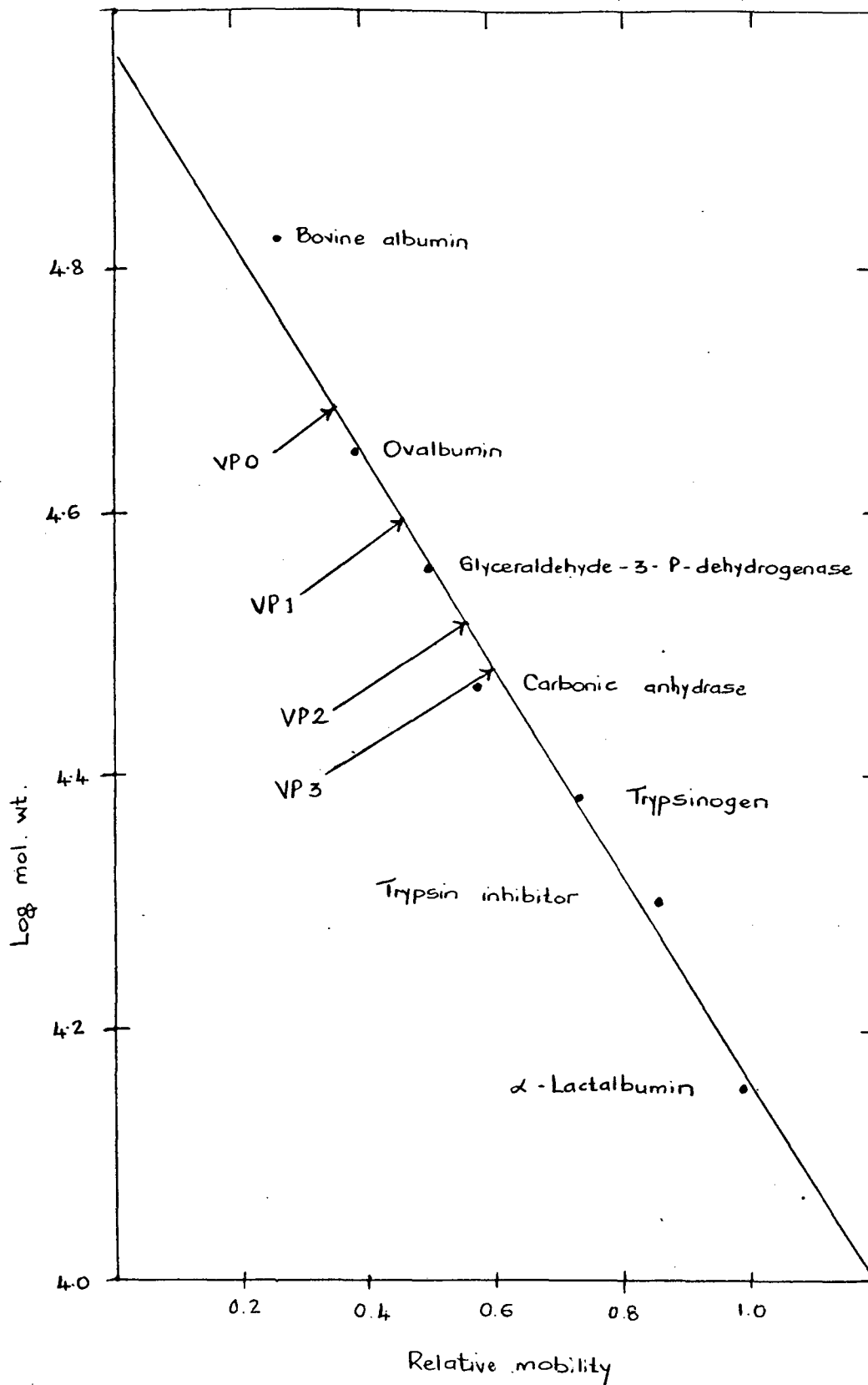


Figure 2.3: Determination of molecular weights of the structural proteins of BEV by polyacrylamide gel electrophoresis.

of 25 μM and 100 μM . The cells were incubated at 37°C until they reached monolayer.

2.10 RADIOLABELLING OF VIRUS

Monolayers of BHK-21 cells were infected with BEV at a multiplicity of approximately 100 p.f.u./cell at 37°C. After a 1 hour adsorption period the monolayers were washed three times with methionine-free medium (MFM) and then incubated in MFM containing [³⁵S]methionine at 10 $\mu\text{Ci/ml}$. After approximately 7 hours, when the cells had become detached from the flask, the culture was transferred to -70 ° C. After freezing and thawing twice the virus was purified using the method described in 2.7 above.

2.11 RADIOLABELLING OF VIRUS-DIRECTED PROTEINS

Monolayers of BHK-21, HeLa and Vero cells were infected at multiplicities of 100 with appropriate viruses at 37°C (33°C for HRV-1B). The infecting virus was allowed to attach to the cells for 1 hour after which the monolayers were washed twice with MFM. Cells infected with BEV, poliovirus, coxsackievirus and EMCV were incubated for a further 1 hour then rewashed with MFM. Cells infected with HRV were incubated for 4 hours before being washed again with MFM. Infected cells were then incubated with [³⁵S]methionine at 5 $\mu\text{Ci/ml}$. After a further 1 hour, infected monolayers were washed with phosphate-buffered saline at 4°C. The radiolabelled proteins were recovered

from the cells with dissociation buffer and analysed on 10% polyacrylamide gels (Laemmli, 1970).

2.12 FATTY ACID TREATMENT OF VIRUSES

Fatty acids at 10mM in ethanol were rapidly injected, at room temperature, into vigorously stirred aqueous virus samples in glass bottles to obtain a final concentration of 100 μ M. The mixture was then used immediately to infect cells or held at room temperature for 1 hour before infection.

For extraction of the fatty acid a BEV/lauric acid mixture was added to an equal volume of chloroform and shaken for 1 minute at room temperature. The mixture was then centrifuged at 10 000 rpm for 5 minutes and the radioactivity in each phase was determined, or the virus in the aqueous phase was used to infect BHK-21 cells.

RESULTS

3.1 MYRISTIC ACID COMPETITION EXPERIMENTS

3.1.1 Incorporation of Lauric Acid (C=12) into VP4 of Bovine enterovirus

Previous studies undertaken in the Department of Microbiology at Rhodes University have shown that radioactive lauric acid (C=12) can be covalently bound to VP4 and incorporated into picornavirus particles. In this research BEV grown in BHK-21 cells was used as a model system, so an experiment was performed to determine whether BEV can incorporate lauric acid into VP4. BEV was grown in the presence of 50 μ Ci [14 C]lauric acid and purified as described in chapter 2. The proteins were recovered by acetone precipitation and hydrolysed with 6N HCl at 110°C for 18 hours. The liberated fatty acids were analysed by ascending chromatography in lanes on C18 reverse-phase TLC plates (Whatman) with glacial acetic acid/acetonitrile (1:1). Parallel lanes contained authentic [3 H]myristic and [14 C]lauric acid markers. Radioactivity in 0.5 cm cuts across each lane was determined using a liquid scintillation counter. Fig. 3.1 shows that mostly myristic acid was recovered from the [14 C]lauric acid-labelled BEV. However, a small amount of lauric acid was also recovered indicating that some virus particles incorporate

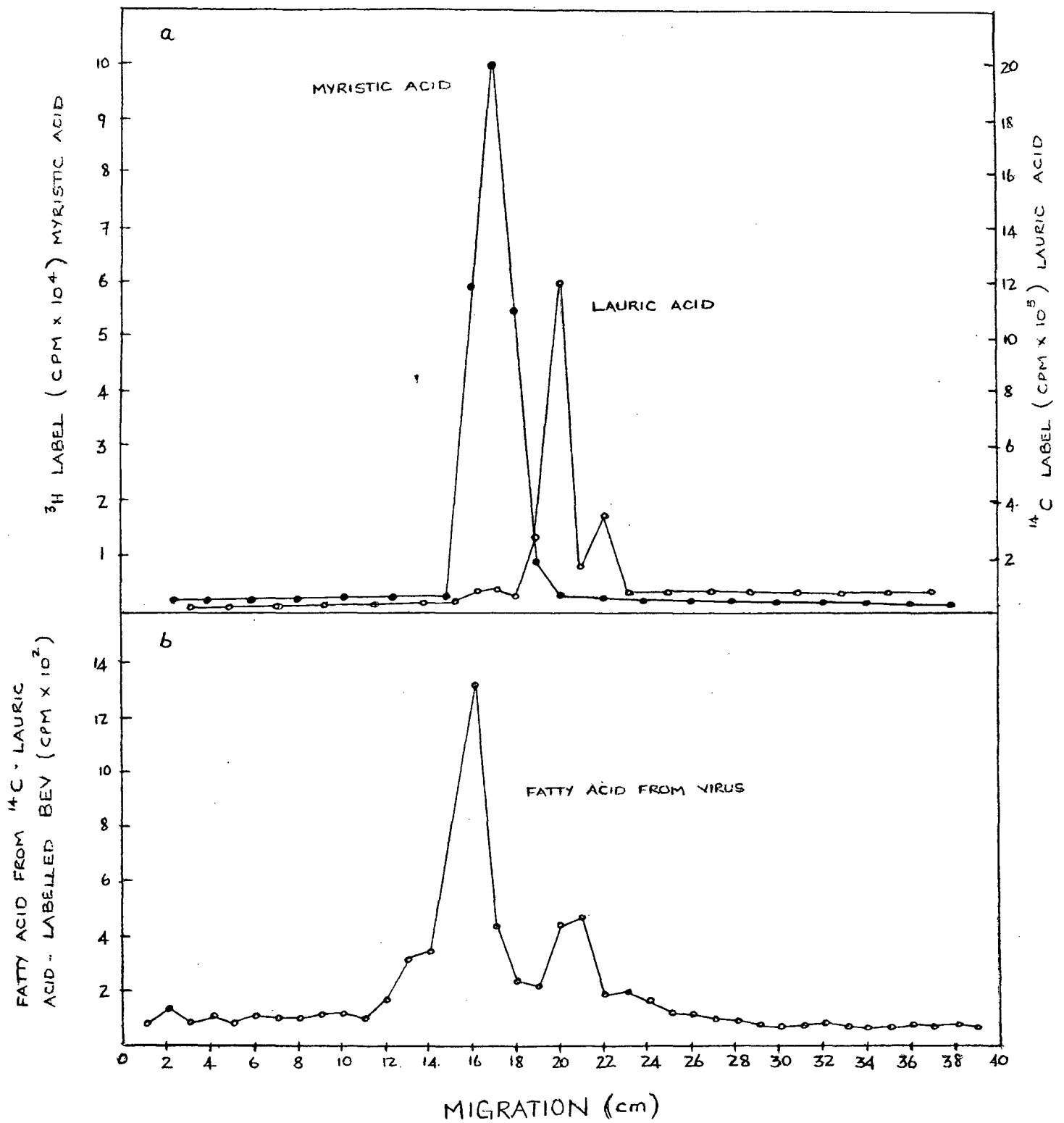


Figure 3.1: Identification of the protein-linked fatty acid on VP4 by ascending chromatography on reverse-phase TLC plates.

lauric acid into VP4 instead of myristic acid. Chow et al. (1987) showed that myristic acid is specifically incorporated into VP4 of poliovirus (serotype 1, Mahoney strain) since only myristic acid was recovered from both [³H]myristic acid and [³H]palmitic acid-labelled viruses. To characterize the fatty acid modification in the virus particle, the protein from [³H]myristic acid-labelled poliovirus was analysed by SDS-PAGE. The radioactivity always specifically co-migrated with the VP4 capsid protein, indicating that the myristic acid was covalently bound to VP4. In this study the protein from [³H]myristic acid- and [³⁵S]methionine-labelled BEV (Fig. 3.2) showed similar bands to that of Chow et al. (1987). The results obtained with BEV therefore indicate that radioactive lauric acid can be covalently bound to VP4 and incorporated into virus particles.

3.1.2 Toxicity of Fatty Acids for BHK-21 cells

Before antiviral activity experiments could be performed with other fatty acid derivatives (Appendix A), the toxicity of these fatty acids for BHK-21 cells had to be determined. Initially, the effect of these fatty acids on BHK-21 cells was simply determined by microscopic observation. Table 3.1 shows the concentrations of fatty acids that were observed to have no effect on BHK-21 cells.

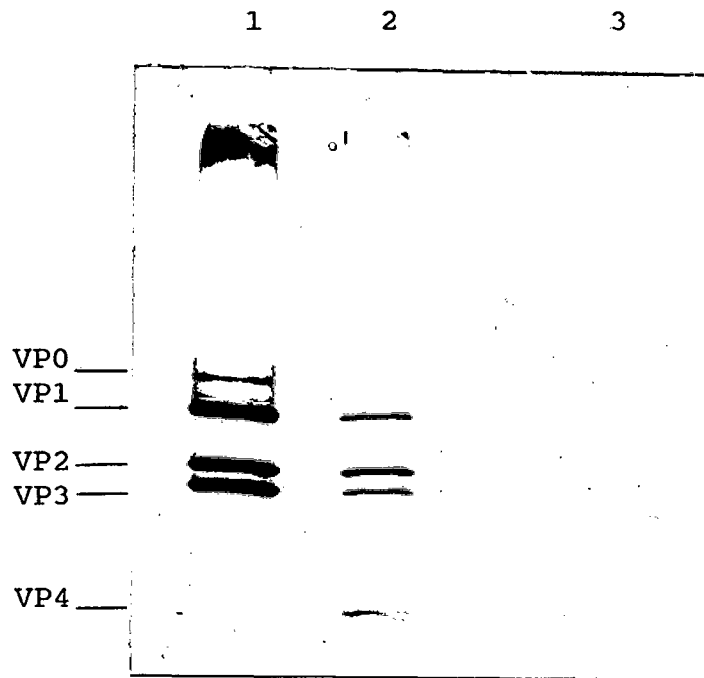


Figure 3.2: SDS-PAGE separation of radiolabelled BEV proteins. [³⁵S]methionine-BEV, lane 1; [¹⁴C]protein hydrolysate-BEV, lane 2; [³H]myristic acid-BEV, lane 3; showing that the [³H] label specifically co-migrated with VP4.

TABLE 3.1: MAXIMUM CONCENTRATION OF FATTY ACIDS THAT ARE NOT TOXIC TO BHK-21 CELLS

FATTY ACID	CONCENTRATION/ μ M
Decyl alcohol	32.82
Capric acid	43.75
Lauric acid	65.63
Tridecanoic acid	65.63
Pentadecanoic acid	21.88
Tetradecane	43.75
Tetradecanol	87.50
2-Bromo-tetradecanoic acid	21.88
Pentadecanoyl chloride	21.88
Myristic anhydride	21.88
Methyl myristate	43.75
Pentadecanol	21.88

3.1.3 Competition with Myristylation of BHK-21 cell Proteins

Fig. 3.3 shows that some of the fatty acid derivatives used above were able to compete with myristylation of BHK-21 cell proteins, as the amount of radioactivity in the cells decreased with increasing concentration of the fatty acid. This indicated that these fatty acids may possibly be able to compete with the myristylation site in BEV-infected BHK-21 cells.

3.1.4 Titration of Virus harvests grown in the presence and absence of Fatty acids

The results of the toxicity experiments gave an indication as to which concentration of fatty acid could safely be used in experiments with infected cells. The effect of the fatty acid on virus growth was determined by titrating virus harvests grown in the presence and absence of fatty acid according to the method of Bey and Golombick (1984).

Fig. 3.4 shows the reduction in BEV titre when grown in the presence of lauric acid. 30 μM -lauric acid reduces the titre by 0.5 log units, 60 μM -lauric acid reduces the titre by 1 log unit, and 80 μM -lauric acid reduces the titre by 2 log units, indicating some antiviral activity of lauric acid. In contrast, capric acid, at all three concentrations used, seemed to have no such activity. When this experiment was attempted with other fatty acids no clear results were

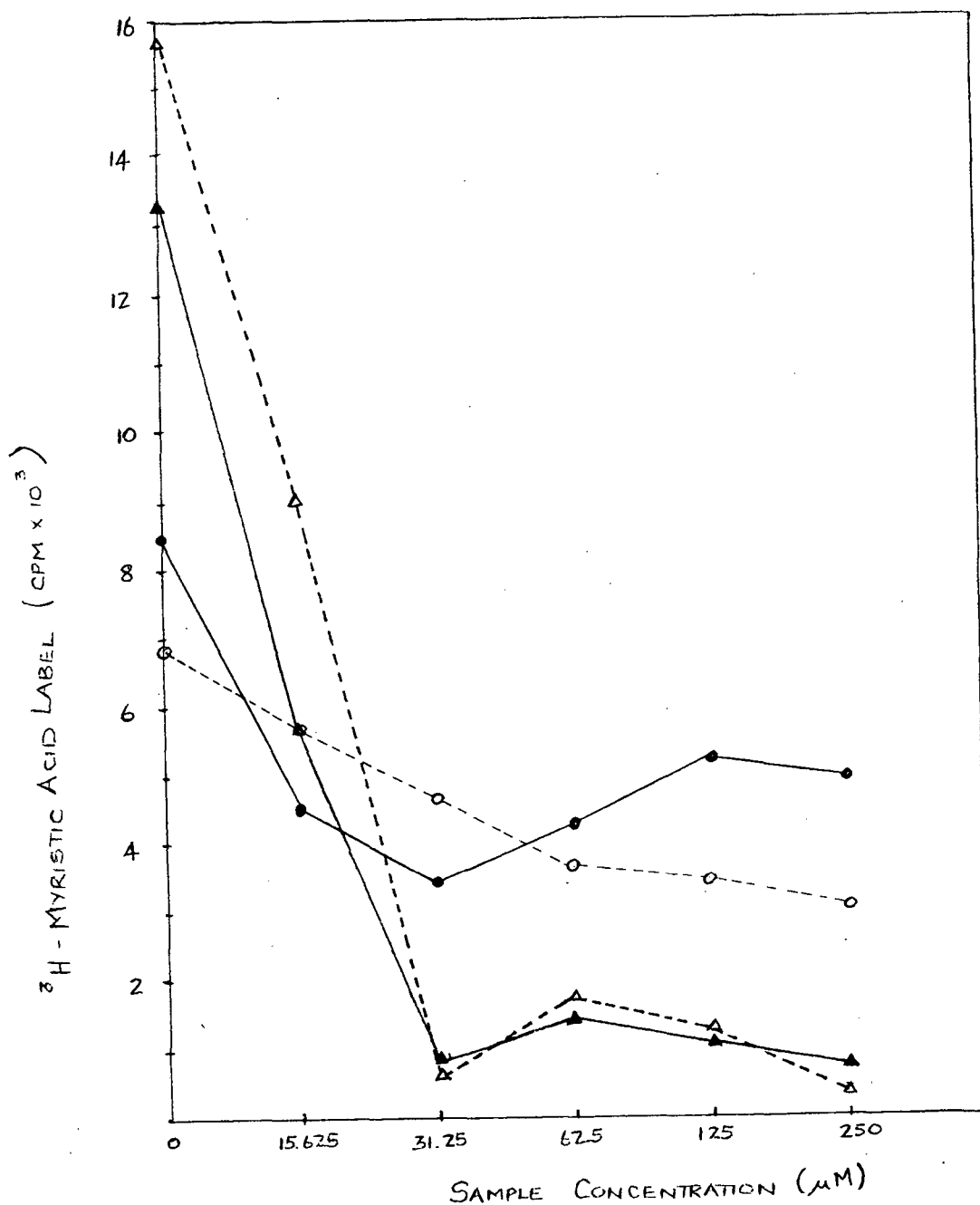


Figure 3.3: Inhibition of the incorporation of [^3H] myristic acid into cell proteins by various fatty acids, as measured by scintillation counting. Lauric acid (●—●), tetradecane (○---○), 2-bromo-tetradecanoic acid (▲—▲), pentadecanoyl chloride (△--△). The amount of radioactivity taken up by the cells decreases as the concentration of fatty acid increases, indicating competition with myristic acid.

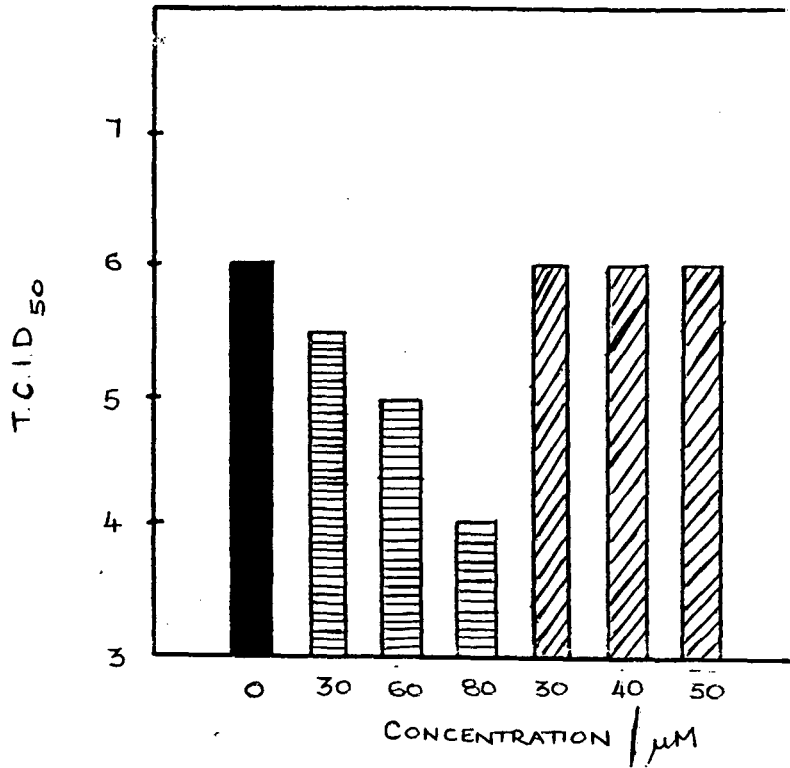


Figure 3.4: Titres of BEV grown in the presence and absence of lauric acid and capric acid. Control , lauric acid , capric acid .

obtained.

3.1.5 Effect of Lauric Acid on Virus Yield

Once it was shown that lauric acid could be incorporated into VP4 of BEV, an experiment was performed to determine the effect of lauric acid on virus yield. BEV was grown in the presence of 30 μ M-lauric acid (found to be non-toxic), radiolabelled with 60 μ Ci [35 S]methionine and purified as before. A radiolabelled culture of BEV without lauric acid served as a control. The radioactivity, as well as the optical density in each of the fractions was read. The yield of virus was estimated from the optical density (1 OD unit = 143 μ g/ml virus). Fig. 3.5 shows that 30 μ M-lauric acid reduces the virus yield by about 50%. This is in correlation with the titres obtained above.

It has been established that picornaviruses generally produce two types of particles during replication. Johnston and Martin (1971) showed that BEV (serotype VG-5-27) grown in BHK-21 cells and purified produced two types of particles, infective particles sedimenting at 165S and empty capsids or procapsids at 75S. PAGE of proteins extracted from both types of components showed that the infective component yielded three major polypeptides (VP1, VP2, VP3) and a fast moving minor component (VP4), whereas the empty capsids contain only three polypeptides (VP0, VP1, VP3). Cleavage of the largest procapsid polypeptide occurs during virus maturation to form VP2 and VP4.

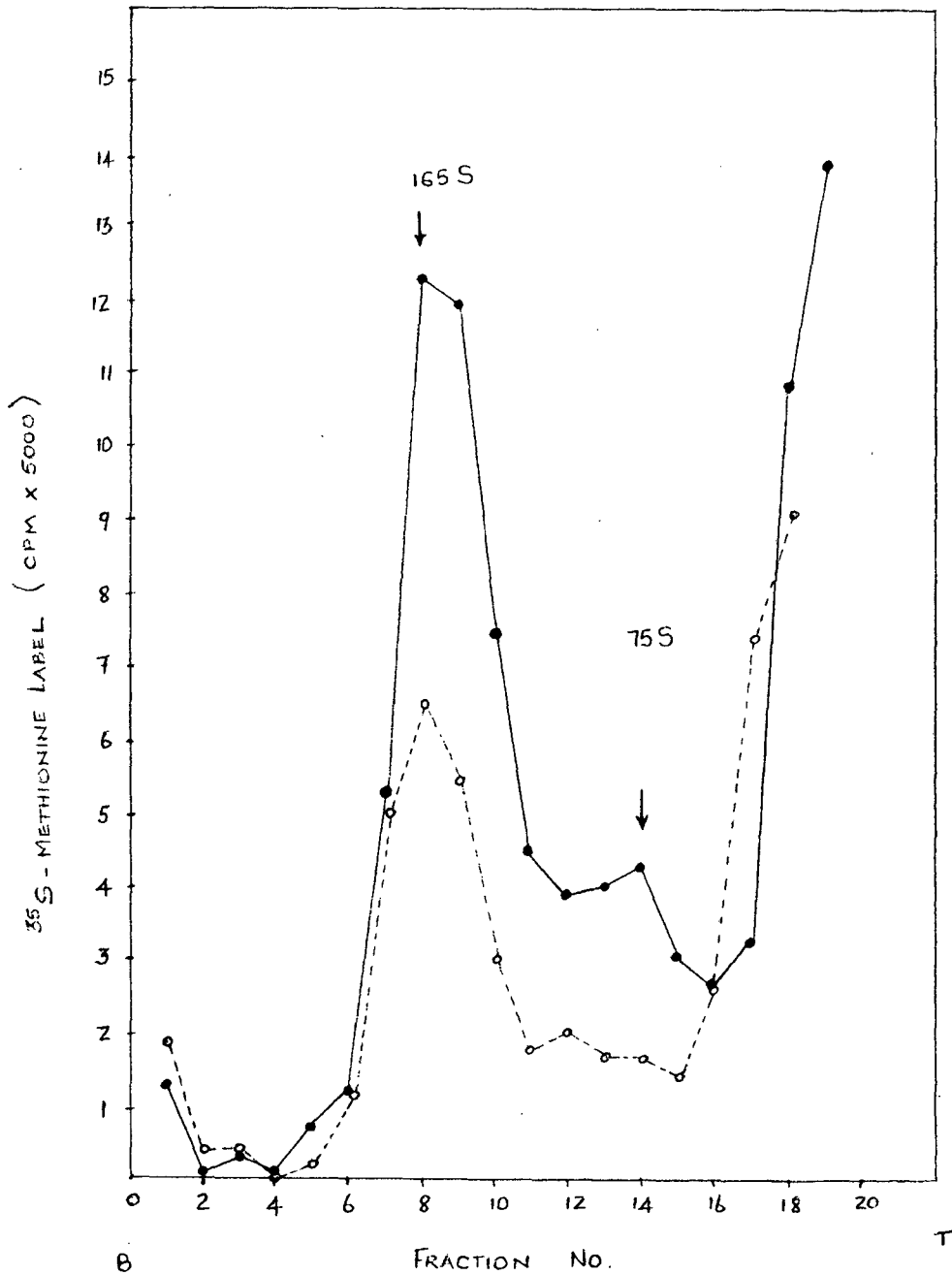


Figure 3.5: Sedimentation through a 15-45% sucrose gradient of BEV grown in normal MEM ●—●, and BEV grown in MEM containing 30 μM lauric acid ○---○.

Fig. 3.5 shows that BEV grown in the presence of lauric acid also produces both types of components.

To show that the two components were indeed corresponding to infective particles and procapsids, [³⁵S]methionine (90 μ Ci) and [³H]uridine (1 mCi)-labelled BEV were subjected to sucrose density gradient centrifugation. [³H]uridine was used to label the virus RNA. The distribution of radioactivity after centrifugation is shown in Fig. 3.6. The fastest sedimenting peak (165S) contains RNA. This has previously been shown to be the infective component (Martin et al. 1970). The second component is not labelled with [³H]uridine and would therefore appear to correspond to the procapsid component (75S).

Fractions containing both whole infective particles or virions (fractions 7-11, Fig.3.5) and empty particles or procapsids (fractions 12-15, Fig.3.5) from both preparations (BEV alone and BEV with lauric acid) were pooled separately and the proteins precipitated with acetone. PAGE of the proteins showed that BEV grown in the presence of 30 μ M-lauric acid (Fig. 3.7, lanes 3 & 4) contains the same proteins as BEV without lauric acid (figure 3.7, lanes 1 & 2). This indicates that whole virus particles are being formed in the presence of lauric acid.

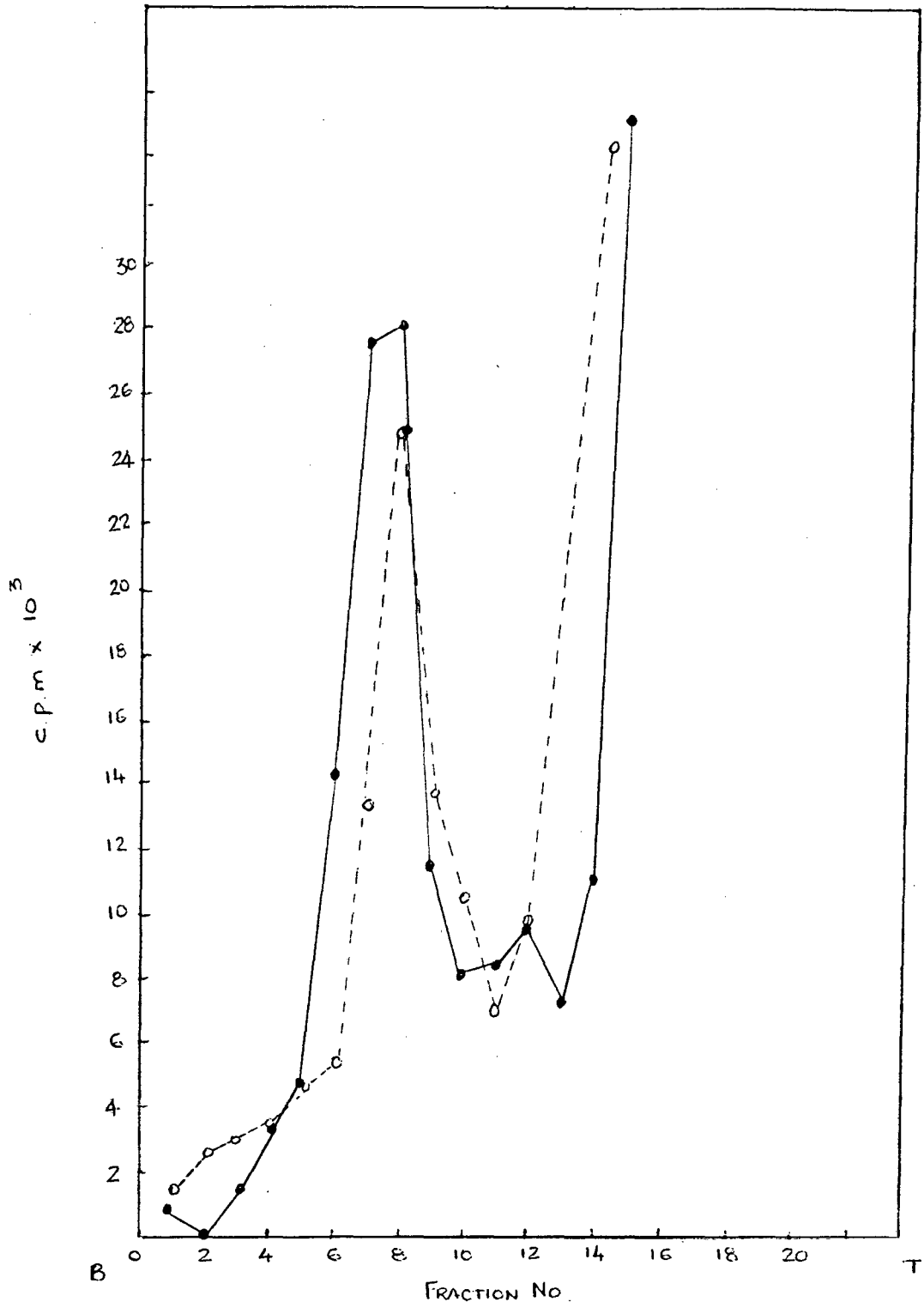


Figure 3.6: Sucrose density gradient fractionation of BEV radiolabelled with [³⁵S]methionine (○---○) and [³H]uridine (●—●) showing that BEV empty particles (fractions 10-13) do not contain RNA.

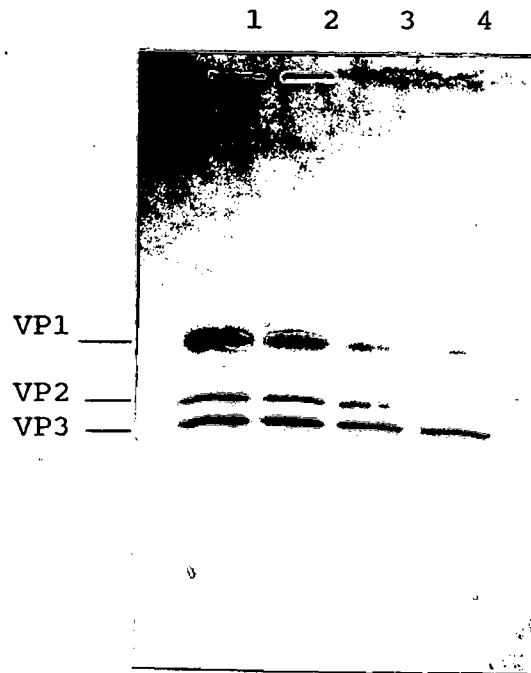


Figure 3.7: PAGE separation of BEV grown in the presence and absence of 30 μ M-lauric acid. BEV full particles, lane 1; BEV empty particles, lane 2; BEV + lauric acid full particles, lane 3; BEV + lauric acid empty particles, lane 4. Theoretically, the empty particles should contain VP0, 1 and 3 and the full particles VP1, 2, 3 and 4. However, the intensity of the VP1 and VP3 bands are darker in the empty particles (lane 2 and 4) indicating more of VP1 and VP3.

3.2 LAURIC ACID EXPERIMENTS

3.2.1 Effect of Fatty Acids on Normal Cell Protein Synthesis

The results from microscopy indicated that most fatty acids seemed to have been toxic to BHK-21 cells at low concentrations, with the exception of a few which were toxic at much higher concentrations. However, these results gave an indication of which concentration levels were safe to use in infected cells, but before these could be used in infected cells, their effect on host cell protein synthesis had to be determined.

Since lauric acid (C=12) seemed to compete with myristylation, it was decided to look at the effect of this fatty acid first. BHK-21 cells were grown in medium containing lauric acid, at final concentrations of 30 μ M, 60 μ M, and 80 μ M, and medium containing a shorter chain fatty acid, capric acid (C=10), at final concentrations of 30 μ M, 40 μ M, and 50 μ M. Fig. 3.8 shows that both lauric acid (lanes 2, 3, and 4) and capric acid (lanes 5, 6, and 7) had no detectable effect on host protein synthesis since the pattern of protein synthesis in the presence of these fatty acids resembled the pattern of protein synthesis in BHK-21 cells grown without any fatty acid (Fig. 3.8, lane 1). The same concentrations of lauric- and capric acids were then used to test their effect on virus-directed

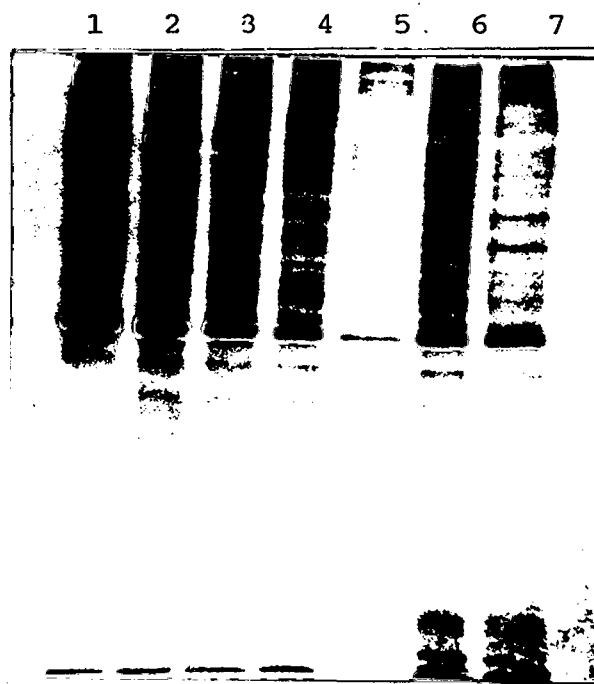


Figure 3.8: PAGE of radiolabelled proteins from BHK-21 cells grown in the presence and absence of lauric acid and capric acid. BHK-21 cells alone, lane 1; cells + lauric acid: 30 μM (lane 2), 60 μM (lane 3), 80 μM (lane 4); cells + capric acid: 30 μM (lane 5), 40 μM (lane 6), 50 μM (lane 7).

protein synthesis.

BHK-21 cells were also grown with a number of other fatty acids (Appendix A) each at final concentrations of 25 μM and 100 μM . All the fatty acids tested were shown to have no effect on BHK-21 cell protein synthesis at both the concentrations used (Fig. 3.9). From this it was deduced that these fatty acids could safely be used at final concentrations of 100 μM in experiments with infected cells.

3.2.2 Effect of Fatty Acids on Virus-directed Protein Synthesis

As indicated, the intention of this research was to concentrate on competing for the myristylation site on picornavirus protein VP4. However in experiments to determine the effect of fatty acid on infected cell macromolecular synthesis, it was observed that fatty acids present during infection had a marked effect on the production of BEV proteins.

Since lauric acid and capric acid were first shown to have no effect on BHK-21 cell protein synthesis (Fig. 3.8), experiments were performed to determine their effect on infected cell protein synthesis. Fig. 3.10 shows that lauric acid, at all three concentrations used, present during infection had a significant effect on the production of BEV proteins. In BEV-infected BHK-21 cells with lauric

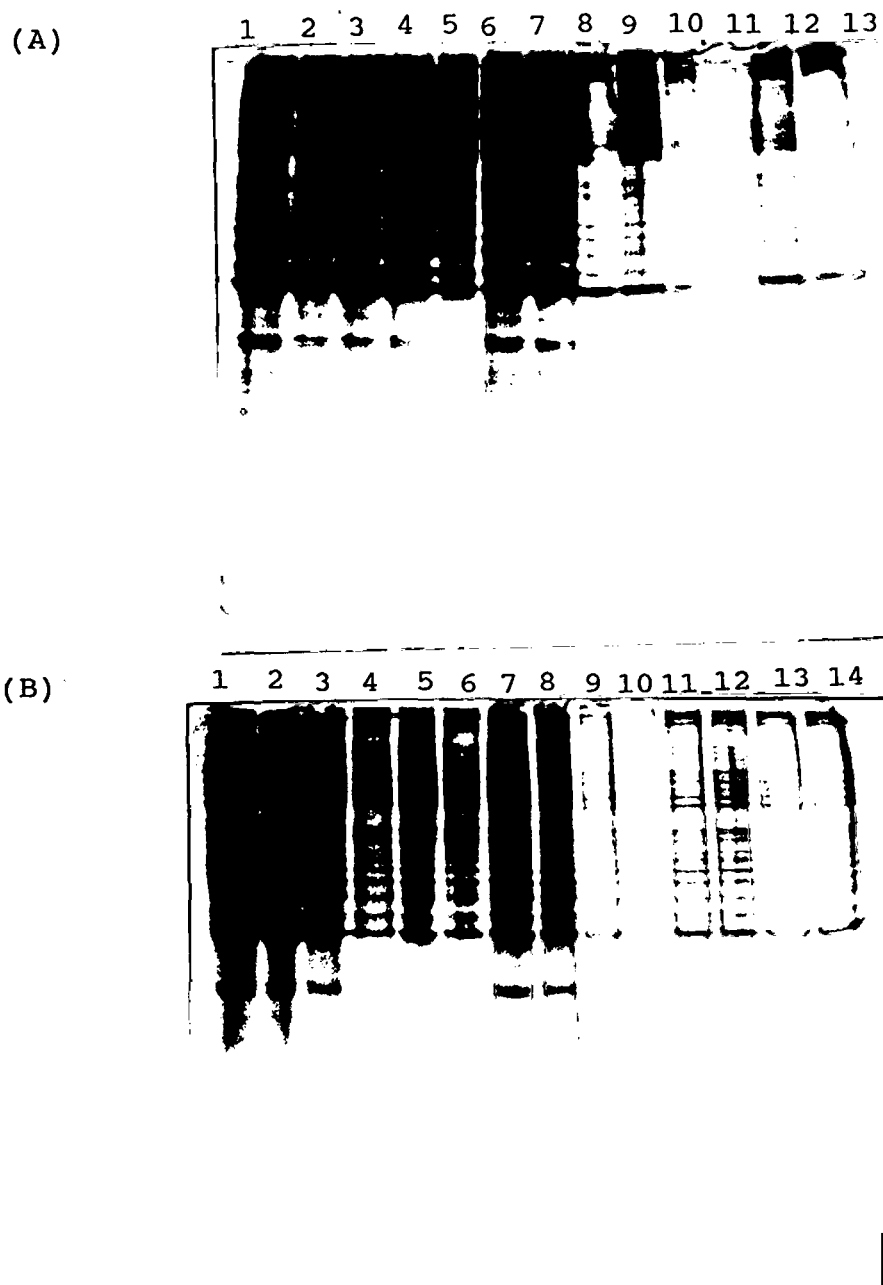


Figure 3.9: PAGE of radiolabelled proteins from BHK-21 cells grown in the presence of fatty acids and related compounds. (A): BHK-21 cell proteins without fatty acid, lane 1; cells + decyl alcohol: 25 μ M (lane 2), 100 μ M (lane 3); cells + capric acid: 25 μ M (lane 4), 100 μ M (lane 5); cells + lauric acid: 25 μ M (lane 6), 100 μ M (lane 7); cells + tridecanoic acid: 25 μ M (lane 8), 100 μ M (lane 9); cells + pentadecanoic acid: 25 μ M (lane 10), 100 μ M (lane 11); cells + tetradecane: 25 μ M (lane 12), 100 μ M (lane 13). (B): Cells + 2-bromo-tetradecanoic acid: 25 μ M (lane 1), 100 μ M (lane 2); cells + pentadecanoyl chloride: 25 μ M (lane 3), 100 μ M (lane 4); cells + myristic anhydride: 25 μ M (lane 5), 100 μ M (lane 6); cells + methyl myristate: 25 μ M (lane 7), 100 μ M (lane 8); cells + pentadecanol: 25 μ M (lane 9), 100 μ M (lane 10); cells + sodium laurate: 25 μ M (lane 11), 100 μ M (lane 12); cells + α -naphthyl myristate: 25 μ M (lane 13), 100 μ M (lane 14).

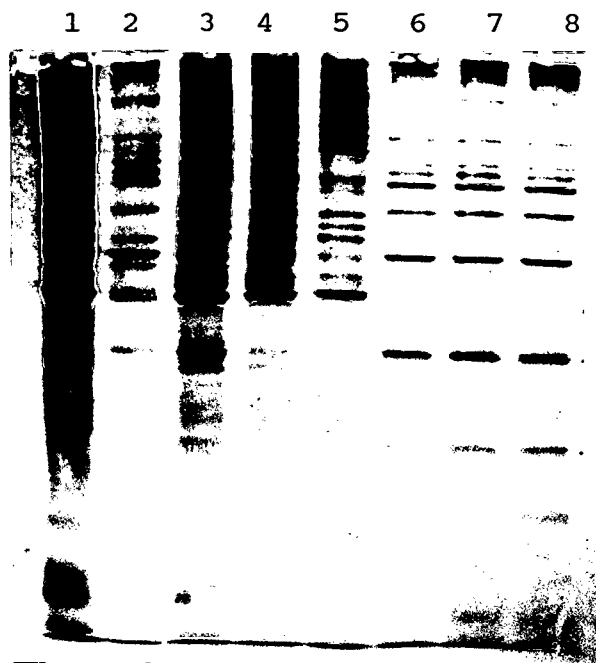


Figure 3.10: PAGE of radiolabelled proteins from BHK-21 cells infected with BEV in the presence and absence of lauric acid and capric acid. Mock-infected BHK-21 cells, lane 1; BEV-infected BHK-21 cells, lane 2; BEV-infected BHK-21 cells with 30 μ M lauric acid, lane 3; BEV-infected BHK-21 cells with 60 μ M lauric acid, lane 4; BEV-infected BHK-21 cells with 80 μ M lauric acid, lane 5; BEV-infected BHK-21 cells with 30 μ M capric acid, lane 6; BEV-infected BHK-21 cells with 40 μ M capric acid, lane 7; BEV-infected BHK-21 cells with 50 μ M capric acid, lane 8.

acid there seemed to be a block in virus-directed protein synthesis (lanes 3, 4, and 5) when compared with BEV-infected cells without lauric acid (lane 2). In the presence of lauric acid the pattern obtained resembled that of non-infected BHK cells (lane 1).

In contrast, in BEV-infected BHK-21 cells with capric acid there seemed to be no effect on virus-directed protein synthesis (lanes 6, 7, and 8) since the pattern obtained resembled that of BEV-infected cells without capric acid (lane 2). However, Fig. 3.11 shows that in similar experiments with EMCV, lauric acid and capric acid present during infection had no effect on virus-directed protein synthesis. The pattern obtained with both lauric acid (lanes 3, 4, and 5) and capric acid (lanes 6, 7, and 8) resembled that of EMCV-infected cells without fatty acid (lane 2). In a similar experiment using HRV-infected HeLa cells, lauric acid seemed to have no effect on HRV-induced proteins (Fig. 3.12).

Since it seemed as though lauric acid only affected the production of BEV-induced proteins and not EMCV- and HRV-induced proteins the experiment was repeated with BEV-infected BHK-21 cells using a higher concentration of lauric acid (100 μ M). Fig. 3.13 shows that there is an almost total block in virus-directed protein synthesis with BEV grown in the presence of 100 μ M-lauric acid (lane 4) compared with BEV grown in the absence of lauric acid (lane 3). Controls were run in parallel i.e. non-infected BHK-21

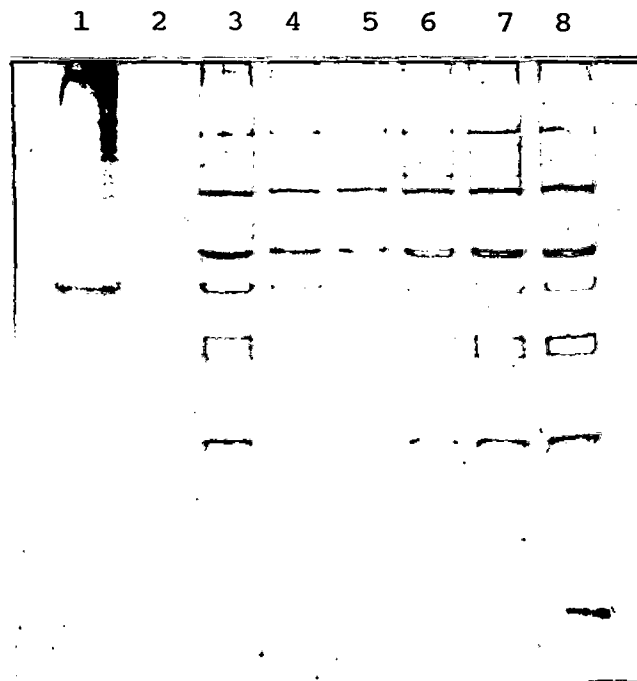


Figure 3.11: PAGE of radiolabelled proteins from BHK-21 cells infected with EMCV in the presence and absence of lauric acid and capric acid. Mock-infected BHK-21 cells, lane 1; EMCV-infected BHK-21 cells, lane 2; EMCV-infected BHK-21 cells with 30 μM lauric acid, lane 3; EMCV-infected BHK-21 cells with 60 μM lauric acid, lane 4; EMCV-infected BHK-21 cells with 80 μM lauric acid, lane 5; EMCV-infected BHK-21 cells with 30 μM capric acid, lane 6; EMCV-infected BHK-21 cells with 40 μM capric acid, lane 7; EMCV-infected BHK-21 cells with 50 μM capric acid, lane 8.



Figure 3.12: PAGE of radiolabelled proteins from HeLa cells infected with HRV-1B in the presence and absence of 30 μ M-lauric acid. Mock-infected HeLa cells, lane 1; HRV-infected HeLa cells, lane 2; Mock-infected HeLa cells with lauric acid, lane 3; HRV-infected HeLa cells with lauric acid, lane 4.

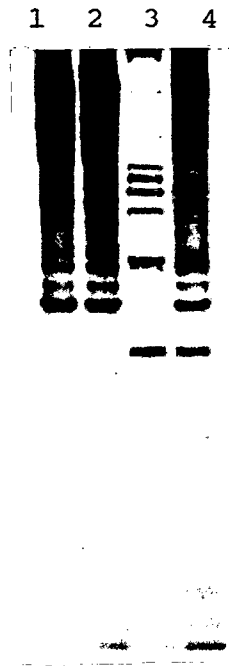


Figure 3.13: PAGE of radiolabelled proteins from BHK-21 cells infected with BEV in the presence of 100 μ M-lauric acid. Mock-infected BHK-21 cells, lane 1; Mock-infected BHK-21 cells with lauric acid, lane 2; BEV-infected BHK-21 cells, lane 3; BEV-infected BHK-21 cells with lauric acid, lane 4.

cells with lauric acid (lane 2) and without lauric acid (lane 3). In similar experiments with myristic- and palmitic-acids, 100 μ M-myristic acid seemed to block virus-directed proteins slightly (Fig. 3.14, lane 8) whereas 100 μ M-palmitic acid seemed to have no effect on virus-directed protein synthesis (Fig. 3.14, lane 10).

Experiments were then performed to determine the effect of lauric acid on the production of proteins in other picornaviruses. Fig. 3.15 shows a PAGE separation of [³⁵S]methionine-labelled proteins synthesized in cells infected with a high multiplicity of infection of enteroviruses (poliovirus type 1, coxsackievirus B5 and BEV VG-5-27), a cardiovirus ((EMCV) and HRV1B. Cells were infected with virus in the absence and presence of 100 μ M-lauric acid and radiolabelling times were chosen to demonstrate the maximum virus-directed protein synthesis. As above, in BHK-21 cells infected with BEV in the presence of lauric acid, there was an almost total block in virus-directed protein synthesis (lane 3) compared with infected cells in the absence of the fatty acid (lane 2). In the presence of lauric acid few virus-directed proteins were synthesized and the pattern obtained resembled that of non-infected BHK-21 cell proteins (lane 1). In contrast, in the absence or presence of lauric acid, EMCV (lanes 4 and 5) compared with BHK-21 cell proteins (lane 1), poliovirus (lanes 7 and 8) and coxsackievirus (lanes 9 and 10) compared with Vero cell proteins (lane 6) and HRV (lanes 12 and 13) compared with HeLa cell proteins (lane 11) showed

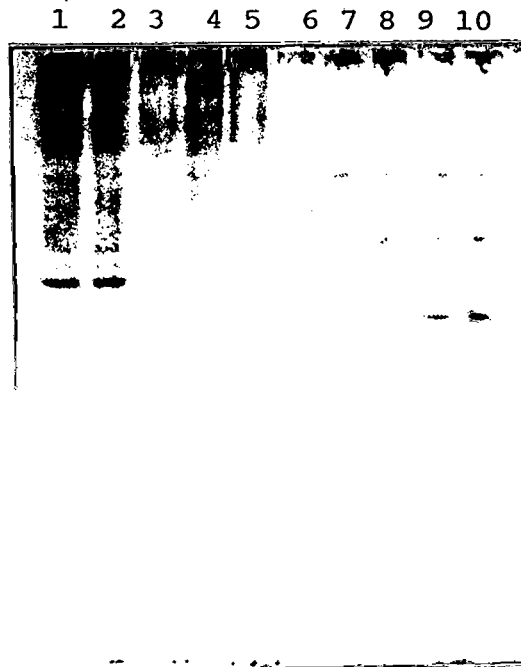


Figure 3.14: PAGE of radiolabelled proteins from BHK-21 cells infected with BEV in the presence and absence of myristic- and palmitic acids. Mock-infected BHK-21 cells, lane 1; Mock-infected BHK-21 cells with 25 μ M myristic acid, lane 2; Mock-infected BHK-21 cells with 100 μ M myristic acid, lane 3; Mock-infected BHK-21 cells with 25 μ M palmitic acid, lane 4; Mock-infected BHK-21 cells with 100 μ M palmitic acid, lane 5; BEV-infected BHK-21 cells, lane 6; BEV-infected BHK-21 cells with 25 μ M myristic acid, lane 7; BEV-infected BHK-21 cells with 100 μ M myristic acid, lane 8; BEV-infected BHK-21 cells with 25 μ M palmitic acid, lane 9; BEV-infected BHK-21 cells with 100 μ M palmitic acid, lane 10.

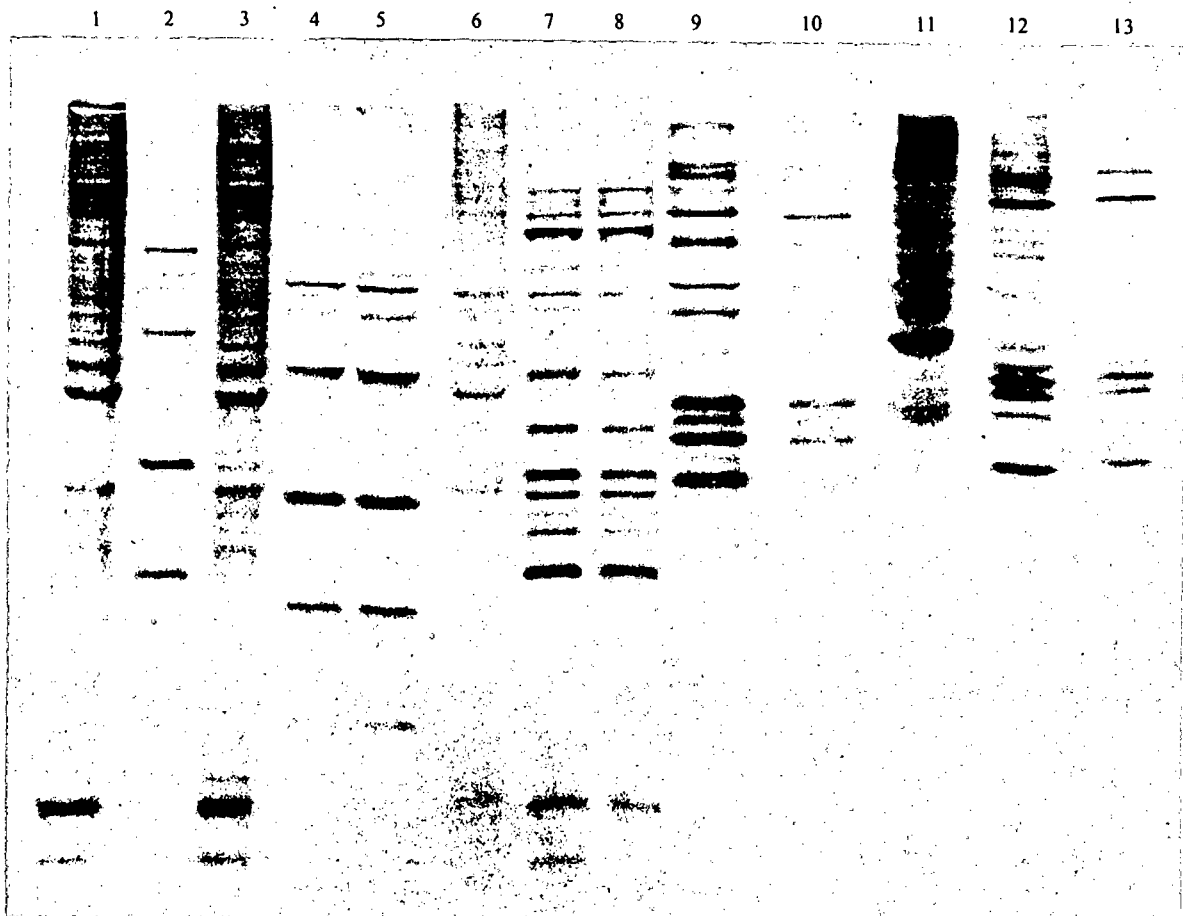


Figure 3.15: PAGE of radiolabelled proteins from cells infected with picornaviruses in the presence and absence of lauric acid. Mock-infected BHK-21 cells, lane 1; BEV-infected BHK-21 cells, lane 2; BEV-infected BHK-21 cells with lauric acid, lane 3; EMCV-infected BHK-21 cells, lane 4; EMCV-infected BHK-21 cells with lauric acid, lane 5; mock-infected Vero cells, lane 6; poliovirus-infected Vero cells, lane 7; poliovirus-infected Vero cells with lauric acid, lane 8; coxsackievirus-infected Vero cells, lane 9; coxsackievirus-infected Vero cells with lauric acid, lane 10; mock-infected HeLa cells, lane 11; HRV-infected HeLa cells, lane 12; HRV-infected HeLa cells with lauric acid, lane 13.

that very little inhibition of virus replication occurred.

These experiments indicate that lauric acid, present at the time of infection with BEV, prevents both the virus-induced inhibition of cellular protein synthesis and the synthesis of virus-directed proteins. However, when the fatty acid was added to BEV-infected cells 5 minutes post infection a typical virus-directed protein pattern was obtained (Fig. 3.16, lane 14). These findings suggest that lauric acid directly inhibits an early event in virus replication. As found with other compounds which inhibit early events in picornavirus replication (McSharry *et al.*, 1979) it was found that adding the fatty acid to the infecting virus for up to 1 hour before infection produced a more clear-cut inhibition of virus protein synthesis. BEV treated with 100 μ M-lauric acid and cultivated in Vero cells also showed a complete cut-off of virus protein synthesis, demonstrating that inhibition was not confined to one cell type.

To establish whether other fatty acids and simple derivatives could inhibit BEV infection, a number of compounds at 100 μ M were mixed with virus for 1 hour before infecting BHK-21 cells. As has been determined previously (results above), by microscopy and the synthesis of host cell proteins, these compounds at 100 μ M were not toxic for BHK-21 cells in culture. The polyacrylamide gel separation in Fig. 3.16 shows that capric acid (C=10, lane 3) failed to inhibit virus protein synthesis but some host protein is visible. Lauric acid (C=12, lane 4), tridecanoic acid

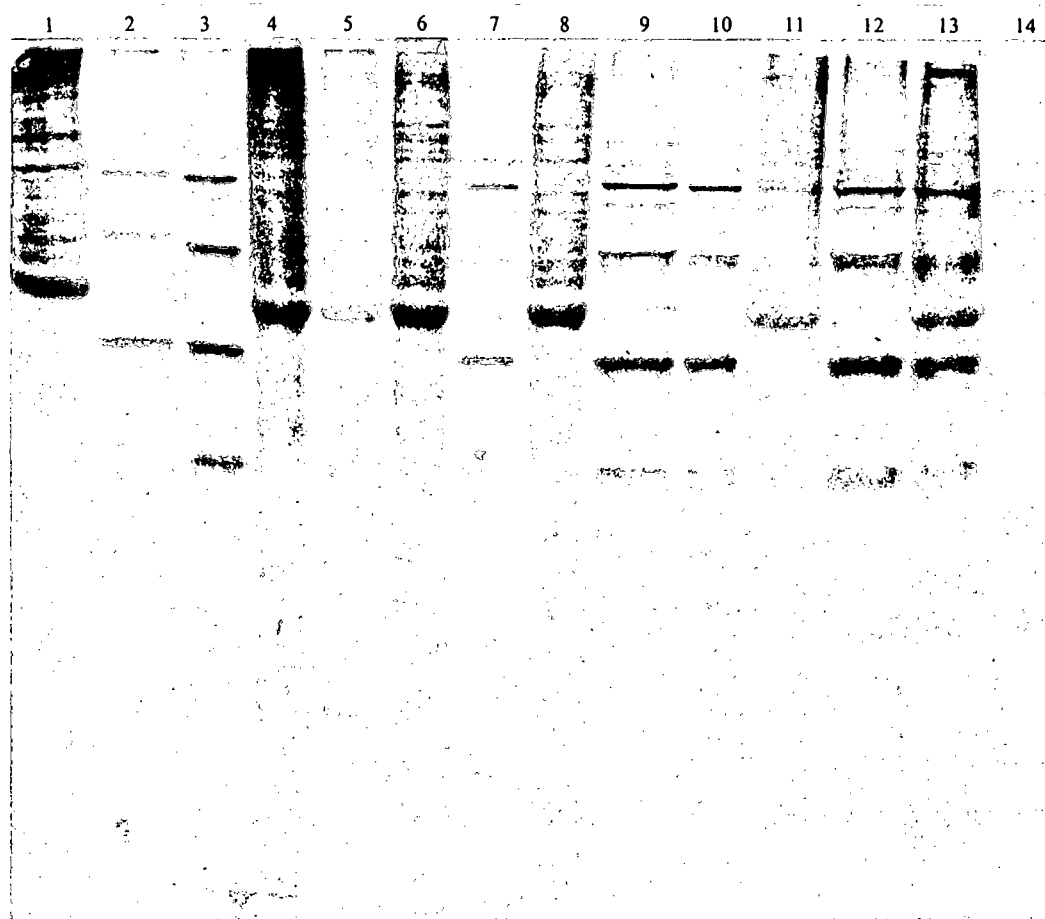


Figure 3.16: PAGE of radiolabelled proteins from BHK-21 cells infected with BEV in the presence of fatty acids and related compounds. Mock-infected cells, lane 1; infected cells, lane 2. Cells infected in the presence of fatty acids: capric acid, lane 3; lauric acid, lane 4; tridecanoic acid, lane 5; myristic acid, lane 6; tetradecane, lane 7; 2-bromo-tetradecanoic acid, lane 8; myristyl bromide, lane 9; myristic anhydride, lane 10; pentadecanoic acid, lane 11; pentadecanol, lane 12; palmitic acid, lane 13; lauric acid added to cells 5 min after infection, lane 14.

(C=13, lane 5), myristic acid (C=14, lane 6) and pentadecanoic acid (C=15, lane 11) inhibited virus protein synthesis. Palmitic acid (C=16, lane 13) was a far less effective inhibitor with the protein separation showing a mixture of virus-directed and host cell proteins. Stearic acid (C=18) failed to inhibit virus protein synthesis (not shown on PAGE). The only substituted fatty acid used in this study which was found to inhibit virus protein synthesis was 2-bromo-tetradecanoic acid (lane 8).

3.2.3 Attachment of Virus to Susceptible Cells

To determine whether fatty acid inhibition of BEV replication was due to failure of the virus to attach to cell receptors, purified [³⁵S]methionine-labelled virus was added to BHK-21 cell monolayers in the presence and absence of 100 μ M-lauric acid. Aliquots were removed from the infecting virus at intervals and the amount of unadsorbed virus was measured on a scintillation counter.

Fig. 3.17 shows that there is a rapid association of radiolabelled BEV with the BHK-21 cells with approximately 40% of the input being cell associated within 4 minutes. The attachment kinetics for radiolabelled virus in the presence and absence of lauric acid were similar.

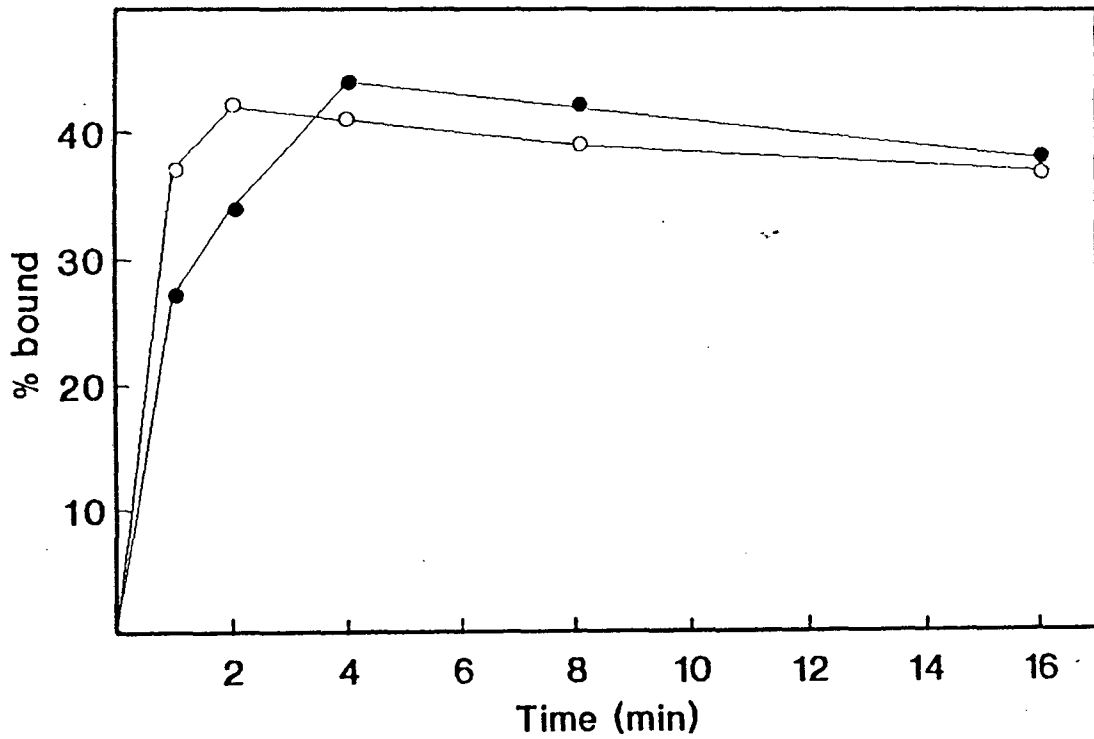


Figure 3.17: Kinetics of attachment of [³⁵S]methionine-labelled BEV to BHK-21 cells at 37°C. (●) Virus alone; (○) Virus with 100 μM-lauric acid.

3.2.4 Binding of Lauric Acid to Virus Particles

Purified unlabelled BEV was mixed with 5 μ Ci [3 H]lauric acid and allowed to stand at 20°C for 30 minutes. Virus-bound fatty acid was then assayed by centrifugation of the virus through a linear sucrose gradient. Fig. 3.18 shows radioactive lauric acid at the same position as the virus on a gradient, suggesting that binding had occurred. When the peak fractions were pooled and extracted with chloroform the radioactive fatty acid was recovered in the organic phase. The non-virucidal reversible binding of fatty acid was confirmed when it was found that chloroform extraction of lauric acid-treated BEV allowed virus replication to occur (Fig. 3.19, lane 4). In a similar binding experiment radiolabelled lauric acid bound only poorly to poliovirus particles.

3.2.5 Stabilization of Virus Particles with Lauric Acid

To examine the effect of fatty acids on virus stability [35 S]methionine-labelled BEV was heated in the presence and absence of lauric acid. Thermal degradation was assayed by sucrose gradient centrifugation. Fig. 3.20 (b) shows that heating at 52°C for 1 hour caused the breakdown of BEV particles, with a radioactive peak sedimenting at about 80S compared with 160S for untreated virus (Fig. 3.20a). In the presence of 100 μ M-lauric acid, breakdown was significantly reduced (Fig. 3.20c). Using 1 mM-lauric acid

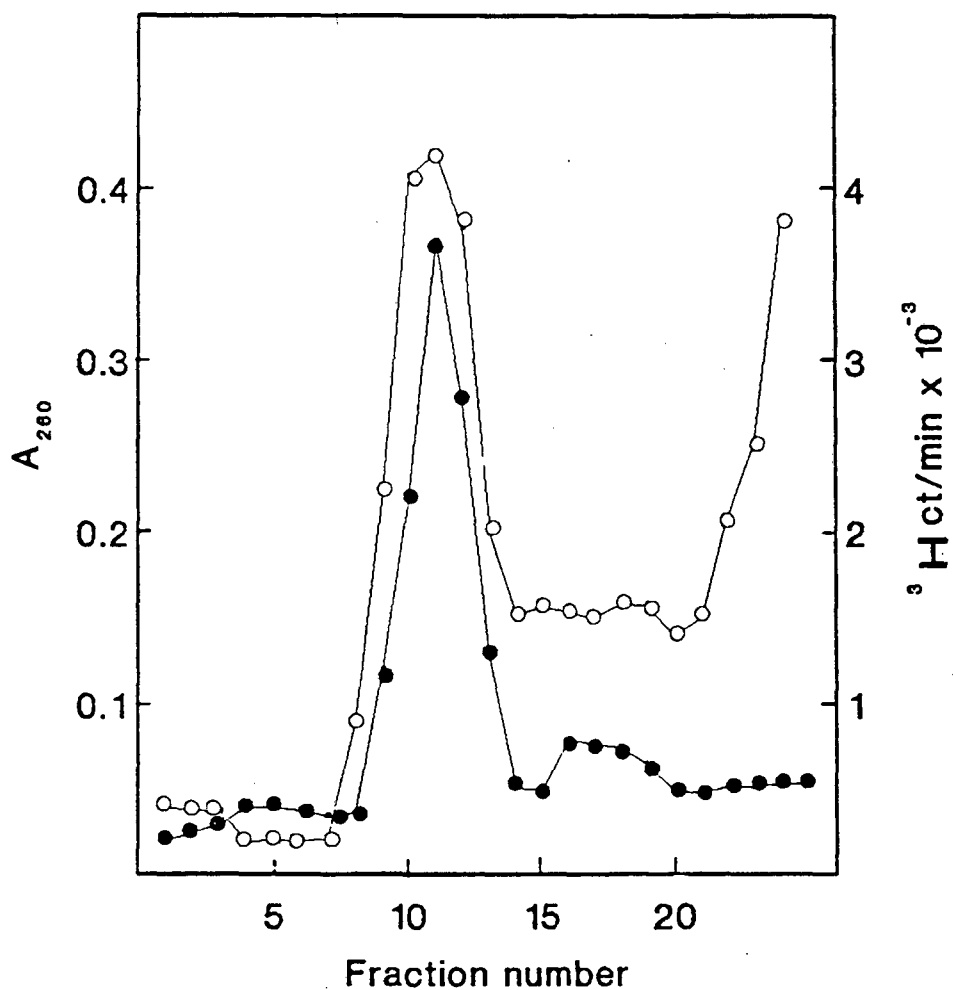


Figure 3.18: Sucrose gradient of [³H]lauric acid bound to purified BEV. (○) Lauric acid (c.p.m.); (●) BEV (absorbance at 260 nm, A₂₆₀).

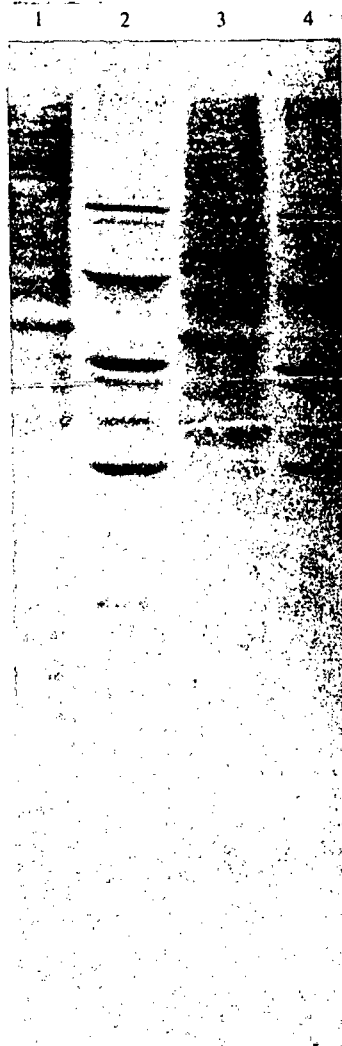


Figure 3.19: PAGE of radiolabelled proteins from BHK-21 cells infected with BEV. Mock-infected cells, lane 1; BEV-infected cells, lane 2; BEV-infected cells with 100 μ M-lauric acid, lane 3; cells infected with BEV incubated with 100 μ M-lauric acid for 1 h and then extracted with chloroform, lane 4.

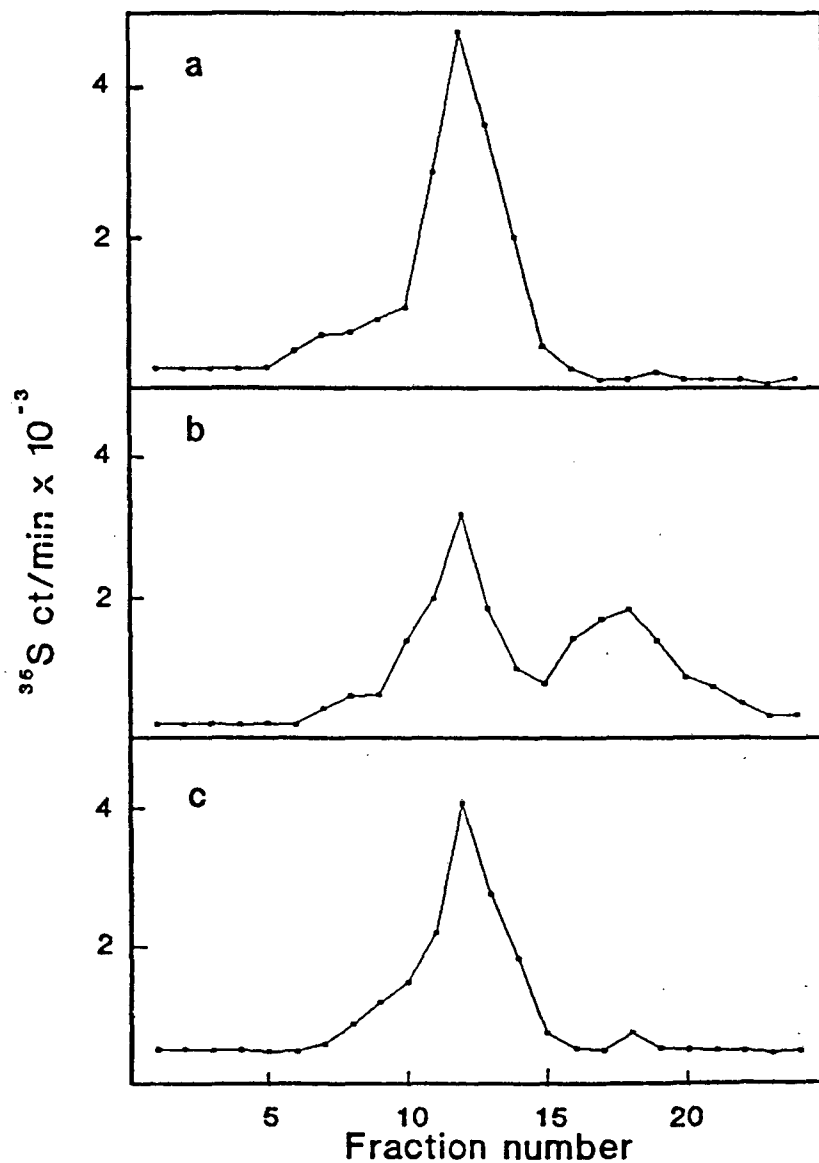


Figure 3.20: Sucrose gradients showing the protective activity of fatty acids against degradation by heating at 52 °C. (a) Untreated BEV; (b) BEV after heating at 52°C for 1 h; (c) BEV with 100 μM -lauric acid for 1 h and then heated at 52°C for 1 h.

it was found later that complete protection from degradation at 52°C could be achieved. In similar experiments 100 µM-lauric acid failed to stabilize poliovirus 1.

3.2.6 Inhibition of Cell-mediated Uncoating

As lauric acid was found to bind to and stabilize BEV particles, while still allowing attachment to susceptible cells, it was determined whether virus particles could undergo cell-mediated uncoating. [³⁵S]methionine-labelled BEV was added to BHK-21 cell monolayers in the presence or absence of 100 µM-lauric acid. After incubation at 37°C for 1 hour the cells were washed with fresh medium and then lysed with a mixture of 0.5% sodium deoxycholate and 1%NP40. Radioactivity in the cell lysate was assayed by sucrose gradient centrifugation. Figure 3.21 (b) shows that after 1 hour a significant proportion of the virus, added to cells in the absence of lauric acid, sedimented to about 80S compared with 160S for the control virus (Fig. 3.21a). Most of the radioactive virus material extracted from cells infected with BEV in the presence of lauric acid sedimented to 160S (Fig. 3.21c).

Owing to the difficulty in making this type of experiment fully quantitative it is possible that the finding of only 160S particles in Fig. 3.21 (c) could be due to 80S particles being rendered unstable by the presence of lauric acid. However this is unlikely in view of the findings in

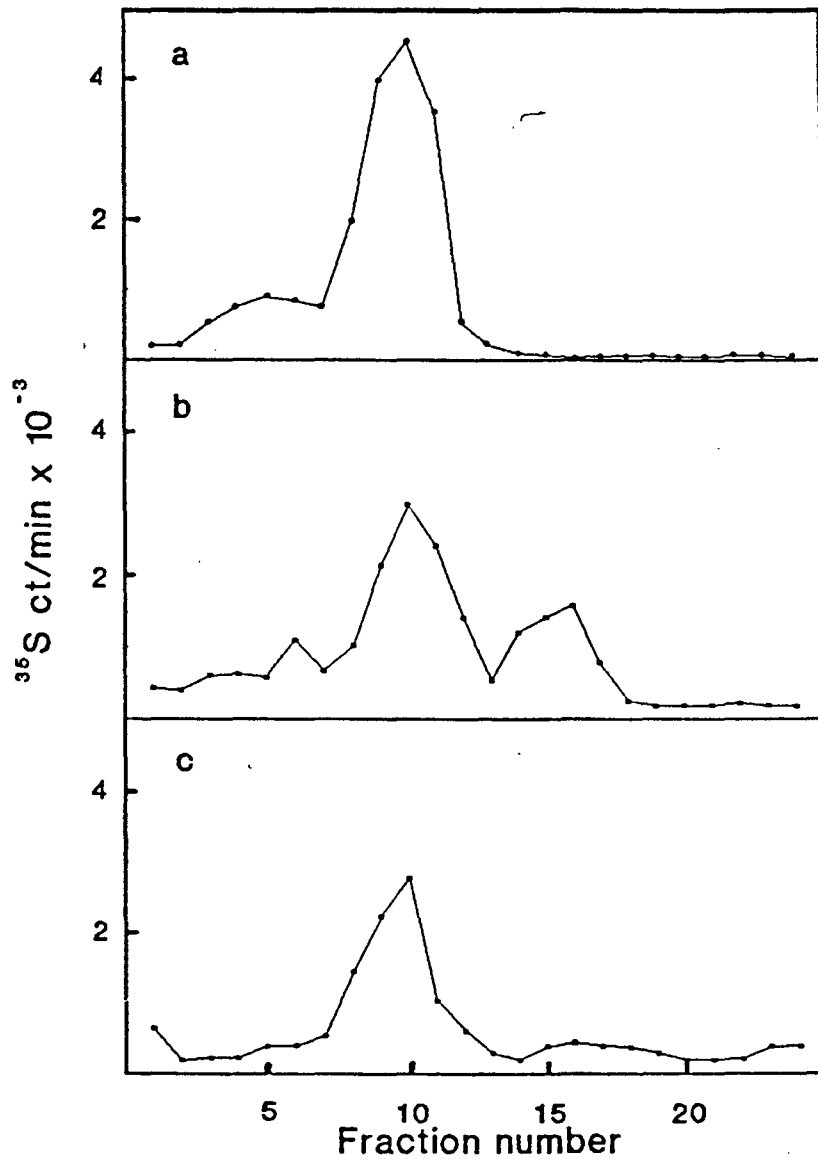


Figure 3.21: Sucrose gradients showing the inhibition of cell-mediated uncoating by lauric acid. (a) Untreated BEV; (b) radiolabel isolated from cells 1 h after infection; (c) radiolabel isolated from cells 1 h after infection with virus mixed with 100 μM -lauric acid.

other experiments where infected cells have been incubated for 4 hours. In cells infected with virus alone there was an almost complete absence of 160S particles whereas in cells infected with virus, in the presence of lauric acid, 160S particles were readily detected. The block in the formation of eclipse products is similar to that described for poliovirus treated with Arildone (Everaert et al., 1989) and suggests that bound lauric acid prevents cell-mediated uncoating.

DISCUSSION AND CONCLUSIONS

4.1 MYRISTIC ACID COMPETITION EXPERIMENTS

As mentioned before, the aim of this research project was; to determine whether analogues of myristic acid would compete for the myristylation site during myristylation, and whether these compounds would have any antiviral activity. The results obtained showed that radioactive lauric acid can be covalently bound to BEV VP4 and incorporated into virus particles. However, this is accompanied by a significant reduction in virus produced. Enzymic studies have shown that the enzyme responsible for myristylation can, in the presence of excess lauric acid, covalently add the shorter chain fatty acid to some proteins, but much less efficiently. Knowing that virus particles containing lauric acid can be made indicated that other fatty acid derivatives could also possibly be incorporated into VP4 and the function of the fatty acid could possibly have been determined. However, when the effect of these fatty acids on virus replication was examined by polyacrylamide gel electrophoresis, it was unexpectedly found that lauric acid inhibits BEV protein synthesis.

4.2 LAURIC ACID EXPERIMENTS

The results obtained in this research have shown that short chain fatty acids have a marked effect on the replication of BEV but this activity does not appear to extend to other picornaviruses or even other members of the enterovirus genus. The presence of lauric acid early in infection inhibits BEV-directed protein synthesis almost completely while having negligible effect on that of poliovirus type 1, coxsackievirus B5, EMCV and HRV1B. Studies with BEV suggest that lauric acid binds to the virus particle and stabilizes its structure against heat degradation. Bound lauric acid has no effect on the ability of the virus to attach to susceptible cells but does appear to prevent cell-mediated uncoating. The binding site for fatty acids has not been determined; however the interaction between the virus particle and lauric acid is reversible with chloroform, suggesting that it is due to hydrophobic bonding and that it is not virucidal.

These findings are similar to those described for a number of other compounds which are capable of inhibiting the uncoating of picornaviruses while not interfering with attachment and penetration of host cells (Lonberg-Holm and Noble-Harvey, 1973; Lonberg-Holm et al., 1975; Ninomiya et al., 1984; Tisdale and Selway, 1984; Otto et al., 1985; Smith et al., 1986; Kenny et al., 1988; Rossmann, 1989). Detailed studies undertaken by Rossmann and his colleagues,

using X-ray crystallography, have shown that the antiviral activity of a series of compounds synthesized by the Sterling Winthrop Institute (WIN compounds) is due to a strong hydrophobic bonding occurring in a small pocket found in the floor of the canyon which encircles each of the 12 vertices on HRV14 particles (see Fig. 1.20). Following this finding it was proposed that viral uncoating is inhibited by the drug preventing the collapse of the hydrophobic pocket or by blocking the flow of ions to the interior of the virus particle (Smith et al., 1986). The cross-resistance of HRV1B to Arildone, SDS and dichloroflavan suggests that these compounds share common binding sites (Tisdale and Selway, 1984) and Rossmann (1989) has suggested that compounds that inhibit the uncoating of picornaviruses probably all bind at essentially the same hydrophobic site. The finding that fatty acids interact hydrophobically and require a carbon chain length of 12 to 15 to inhibit the replication of BEV suggests that these molecules may also have to fit into a restricted hydrophobic domain. This possible restriction of size and hydrophobicity is similar to that found for some WIN compounds where aliphatic chains of 5 or 7, linking oxazoline-phenoxy groups and the isoxazole group, produce molecules that fit best into the hydrophobic pocket of HRV14 (Smith et al., 1986). In this study the finding that capric acid (C=10) did not inhibit BEV may indicate that it is not sufficiently hydrophobic to have a high affinity for the hydrophobic domain in the virus particle. Previously it has been shown that increasing the hydrophobicity of some

WIN compounds, by suitable additions to the phenyl group, increased their antiviral activity (Smith et al., 1986). Similarly, removal of hydrophobic substituents from Arildone decreased antiviral activity (Diana et al., 1977).

The observation that WIN compounds 51711 and 52084 inhibit rhino- and polioviruses but not mengo, foot-and-mouth disease (FMDV) and hepatitis A viruses is thought to reflect small differences in the capsid structure (Smith et al., 1986). Mengovirus, which is structurally similar to HRV14, has a partially blocked hydrophobic pocket which may influence accessibility to WIN compounds. The specificity of compounds such as the chalcone Ro 09-0410, which inhibits rhinoviruses but is ineffective against coxsackie-, echo-, polio- and mengo-viruses (Ishutsuka et al., 1982; Ninomiya et al., 1984), the inhibition of HRV2 but not HRV14 by low concentrations of SDS (Lonberg-Holm and Noble-Harvey, 1973) and the findings presented in this study are less easy to explain and may argue against a common binding site. The possibility that poliovirus type 1 (a South African isolate made in 1986), HRV1B and the coxsackievirus B5 used in this study (for which there are no structural data) may have inaccessible hydrophobic pockets cannot be ruled out. However this appears to be unlikely in the case of poliovirus, as recent experiments have shown that poliovirus type 1 (LSc) is also not inhibited by lauric acid (J. F. E. Newman, unpublished observations). It is also possible that fatty acids, even

if they enter the canyon pockets of these viruses, are not retained there because of insufficient hydrophobic affinity. Smith et al. (1986) have presented comparative data showing differences in amino acids found in the hydrophobic pockets of poliovirus, HRV and FMDV which suggest that such variable size, shape and affinity is possible. If this model for the hydrophobic pocket is correct, the findings in this study would suggest that fatty acids with chain lengths of 12 to 15 are of the correct size and shape to penetrate BEV particles and, because of a high affinity, become tightly bound. An alternative explanation might be that there are other sites on some picornaviruses that interact with hydrophobic fatty acids in such a way that uncoating is inhibited. It has been proposed for the antiviral chalcone Ro 09-0410 that some rhinoviruses have specific binding sites on their capsids not found on other picornaviruses (Ninomiya et al., 1984). Competition studies with WIN compounds and RNA sequence analysis of escape mutants should go some way to answering this question.

From the results and discussion of this study, it can be concluded that short chain fatty acids may act on bovine enterovirus in a similar way as the WIN compounds. Fatty acids have the added advantage in that they are relatively inexpensive as compared to the WIN compounds.

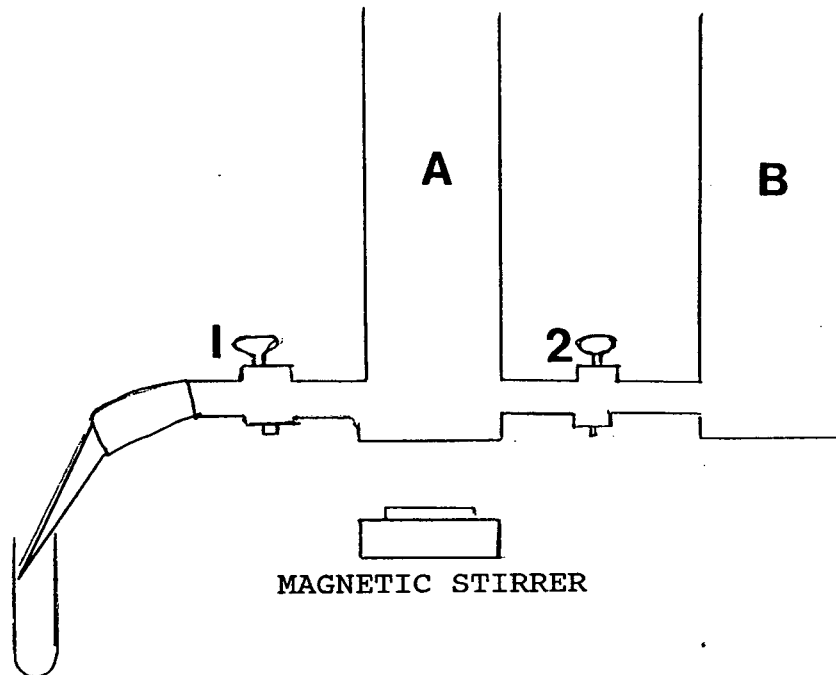
APPENDIX A:

TABLE OF FATTY ACIDS

Fatty acid	Carbon chain length	MW
Capric acid	10	172.27
Decyl alcohol	10	158.29
Lauric acid	12	200.32
Sodium laurate	12	222.30
Tridecanoic acid	13	214.35
Myristic acid	14	228.40
β -Naphthyl myristate	14	354.50
Tetradecane	14	198.40
2-Bromo-tetradecanoic acid	14	307.28
Methyl myristate	15	242.40
Pentadecanoyl chloride	15	260.90
Pentadecanoic acid	15	242.40
Pentadecanol	15	228.42
Palmitic acid	16	256.40
Stearic acid	18	284.20

APPENDIX B:

PREPARATION OF SUCROSE DENSITY GRADIENT



Make sure that the two taps (1 & 2) are closed

Pour 15% sucrose solution in chamber B and open tap 2 slightly to remove any air bubbles

Pour 45% sucrose solution in chamber A and switch on the magnetic stirrer

Open tap 2 first, followed by tap 1 and allow the solutions to flow through slowly down the side of the centrifuge tube (for SW 41 rotor)

APPENDIX C:

DISCONTINUOUS POLYACRYLAMIDE GEL ELECTROPHORESIS

Resolving gel buffer stock solution (1.5 M Tris-HCL pH 8.8)

Tris	90.9 g
conc HCL	10.95 ml
Distilled H ₂ O	500 ml

Stacking gel buffer stock solution (0.5 M Tris-HCL pH 6.8)

Tris	30.3 g
conc HCL	20.5 ml
Distilled H ₂ O	500 ml

Bath buffer stock solution

Tris	30.3 g
Glycine	144.1 g
SDS	10.0 g
Distilled H ₂ O	1.0 l

Diluted 10x before use

Acrylamide stock solution

Acrylamide	150.0 g
bis-acrylamide	4.0 g
Distilled H ₂ O	500 ml

Dissociation buffer

SDS	5.0 g
Mercaptoethanol	5.0 ml
Glycerol	7.5 ml
Bromophenol blue (0.2%)	2.5 ml
1 M Tris-HCL pH 6.8	6.3 ml
Distilled H ₂ O	<u>28.7 ml</u>
	50 ml

Slab gel formulations

<u>Resolving gel:</u>	Acrylamide stock solution	13.3 ml
(10% acrylamide)	1.5 M Tris-HCL pH 8.8	15.0 ml
	Distilled H ₂ O	9.3 ml
	10% SDS	0.4 ml
	1.5% (NH ₄) ₂ S ₂ O ₈	2.0 ml
	(prepared fresh)	
	TEMED	10 µl

<u>Stacking gel:</u>	Acrylamide stock solution	2.0 ml
(4% acrylamide)	0.5 M Tris-HCL pH 6.8	1.9 ml
	Distilled H ₂ O	9.25 ml
	80% glycerol	1.0 ml
	10% SDS	0.15 ml
	1.5% (NH ₄) ₂ S ₂ O ₈	0.7 ml
	(prepared fresh)	
	TEMED	20 µl

After electrophoresis the gels were removed from the plates, stained for 2 hours in coomassie brilliant blue and then destained.

Staining solution

Methanol	45 ml
Glacial acetic acid	10 ml
Coomassie brilliant blue	0.2 g
Distilled H ₂ O	45 ml

The dye was dissolved in a small amount of methanol and filtered. Then the remaining methanol, H₂O and acetic acid were added.

Destaining solution

Methanol	500 ml
Glacial acetic acid	200 ml
Glycerol	20 ml
Distilled H ₂ O	<u>1 280 ml</u>
	2 l

For autoradiography, the gel was soaked in Amplify for at least 30 minutes, dried and exposed to X-ray film at -20°C.
(This was for detection of radioactive proteins)

REFERENCES

ACHARYA, R., FRY, E., STUART, D., FOX G., ROWLANDS D. & BROWN, F. (1989). The three-dimensional structure of foot-and-mouth disease virus at 2.9 . resolution. *Nature, London* 337, 709-716.

ARNOLD, E., LUO, M., VRIEND, G., ROSSMANN, M. G., PALMENBERG, A. C., PARKS G. D., NICKLIN, M. J. H. & WIMMER, E. (1987). Implications of the picornavirus capsid structure for polyprotein processing. *Proceedings of the National Academy of Sciences, U.S.A.* 84, 21-25.

AUVINEN, P. & HYPPIA, T. (1990). Echoviruses include genetically distinct serotypes. *Journal of General Virology* 71, 2133-2139

BALTIMORE, D. & GIRARD, M. (1966). An intermediate in synthesis of poliovirus RNA. *Proceedings for the National Academy of Sciences, U.S.A.* 56, 741-748.

BALTIMORE, D., GIRARD. M. & DARNELL, J. E. (1966). Aspects of the synthesis of poliovirus RNA and the formation of virus particles. *Virology* 29, 179-189.

BEY, E. & GOLOMBICK, T. (1984). A comparison of three methods for titration of poliovirus vaccines. *Journal of Virological Methods* 9, 123-130

BIENZ, K., EGGER, D., RASSER, Y. & BOSSART, W. (1980). Kinetics and location of poliovirus macromolecular synthesis in correlation to virus-induced cytopathology. *Virology* 100, 390-399.

BOULANGER, P. & LONBERG-HOLM, K. (1981). Components of non-enveloped viruses which recognize receptors. In: *Receptors and Recognition. Series B, Vol 8: Virus Receptors. Part 2: Animal Viruses*, edited by K. Lonberg-Holm and L. Philipson, 21-46. Chapman and Hall, New York.

BROWN, F., CARTWRIGHT, B. & STEWART, D. L. (1962). Further studies on the infection of pig-kidney cells by foot-and-mouth disease virus. *Biochem. Biophys. Acta* 55, 768-774.

BROWN, F. & CARTWRIGHT, B. (1963). Purification of radioactive foot-and-mouth disease virus. *Nature, London* 199, 1169-1170.

BROWN, F., NEWMAN, J. F. E., STOTT, J., PORTER, A., FRISBY, D., NEWTON, C., CAREY, N. & FELLNER, P. (1974). Poly C in animal viral RNAs. *Nature, London* 251, 342-344.

BROWN, F. (1983). Neutralizing site of poliovirus. *Nature, London* 304, 395.

BUTTERWORTH, B. E. & RUECKERT, R. R. (1972). Gene order of encephalomyocarditis virus as determined by studies with pactamycin. *Journal of Virology* 9, 823-828.

BUTTERWORTH, B. E., SHIMSHICK, E. J. & YIN, F. H. (1976). Association of the polioviral RNA complex with phospholipid membranes. *Journal of Virology* 19, 457-466.

CALIGUIRI, L. A. & TAMM, I. (1970). Characterization of poliovirus specific structures associated with cytoplasmic membranes. *Virology* 42, 112-122.

CALIGUIRI, L. A. & MOSSER, A. G. (1971). Protein associated with the poliovirus RNA replication complex. *Virology* 46, 375-386.

CALIGUIRI, L. A., MCSHARRY, J. J. & LAWRENCE, G. W. (1980). Effect of Arildone on modifications of poliovirus in vitro. *Virology* 105, 86-93.

CALLAHAN, P. L., MIZUTINI, S. & COLONNO, R. J. (1985). Molecular cloning and complete sequence determination of human rhinovirus type 14 genome RNA. *Proceedings of the National Academy of Sciences, U.S.A.* 82.

CARROLL, A. R., ROWLANDS, D. J. & CLARK, B. E. (1984). The complete nucleotide sequence of the RNA coding for the primary translation product of foot-and-mouth disease virus. *Nucleic Acids Research* 12, 2461-2472.

CHOW, M., NEWMAN, J. F. E., FILMAN, D., HOGLE, J. M., ROWLANDS, D. J. & BROWN, F. (1987). Myristylation of picornavirus capsid protein VP4 and its structural significance. *Nature, London* 327, 482-486.

CORDS, C. E., JAMES, C. G. & McLAREN, L. C. (1975). Alteration of capsid proteins of coxsackievirus A13 by low ionic concentrations. *Journal of Virology* 15, 244-252.

COULEPSIS, A. G., LOCARNI, S. A., WESTAWAY, E. G., TANNOCK, G. A. & GUST, I. D. (1982). Biophysical and biochemical characterization of hepatitis A virus. *Intervirology* 18, 107-127.

CRAWFORD, N., FIRE, A., SAMUELS, M., SHARP, P. A. & BALTIMORE, D. (1981). Inhibition of transcription factor activity by poliovirus. *Cell* 27, 555-561.

CRAWFORD, N. M. & BALTIMORE, D. (1983). Genome-linked protein VPg of poliovirus present as VPg and VPg-pUp in poliovirus-infected cells. *Proceedings for the National Academy of Sciences, U.S.A.* 80, 7452-7455.

CROWELL, R. L. & PHILIPSON, L. (1971). Specific alterations of coxsackievirus B3 eluted from HeLa cells. *Journal of Virology* 8, 509.

CROWELL, R. L. & LANDAU, B. J. (1983). Receptors in the initiation of picornavirus infections. In: *Comprehensive Virology*, edited by H. Fraenkel-Conrat and R. R. Wagner, 18, 1-42. Plenum, New York.

DAS GUPTA, A., ZABEL, P. & BALTIMORE, D. (1980). Dependence of the activity of the poliovirus replicase on a host cell protein. *Cell* 19, 423-429.

DENOYA, C. D., SCODELLER, E. A., VASQUEZ, C. & LA TORRE, J. L. (1978). Foot-and-mouth disease virus. II. Endoribonuclease activity within purified virions. *Virology* 89, 67-74.

DIANA, G. D., SALVADOR, U. J., ZULAY, E. S., JOHNSON, R. E., COLLINS, J. C., JOHNSON, D., HINSHAW, W. B., LORENZ, R. R., THIELKING, W. H. & PANCIC, F. (1977). Antiviral activity of some β -diketones. I. Aryl alkyl diketones. *In vitro* activity against both RNA and DNA viruses. *Journal of Medicinal Chemistry* 20, 750-756.

DUNKER, A. K. & RUECKERT, R. R. (1971). Fragments generated by pH dissociation of ME virus and their relation to the structure of the virion. *Journal of Molecular Biology* 58, 217-235.

EHRENFELD, E. (1982). Poliovirus-induced inhibition of host-cell protein synthesis. *Cell* 28, 435-436.

EMINI, E. A., JAMESON, B. A. & WIMMER, E. (1983). Identification of multiple neutralization sites on poliovirus type 1 and the priming of the immune response with synthetic peptides. In: *Modern Approaches to Vaccines*, edited by R. M. Channock and R. A. Lerner, 65-75. Cold Spring Harbor Laboratory, Cold Springs Harbor, New York.

ETCHISON, D., HANSEN, J., EHRENFELD, E., EDERY, I., SONENBERG, N., MILBURN, S. & HERSHEY, J. W. B. (1984). Demonstration in vitro that eucaryotic initiation factor 3 is active but that a cap-binding protein complex is inactive in poliovirus-infected HeLa cells. *Journal of Virology* 51, 832-837.

EVERAERT, L., VRUSEN, R. & BOEYE, A. (1989). Eclipse products of poliovirus after cold-synchronized infection of HeLa cells. *Virology* 171, 76-82.

FERNANDEZ-MUNOZ, R. & DARNELL, J. (1976). Structural differences between the 5'-termini of viral and cellular mRNA in poliovirus infected cells: Possible basis for the inhibition of host protein synthesis. *Journal of Virology* 18, 719-726.

FERNANDEZ-TOMAS, C. B. & BALTIMORE, D. (1973). Morphogenesis of poliovirus II. Demonstration of a new intermediate, the provirion. *Journal of Virology* 12, 1122-1130.

FLANEGAN, J. B. & BALTIMORE, D. (1977). Poliovirus-specific primer-dependent RNA polymerase able to copy poly(A). *Proceedings of the National Academy of Sciences, U.S.A.* 74, 2677-2680.

FLANEGAN, J. B., PETERSSON, R. F., AMBROS, V., HEWLETT, M. J. & BALTIMORE, D. (1977). Covalent linkage of a protein to a defined nucleotide sequence at the 5' terminus of the virion and replicative intermediate RNAs of poliovirus. *Proceedings of the National Academy of Sciences, U.S.A.* 74, 961-965.

FOX, M. P., OTTO, M. J. & MCKINLAY, M. A. (1986). Prevention of rhinovirus and poliovirus uncoating by WIN 51711, a new antiviral drug. *Antimicrobial Agents and Chemotherapy* 30, 110-116.

GAUNTT, C. & GRIFFITH, M. M. (1974). Fragmentation of RNA in virus particles of rhinovirus type 14. *Journal of General Virology* 21, 253-267.

GOLINI, F., SEMLER, B. L., DORNER, A. J. & WIMMER, E. (1980). Protein-linked RNA of poliovirus is competent to form an initiation complex of translation in vitro. *Nature, London* 287, 600-603.

GUTTMAN, N. & BALTIMORE, D. (1977). Morphogenesis of poliovirus. IV. Existence of particles sedimenting at 150S and having the properties of provirion. *Journal of Virology* 23, 363-367.

GWALTNEY, J. M. (1982). Rhinoviruses. In: *Viral Infections of Humans: Epidemiology and Control*, edited by A. S. Evans, 491-517. Plenum, New York.

HERSHEY, H. V. & TAYLOR, M. W. (1987). Replication of Viral Genomes. In: *The Molecular Basis of Viral Replication*, edited by R. P. Bercoff 136, 51-55. Plenum, New York.

HEWLETT, M. J., ROSE, J. K. & BALTIMORE, D. (1976). 5' Terminal structure of poliovirus polyribosomal RNA is pUp. *Proceedings of the National Academy of Sciences, U.S.A.* 73, 327-330.

HOGLE, J. M., CHOW, M. & FILMAN, D. J. (1985). Three-dimensional structure of poliovirus at 2.9 resolution. *Science* 229, 1358-1365.

HRUBY, D. E. & ROBERTS, W. K. (1976). Variations in polyadenylic acid content and biological activity. *Journal of Virology*, 19, 325-330.

ICENOGLE, J., HONG, S., DUKE, G., GILBERT, S., RUECKERT, R. & ANDEREGG, J. (1983). Neutralization of poliovirus by a monoclonal antibody: Kinetics and stoichiometry. *Virology* 127, 412-425.

ISHUTSUKA, H., NINOMIYA, Y., OHSAWA, C., FUJII, M. & SUHARA, Y. (1982). Direct and specific inactivation of rhinovirus by a chalcone, Ro 09-0410. *Antimicrobial Agents and Chemotherapy* 22, 617-621.

JACOBSON, M. F., ASSO, J. & BALTIMORE, D. (1970). Further evidence on the formation of poliovirus proteins. *Journal of Molecular Biology* 49, 657-669.

JEN, G. & THACH, R. E. (1982). Inhibition of host translation in encephalomyocarditis virus-infected L cells: A novel mechanism. *Journal of Virology* 43, 250-261.

JOHNSTON, M. D. & MARTIN, S. J. (1971). Capsid and procapsid proteins of a bovine enterovirus. *Journal of General Virology* 11, 71-79.

KAMPS, M. P., BUSS, J. E. & SEFTON, B. M. (1985). Mutation of NH₂-terminal glycine of p60^{src} prevents both myristoylation and morphological transformation. *Proceedings of the National Academy of Sciences, U.S.A.* 82, 4625-4628.

KAPIKIAN, A. Z. (1971). A collaborative report: Rhinoviruses-extension of the number system. *Virology* 43, 524-526.

KATAGIRI, S., HINUMA, Y. & ISHIDA, N. (1967). Biophysical properties of poliovirus particles irradiated with ultraviolet light. *Virology* 32, 337-343.

KAUFMANN, Y., GOLDSTEIN, E. & PENMAN, S. (1976). Poliovirus-induced inhibition of polypeptide initiation in vitro on native polyribosomes. *Proceedings of the National Academy of Sciences, U.S.A.* 73, 1834-1838.

KEAN, K. M., TETERINA, N. & GIRARD, M. (1990). Cleavage specificity of the poliovirus 3C is not restricted to Gln-Gly in the 3C/3D junction. *Journal of General Virology* 71, 2553-2563.

KENNY, M. T., TORNEY, H. L. & DULWORTH, J. K. (1988). Mechanism of action of the antiviral compound MDL 20,610. *Antiviral Research* 9, 249-261.

KITAMURA, N., SEMLER, B., ROTHBERG, P. G., LARSON, G. R., ADLER, C. J., DORNER, A. J., EMINI, E. A., HANECAK, R., LEE, J. J., VAN DE WERF, S., ANDERSON, C. W. & WIMMER, E. (1981). Primary structure, gene organization and polypeptide expression of poliovirus RNA. *Nature, London* 291, 547-553.

KORANT, B. D., LONBERG-HOLM, K., NOBLE, J. & STASNY, J. T. (1972). Naturally occurring and artificially produced components of three rhinoviruses. *Virology* 48, 71-86.

LAEMMLI, U. K. (1970). Cleavage of structural proteins during the assembly of the head of bacteriophage T4. *Nature, London* 227, 680-685.

LAWRENCE, C. & THACH, R. E. (1975). Identification of a viral protein involved in post-translational maturation of the EMC virus capsid precursor. *Journal of Virology* 15, 918-928.

LAZARUS, L. H. & BARZILAI, R. (1974). Association of foot-and-mouth disease virus replicase with RNA template and cytoplasmic membranes. *Journal of General Virology* 23, 213-218.

LONBERG-HOLM, K. & KORANT, B. D. (1972). Early interaction of rhinoviruses with host cells. *Journal of Virology* 9, 29-40.

LONBERG-HOLM, K. & NOBLE-HARVEY, J. (1973). Comparison of in vitro and cell-mediated alteration of a human rhinovirus and its inhibition by sodium dodecyl sulphate. *Journal of Virology* 12, 819-826.

LONBERG-HOLM, K., GOSSER, L. B. & KAUER, J. C. (1975). Early alteration of poliovirus in infected cells and its specific inhibition. *Journal of General Virology* 27, 329-342.

LONBERG-HOLM, K. & WHITELEY, N. M. (1976). Physical and metabolic requirements for early interaction of poliovirus and human rhinovirus with HeLa cells. *Journal of Virology* 19, 857-870.

LONGWORTH, J. F. (1978). Small isometric viruses of insects. *Advances in Virus Research* 23, 103-157.

LUND, G. A., ZIOLA, B. R., SALMI, A. & SCRABA, D. G. (1977). Structure of the Mengo virion. V. Distribution of the capsid polypeptides with respect to the surface of the virus particle. *Virology* 78, 35-44.

LUNDQUIST, R. E., EHRENFELD, E. & MAIZEL, J. V. (1974). Isolation of a viral polypeptide associated with the poliovirus replication complex. Proceedings of the National Academy of Sciences, U.S.A. 71, 4774-4777.

LUO, M., VRIEND, G., KAMER, G., MINOR, I., ARNOLD, E., ROSSMANN, M. G., BOEGE, U., SCRABA, D. G., DUKE, G. M. & PALMENBERG, A. C. (1987). The atomic resolution structure of Mengo virus at 3.0 . resolution. Science 235, 182-191.

LUO, M., ROSSMANN, M. G. & PALMENBERG, A. C. (1988). Prediction of three-dimensional models for foot-and-mouth disease virus and hepatitis A virus. Virology 166, 503-514.

MAIZEL, J. V. (1964). Preparative electrophoresis of proteins in acrylamide gels. N. Y. Acad. Symp. Gel Electrophoresis 121 (Art 2), 382-390.

MAIZEL, J. V., PHILLIPS, B. A. & SUMMERS, D. E. (1967). Composition of artificially produced and naturally occurring empty capsids of poliovirus type I. Virology 32, 692-699.

MANDEL, B. (1976). Neutralization of poliovirus: a hypothesis to explain the mechanism and the one-hit character of the neutralization reaction. Virology 69, 500.

MAPOLES, J. E., ANDEREGG, J. W. & RUECKERT, R. R. (1978). Properties of poliovirus propagated in medium containing cesium chloride. Implications for picornaviral structure. *Virology* 90, 103-111.

MARTIN, S. J., JOHNSTON, M. D. & CLEMENTS, J. B. (1970). Purification and characterization of bovine enteroviruses. *Journal of General Virology* 7, 103-113.

MATTHEWS, R. E. F. (1982). Classification and nomenclature of viruses. *Intervirology* 17, 1-199.

MAYER, M. M., RAPP, H. J., ROIZMAN, B., KLEIN, S. W., COWAN, K. M., LUKENS, D., SCHWERDT, C. E., SCHAFFER, F. L. & CHARNEY, J. (1957). The purification of poliomyelitis virus as studied by complement fixation. *Journal of Immunology* 78, 435-455.

McFERRAN, J. B. (1962). Bovine enteroviruses. *Annals of the New York Academy of Sciences* 101, 436-443.

McKINLAY, M. A. & STEINBERG, B. A. (1986). Oral efficacy of WIN 51711 in mice infected with human poliovirus. *Antimicrobial Agents and Chemotherapy* 29, 30-32.

McSHARRY, J. J., CALIGUIRI, L. A. & EGGERS, H. J. (1979). Inhibition of uncoating of poliovirus by Arildone, a new antiviral drug. *Virology* 97, 307-315.

MEDAPPA, K. C., McLEAN, C. & RUECKERT, R. R. (1971). On the structure of rhinovirus 1A. *Virology* 44, 259-270.

MELNICK, J. L. (1974). Picornaviridae. *Intervirology* 4, 303-316.

MELNICK, J. L. (1976). Enteroviruses. In: *Viral Infections of Humans*, edited by A. S. Evans, 163-208. Plenum Medical Book Co., New York.

MELNICK, J. L. (1983)a. Classification of hepatitis A virus as enterovirus type 72 and of hepatitis B virus as hepadnavirus type 1. *Intervirology* 18, 105-106.

MELNICK, J. L. (1983)b. Portraits of viruses: The picornaviruses. *Intervirology* 20, 61-100.

MOORE, N. F. & TINSLEY, T. W. (1982). The small RNA viruses of insects. *Archives of Virology* 72, 229-245.

NEWMAN, J. F. E., ROWLANDS, D. J., BROWN, F., GOODRIDGE, D., BURROWS, R. & STECK, F. (1977). Physicochemical characterization of two serologically unrelated equine rhinoviruses. *Intervirology* 8, 145-154.

NINOMIYA, Y., OHSAWA, C., AOYAMA, M., UMEDA, I., SUHARA, Y. & ISHUTSUKA, H. (1984). Antivirus agent, Ro 09-0410, binds to rhinovirus specifically and stabilizes the virus conformation. *Virology* 134, 269-276.

NOMOTO, A., LEE, Y. F. & WIMMER, E. (1976). The 5' end of poliovirus mRNA is not capped with m G(5')⁷pppG(5')-Np. *Proceedings of the National Academy of Sciences, U.S.A.* 73, 375-380.

NOMOTO, A., DETJEN, B. M., POZZATTI, R. & WIMMER, E. (1977). Location of the polio genome protein in viral RNAs and its implication for RNA synthesis. *Nature, London* 268, 208-213.

OTTO, M. J., FOX, M. P., FANCHER, M. J., KUHRT, M. F., DIANA, G. D. & MCKINLAY, M. A. (1985). In vitro activity of WIN 51711, a new broad-spectrum anti-picornavirus drug. *Antimicrobial Agents and Chemotherapy* 27, 883-886.

PALLANSCH, M. A., KEW, O. M., SEMLER, B. L., OMILIANOWSKI, D. R., ANDERSON, C. W., WIMMER, E. & RUECKERT, R. R. (1984). Protein processing map of poliovirus. *Journal of Virology* 49, 873-880.

PALMENBERG, A. C. (1982). In vitro synthesis and assembly of picornaviral capsid intermediate structures. *Journal of Virology* 44, 900-906.

PALMENBERG, A. C., & RUECKERT, R. R. (1982). Evidence for intramolecular self-cleavage of picornaviral replicase precursors. *Journal of Virology* 41, 244-248.

PALMENBERG, A. C., KIRBY, E. M., JANDA, M. R., DRAKE, N. L., DUKE, G. M., POTRATZ, K. F. & COLLETT, M. S. (1984). The nucleotide and deduced sequences of the encephalomyocarditis viral polyprotein coding region. *Nucleic Acids Research* 12, 2969-2985.

PAUL, A. V., SCHULTZ, A., PINCUS, S. E., OROSZLAN, S. & WIMMER, E. (1987). Capsid protein VP4 of poliovirus is N-myristoylated. *Proceedings of the National Academy of Sciences, U.S.A.* 84, 7827-7831.

PELLMAN, D., GARBER, E. A., CROSS, F. R. & HANAFUSA, H. (1985). Fine structural mapping of a critical NH-terminal region of p60^{src}. *Proceedings of the National Academy of Sciences, U.S.A.* 82, 1623-1627.

PENMAN, S. & SUMMERS, D. (1965). Effects on host cell metabolism following synchronous infection with poliovirus. *Virology* 27, 614-620.

PERLIN, M. & PHILLIPS, B. A. (1973). In vitro assembly of polioviruses. III. Assembly of 14S particles into empty capsids by poliovirus-infected HeLa cell membranes. *Virology* 53, 107-114.

PHILLIPS, B. A. (1969). In vitro assembly of polioviruses. I. Kinetics of the assembly of empty capsids and the role of extracts from infected cells. *Virology* 39, 811-821.

PHILLIPS, B. A., LUNDQUIST, R. E. & MAIZEL, J. V. (1980). Absence of subviral particles and assembly activity in HeLa cells infected with defective-interfering (DI) particles of poliovirus. *Virology* 100, 116-124.

PUTNAK, J. R. & PHILLIPS, B. A. (1981). Picornaviral structure and assembly. *Microbiological Reviews* 45, 287-315.

RACANIELLO, V. R. & BALTIMORE, D. (1981). Molecular cloning of poliovirus cDNA and determination of the complete nucleotide sequence of the viral genome. *Proceedings of the National Academy of Sciences, U.S.A.* 78, 4887-4891.

REIN, A., McCLURE, M. R., RICE, N. R., LUFTIG, R. B. & SCHULTZ, M. A. (1986). Myristylation site in Pr65^{gag} is essential for virus particle formation by Maloney murine leukemia virus. *Proceedings of the National Academy of Sciences, U.S.A.* 83, 7246-7250.

RHEE, S.S. & HUNTER, E. (1987). Myristylation is required for intracellular transport but not for assembly of D-type retrovirus capsids. *Journal of Virology* 61, 1045-1053.

RICHARDS, O. C., MORTON, K., MARTIN, S. C. & EHRENFELD, E. (1984). Two forms of poliovirus VPg result from amino acid modification of a single viral protein. *Virology* 136, 453-456.

ROMBAUT, B., VRIJESSEN, R. & BOEYE, A. (1984). *In vitro* assembly of poliovirus empty capsids: Antigenic consequences and immunological assay of the morphopoietic factor. *Virology* 135, 546-550.

ROSSMANN, M. G., ARNOLD, E., ERICKSON, J. W., FRANKENBERGER, E. A., GRIFFITH, J. P., HECHT, H. J., JOHNSON, J. E., KAMER, G., LUO, M., MOSSER, A. G., RUECKERT, R. R., SHERRY, B. & VRIEND, G. (1985). Structure of a human common cold virus and functional relationship to other picornaviruses. *Nature, London* 317, 145-153.

ROSSMANN, M. G., ARNOLD, E., KAMER, G., KREMER, M. J., LUO, M., SMITH, T. J. & VRIEND, G. (1987). Viral particles at atomic resolution. In: *The Molecular Basis of Viral Replication*, edited by R. P. Bercoff, 25-44. Plenum, New York.

ROSSMANN, M. G. & RUECKERT, R. R. (1987). What does the molecular structure of viruses tell us about viral functions?. *Microbiological Sciences* 4, 206-214.

ROSSMANN, M. G. (1989). The structure of antiviral agents that inhibit uncoating when complexed with viral capsids. *Antiviral Research* 11, 3-14.

ROUMIANTZEFF, M., SUMMERS, D. F. & MAIZEL, J. V. (1971). In vitro protein synthetic activity of membrane-bound poliovirus polyribosomes. *Virology* 44, 249-258.

ROWLANDS, D. J., SHIRLEY, M. W., SANGAR, D. V. & BROWN, F. (1975). A high density component in several vertebrate enteroviruses. *Journal of General Virology* 29, 223-234.

RUECKERT, R. R., DUNKER, A. K. & STOLTZFUS, C. M. (1969). The structure of Maus-elberfeld virus: A model. *Proceedings of the National Academy of Sciences, U.S.A.* 62, 912-919.

RUECKERT, R. R. (1976). On the structure and morphogenesis of picornaviruses. In: *Comprehensive Virology*, edited by H. Fraenkel-Conrat and R. R. Wagner, 131-213. Plenum, New York.

RUECKERT, R. R. & WIMMER, E. (1984). Systematic nomenclature of picornavirus proteins. *Journal of Virology* 50, 957-959.

RUECKERT, R. R. (1986). Picornaviruses and their replication. In: Fundamental Virology, edited by B. N. Fields & D. M. Knipe, 357-390. Raven Press, New York.

SANGAR, D.V. (1979). The replication of picornaviruses. Journal of General Virology 45, 1-11.

SCHARFF, M. D. & LEVINTOW, L. (1963). Quantitative study of the formation of poliovirus antigens in infected HeLa cells. Virology 19, 491-500.

SCHARFF, M. D., MAIZEL, J. V. & LEVINTOW, L. (1964). Physical and immunological properties of a soluble precursor of the poliovirus capsid. Proceedings of the National Academy of Sciences, U.S.A. 51, 329-337.

SHERRY, B., MOSSER, A. G., COLONNO, R. J. & RUECKERT, R. R. (1986). Use of monoclonal antibodies to identify four neutralizing immunogens on a common cold picornavirus, human rhinovirus 14. Journal of Virology 57, 246-257.

SMITH, T. J., KREMER, M. J., LOU, M., VRIEND, G., ARNOLD, E., KAMER, G., ROSSMANN, M. G., MCKINLAY, M. A., DIANÁ, G. D. & OTTO, M. J. (1986). The site of attachment in human rhinovirus 14 for antiviral agents that inhibit uncoating. Science 233, 1286-1293.

SPECTOR, D. H. & BALTIMORE, D. (1974). Requirement of 3'-terminal polyadenylic acid for the infectivity of poliovirus RNA. Proceedings of the National Academy of Sciences, U.S.A. 71, 2983-2987.

STANWAY, G. (1990). Structure, function and evolution of the picornaviruses. Journal of General Virology 71, 2483-2501.

SUMMERS, D. F., MAIZEL, J. V. & DARNELL, J. E. (1965). Evidence for virus-specific noncapsid proteins in poliovirus-infected cells. Proceedings of the National Academy of Sciences, U.S.A. 54, 505-513.

SUMMERS, D. F. & MAIZEL, J. V. (1971). Determination of the gene sequence of poliovirus with pactamycin. Proceedings of the National Academy of Sciences, U.S.A. 68, 2852-2856.

TABER, R., REKOSH, D. & BALTIMORE, D. (1971). Effect of pactamycin on synthesis of poliovirus proteins: A method for genetic mapping. Journal of Virology 8, 395-410.

TALBOT, P. & BROWN, F. (1972). A model for foot-and-mouth disease virus. Journal of General Virology 15, 163-170.

TAMM, I. & EGGERS, H. J. (1963). Specific inhibition of replication of animal viruses. Science 142, 24-33.

TAMURA, T. A. (1983). Provirus of M7 baboon endogenous virus: Nucleotide sequence of the gag-pol region. Journal of Virology 47, 137-145.

TISDALE, M. & SELWAY, J. W. T. (1984). Effect of dichloroflavan (BW683C) on the stability and uncoating of rhinovirus type 1B. Journal of Antimicrobial Chemotherapy 14, 97-105.

TOYODA, H., NICKLIN, M. J. H., MURRAY, M. G., ANDERSON, C. W., DUNN, J. J., STUDIER, F. W. & WIMMER, E. (1986). A second virus-encoded proteinase involved in proteolytic processing of poliovirus polyprotein. Cell 45, 761-770.

VAN DYKE, T. A. & FLANEGAN, J. B. (1980). Identification of poliovirus polypeptide p63 as a soluble RNA-dependent RNA polymerase. Journal of Virology 35, 732-740.

WETZ, K., ZEICHARDT, H., WILLINGMANN, P. & HABERMEHL, K. O. (1983). Dense particles and slow sedimenting particles produced by ultraviolet irradiation of poliovirus. Journal of General Virology 64, 1263-1275.

WHITAKER, A. (1972). Estimation of Viruses. In: Tissue and cell culture, 78-81. Bailliere Tindall, London.

YAMAGUCHI-KOLL, U., WIEGER, K. J. & DRZENIEK, R. (1975). Isolation and characterization of "dense particles" from poliovirus-infected HeLa cells. Journal of General Virology 26, 307-319.

YIN, F. H. (1977). Involvement of viral procapsid in the RNA synthesis and maturation of poliovirus. Virology 82, 299-307.